SIMULATION OF AN ACTIVE FILTER USING A 3-LEVEL INVERTER

by

ANIL BISHT

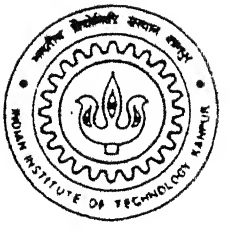

DEPARTMENT OF ELECTRICAL ENGINEERING

INDIAN INSTITUTE OF TECHNOLOGY KANPUR

April, 1999

SIMULATION OF AN ACTIVE FILTER USING A 3-LEVEL INVERTER

A Thesis Submitted
in Partial Fulfilment of the Requirements
for the Degree of
MASTER OF TECHNOLOGY
by
ANIL BISHT

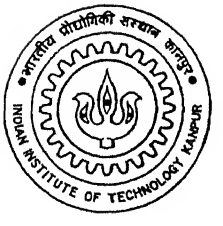

to the
DEPARTMENT OF ELECTRICAL ENGINEERING
INDIAN INSTITUTE OF TECHNOLOGY KANPUR
APRIL, 1999

CERTIFICATE

It is certified that the work contained in the thesis entitled **SIMULATION OF AN ACTIVE FILTER USING A 3-LEVEL INVERTER :** by ***Anil Bisht***, has been carried out under my supervision and that this work has not been submitted elsewhere for a degree.

Dr. A. Joshi
Professor,
Department of Electrical Engineering,
Indian Institute of Technology,
Kanpur 208016.

April, 1999.

Dedicated

to

my parents

Acknowledgement

It is with a deep sense of gratitude that I acknowledge the invaluable guidance received from Dr. A. Joshi. I thank him for his excellent guidance, constructive advice, constant support and encouragement throughout the present work.

I finally thank all my friends, who have, directly or indirectly, assisted me with their valuable suggestions in the completion of this work.

Anil Bisht

Abstract

Power electronics equipments converts power from one form to the other, as required by the consumer, with ease of control and high efficiency. These equipments are used in various applications. These P.E. equipments have inherent non-linear characteristics, introduce harmonics into the source and consume reactive power. In this thesis shunt active filter is analyzed in detail to eliminate these unwanted harmonics of the source and to compensate the reactive power of the load. A three level inverter is discussed, which with the control circuit acts as an active filter. The three level inverter has the advantage that switches with low power ratings can be used, hence one can use high frequency switches. The load currents are sensed and command currents for the active filter are generated, which would make the source currents sinusoidal. Using various controllers the active filter current is forced to follow these command currents. Thus the source only provides the real power, harmonics and reactive power are provided by the active filter. Active filter has been discussed both for balanced and unbalanced loads. In the end active filter is tested for various types of non-linear loads. The active filter is found to be effective in eliminating the harmonics of the source and improving the source power factor to unity.

Contents

List of Figures

List of Tables

Chapter 1

Introduction

1.1 General

Electrical power is processed by power electronics equipments to change it from one form to other as required by consumer. These power electronics equipments are widely used in comparison to the traditional one, as they provide higher efficiency and ease of control. With the recent advances of power electronics [1], more and more innovative circuits are being developed. There are devices with high power ratings and high switching frequency, and high speed micro-electronics chips to control them. These P.E. devices have an inherent characteristic of introducing harmonics into the source, thus making the source current non-sinusoidal. These power electronics devices also consumes reactive power thus decreasing p.f of the source. Non-sinusoidal source currents have various effects [2, 3, 4].

1. Distortion in the supply as current harmonics results in voltage harmonics.

2. Malfunction of sensitive electronic equipment.

3. Increased losses.

4. Inefficient use of energy.

5. Low input power factor.

6. Devices are used at a lower value than their rating.

Traditionally passive filters were used to remove these unwanted harmonic distortions. These passive filters are the filters tuned to the frequency of the harmonics to be removed. These have several disadvantages [4, 5].

1. Large in size weight and volume.

2. As both harmonic and fundamental flow into the filter the capacity of the filter must be rated taking into account both the currents.

3. They are tuned to remove specific frequency components thus providing fixed compensation.

4. At specific frequency parallel resonance occurs between source impedance and shunt passive filter,which is so called harmonic amplification.

5. The passive filter may fall into series resonance with the power system , so that voltage distortion produces excessive harmonic currents flowing into passive filter.

Thus to overcome all these disadvantages of passive filters active filters [3, 6] are proposed. Active Power Filters (APF) injects equal and opposite harmonics into the source, thereby canceling the distortion produced by the non-linear loads and making the source current harmonic free. It is capable of producing variable frequency component, thus can filter all the higher order harmonic component of the source.

Various types of active power filters have been discussed in the literature. A shunt filter [7] is used to eliminate current harmonic. Voltage harmonic can be eliminated by using a series filter [8]. Unified power controllers [9] are also used to simultaneously eliminate both current and voltage harmonics, but they have the disadvantage of large weight and complex control. The active filter can be used with the passive filters to reduce cost and improve efficiency. These filters are known as hybrid filters [10]. Passive filters are used to reduce lower order harmonics where as higher order harmonics are eliminated by active filter.

These filters are controlled in time domain or frequency domain [3]. Compensation in frequency domain is based on the Fourier analysis of distorted voltage or current. Complex calculations are used so the time response is large. The control in time domain is based on the principle of holding instantaneous voltages and currents.

There are various control methods in time domain, (a) instantaneous 'p-q' theory [11, 12], (b) sliding mode control [13], (c) peak source current estimation [14]. The advantage of harmonic correction in time domain is that the response is fast and it is easy to implement.

The active filter currents can be controlled to follow the reference currents using a current controller. Different controllers can be used, some of the controllers discussed in the literature are (a) hysteresis current controller [15], (b) adaptive hysteresis current controller [18, 19], (c) predictive current controller [16, 17], (d) triangularization of error [20].

In this thesis a shunt active filter is used to compensate a non-linear power converter. Further a 3-level inverter [21], instead of conventional 2-level inverter, is proposed. The 3-level inverter can produce the voltage levels of $+\frac{v}{2}$, 0,$-\frac{v}{2}$, as compared to 2-level inverter which produces $+\frac{v}{2}$ and $-\frac{v}{2}$. Thus the terminal voltage waveforms have less harmonics content [21]. The other advantage is that each switch has to block the voltage equal to half the dc link voltage, so it can be used in high power applications with the same switching frequency [22]. The harmonic correction is done in time domain using peak source current estimation. The steady state and transient behavior of two current controllers, hysteresis controller and predictive controller, have been studied.

The active filter is simulated for various types of nonlinear loads. Various differential equations defining the model of load (as given in appendix) and the model of active filter (as given in chapter 3) are solved using 4^{th} order R-K method with a program made in C code. The samples of currents and voltages are taken with a time step of 1.1μsec. The FFT package is used to determine the harmonic spectrum and TDH.

1.2 Thesis Organization

Chapter 1 deals with the introduction and briefly describes the 3-level inverter and the shunt active filter. The operation of the three level voltage source inverter is studied in detail in chapter 2. Its working as a current source, using hysteresis controller and space vector modulation is simulated. In chapter 3 the shunt active filter using three level inverter is discussed. The reference current is generated using peak source current estimation. Hysteresis current controller and predictive current controller are used to control the current of the inverter. The circuits for balanced and unbalanced

loads are discussed. In the end simulation results are presented for different loads and various control strategies. In chapter 4 the thesis work is concluded with the recommendations for future work.

Chapter 2

3-Level Inverter Configuration And Its Operation

2.1 Introduction

A three level voltage source inverter [21, 22, 23] is discussed in this chapter. Its working is explained with the switching strategy. Its output in time domain and as space vector are discussed. This inverter can be changed to current controlled mode using different current controllers. Hysteresis controller [15] and space vector modulation [25, 26] are discussed in detail. In the end the inverter is simulated in the current controlled mode.

2.2 Inverter Configuration with Ideal Voltage Source

The three level inverter with neutral point clamped is shown in the fig. 2.1. It consists of 12 switches with anti-parallel diodes (4 in each leg). The dc source is divided into two parts with ground as the center point, N. The junction of two switches is connected through a diode to point, N, e.g. junction of S_{a1} and S_{a2} is connected through D_{a12}.. There are six such diodes. Use of these diodes facilitates current flow in both directions. The three phase output is provided at points a, b and c. This inverter provides three level of voltages $+\frac{V_{dc}}{2}$, 0 and $-\frac{V_{dc}}{2}$, as compared to the 2 level inverter which provides $+\frac{V_{dc}}{2}$ and $-\frac{V_{dc}}{2}$. The advantage of 3-level inverter is that high power levels can be attained with reduced harmonic content in the output voltage.

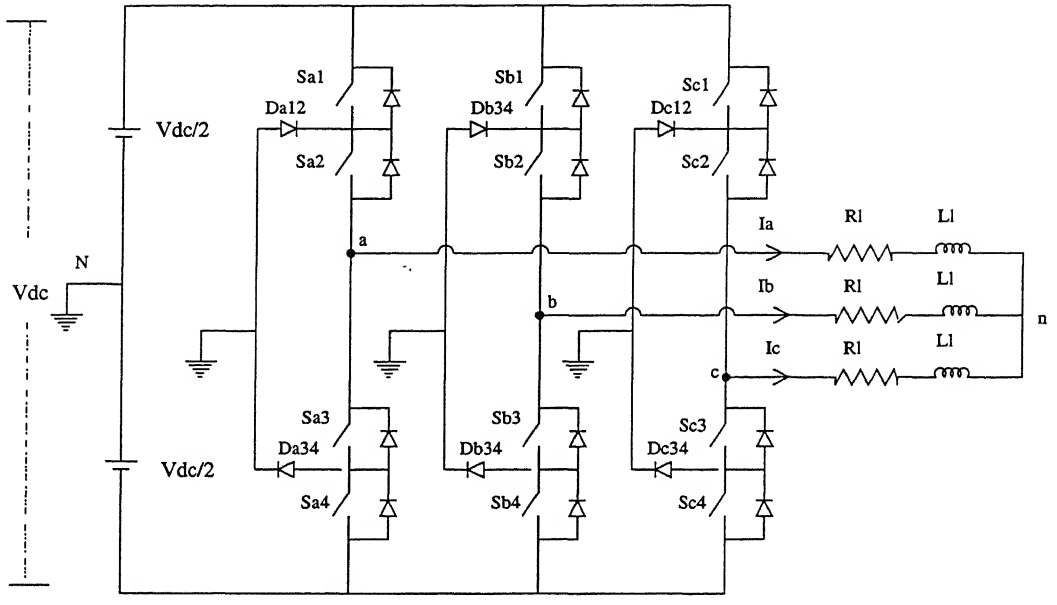

Figure 2.1: A 3-level inverter.

2.3 Switching Strategy for the Inverter Switches

The inverter provides output levels of $+\frac{V_{dc}}{2}$, 0 and $-\frac{V_{dc}}{2}$, by closing a combination of two switches in each leg. The output point 'a' can be connected to $+\frac{V_{dc}}{2}$ by closing S_{a1} and S_{a2}, to N by closing S_{a2} and S_{a3}, to $-\frac{V_{dc}}{2}$ by closing S_{a3} and S_{a4}. Similarly for other two phases. The use of diodes ensures that the output voltage level is independent of the direction of output current.

Now we can define the output states of each leg by just three switching functions, S_a, S_b, S_c instead of 12 switches. The output state of each of the three functions can be defined as '1', '0' and '-1' according to the switching state of the 12 switches, as shown in table 2:1.

Table 2.1: The inverter switching states.

$S_a = 1$	$V_{aN} = \frac{V_{dc}}{2}$	if S_{a1} and S_{a2} are on
$S_a = 0$	$V_{aN} = 0$	if S_{a2} and S_{a3} are on
$S_a = -1$	$V_{aN} = -\frac{V_{dc}}{2}$	if S_{a3} and S_{a4} are on
$S_b = 1$	$V_{bN} = \frac{V_{dc}}{2}$	if S_{b1} and S_{b2} are on
$S_b = 0$	$V_{bN} = 0$	if S_{b2} and S_{b3} are on
$S_b = -1$	$V_{bN} = -\frac{V_{dc}}{2}$	if S_{b3} and S_{b4} are on
$S_c = 1$	$V_{cN} = \frac{V_{dc}}{2}$	if S_{c1} and S_{c2} are on
$S_c = 0$	$V_{cN} = 0$	if S_{c2} and S_{c3} are on
$S_c = -1$	$V_{cN} = -\frac{V_{dc}}{2}$	if S_{c3} and S_{c4} are on

The switching strategy in table above ensures defined output voltages independent of the direction of output current.

2.4 3-level Inverter Output in Time Domain

Inverter output depends on the switching functions of the three legs. Thus output voltage can be defined in terms of the switching functions S_a, S_b, S_c and the dc voltage, V_{dc} .

The pole voltages for different switching function are

$$V_{aN} = S_a \frac{V_{dc}}{2} \tag{2.1}$$

$$V_{bN} = S_b \frac{V_{dc}}{2} \tag{2.2}$$

$$V_{cN} = S_c \frac{V_{dc}}{2} \tag{2.3}$$

Phase voltages can be written as

$$V_{an} = V_{aN} - V_{nN} \tag{2.4}$$

$$V_{bn} = V_{bN} - V_{nN} \tag{2.5}$$

$$V_{cn} = V_{cN} - V_{nN} \tag{2.6}$$

If the neutral point, n, is not grounded sum of output currents is zero. If the load is balanced this implies that $V_{an} + V_{bn} + V_{cn} = 0$. Therefore from equation 2.4, 2.5 and 2.6.

$$V_{nN} = \frac{1}{3}[V_{aN} + V_{bN} + V_{cN}] \tag{2.7}$$

Using equations 2.1 to 2.7 phase voltages can be defined as

$$V_{an} = \frac{V_{dc}}{6}[2S_a - S_b - S_c] \tag{2.8}$$

$$V_{bn} = \frac{V_{dc}}{6}[-S_a + 2S_b - S_c] \tag{2.9}$$

$$V_{cn} = \frac{V_{dc}}{6}[-S_a - S_b + 2S_c] \tag{2.10}$$

Switching states, S_a, S_b, S_c, are independent. Therefore 27 different values (of S_a, S_b, S_c) are possible. However a particular phase voltage, e.g. V_{an}, can attain only nine different values of output voltage. Of these four are +ve, four are -ve and one is zero. As comparison to 2-level inverter which can attain a total of five levels of voltages. Table 2.2 shows the pole voltages and phase voltages for all 27 values of (S_a, S_b, S_c).

Table 2.2: Pole voltages, phase voltages and voltage vector for different switching logic.

S_a	S_b	S_c	V_{aN}	V_{bN}	V_{cN}	V_{an}	V_{bn}	V_{cn}	$\|V\|$	$\angle V$	*voltage vector*
-1	-1	-1	$-\frac{V_{dc}}{2}$	$-\frac{V_{dc}}{2}$	$-\frac{V_{dc}}{2}$	0	0	0	0	0	V_0
-1	-1	0	$-\frac{V_{dc}}{2}$	$-\frac{V_{dc}}{2}$	0	$-\frac{V_{dc}}{6}$	$-\frac{V_{dc}}{6}$	$\frac{V_{dc}}{3}$	$\frac{V_{dc}}{3}$	-120	V_{19}
-1	-1	1	$-\frac{V_{dc}}{2}$	$-\frac{V_{dc}}{2}$	$\frac{V_{dc}}{2}$	$-\frac{V_{dc}}{3}$	$-\frac{V_{dc}}{3}$	$\frac{2V_{dc}}{3}$	$\frac{2V_{dc}}{3}$	-120	V_{21}
-1	0	-1	$-\frac{V_{dc}}{2}$	0	$-\frac{V_{dc}}{2}$	$-\frac{V_{dc}}{6}$	$\frac{V_{dc}}{3}$	$-\frac{V_{dc}}{6}$	$\frac{V_{dc}}{3}$	120	V_{11}
-1	0	0	$-\frac{V_{dc}}{2}$	0	0	$-\frac{V_{dc}}{3}$	$\frac{V_{dc}}{6}$	$\frac{V_{dc}}{6}$	$\frac{V_{dc}}{3}$	180	V_{15}
-1	0	1	$-\frac{V_{dc}}{2}$	0	$\frac{V_{dc}}{2}$	$-\frac{V_{dc}}{2}$	0	$\frac{V_{dc}}{2}$	$\frac{V_{dc}}{\sqrt{3}}$	-150	V_{18}
-1	1	-1	$-\frac{V_{dc}}{2}$	$\frac{V_{dc}}{2}$	$-\frac{V_{dc}}{2}$	$-\frac{V_{dc}}{3}$	$\frac{2V_{dc}}{3}$	$-\frac{V_{dc}}{3}$	$\frac{2V_{dc}}{3}$	120	V_{13}
-1	1	0	$-\frac{V_{dc}}{2}$	$\frac{V_{dc}}{2}$	0	$-\frac{V_{dc}}{2}$	$\frac{V_{dc}}{2}$	0	$\frac{V_{dc}}{\sqrt{3}}$	150	V_{14}
-1	1	1	$-\frac{V_{dc}}{2}$	$\frac{V_{dc}}{2}$	$\frac{V_{dc}}{2}$	$-\frac{2V_{dc}}{3}$	$\frac{V_{dc}}{3}$	$\frac{V_{dc}}{3}$	$\frac{2V_{dc}}{3}$	180	V_{17}
0	-1	-1	0	$-\frac{V_{dc}}{2}$	$-\frac{V_{dc}}{2}$	$\frac{V_{dc}}{3}$	$-\frac{V_{dc}}{6}$	$-\frac{V_{dc}}{6}$	$\frac{V_{dc}}{3}$	0	V_3
0	-1	0	0	$-\frac{V_{dc}}{2}$	0	$\frac{V_{dc}}{6}$	$-\frac{V_{dc}}{3}$	$\frac{V_{dc}}{6}$	$\frac{V_{dc}}{3}$	-60	V_{23}
0	-1	1	0	$-\frac{V_{dc}}{2}$	$\frac{V_{dc}}{2}$	0	$-\frac{V_{dc}}{2}$	$\frac{V_{dc}}{2}$	$\frac{V_{dc}}{\sqrt{3}}$	-90	V_{22}
0	0	-1	0	0	$-\frac{V_{dc}}{2}$	$\frac{V_{dc}}{6}$	$\frac{V_{dc}}{6}$	$-\frac{V_{dc}}{3}$	$\frac{V_{dc}}{3}$	60	V_7
0	0	0	0	0	0	0	0	0	0	0	V_1
0	0	1	0	0	$\frac{V_{dc}}{2}$	$-\frac{V_{dc}}{6}$	$-\frac{V_{dc}}{6}$	$\frac{V_{dc}}{3}$	$\frac{V_{dc}}{3}$	-120	V_{20}
0	1	-1	0	$\frac{V_{dc}}{2}$	$-\frac{V_{dc}}{2}$	0	$\frac{V_{dc}}{2}$	$-\frac{V_{dc}}{2}$	$\frac{V_{dc}}{\sqrt{3}}$	90	V_{10}
0	1	0	0	$\frac{V_{dc}}{2}$	0	$-\frac{V_{dc}}{6}$	$\frac{V_{dc}}{3}$	$-\frac{V_{dc}}{6}$	$\frac{V_{dc}}{3}$	120	V_{12}
0	1	1	0	$\frac{V_{dc}}{2}$	$\frac{V_{dc}}{2}$	$-\frac{V_{dc}}{3}$	$\frac{V_{dc}}{6}$	$\frac{V_{dc}}{6}$	$\frac{V_{dc}}{3}$	180	V_{16}
1	-1	-1	$\frac{V_{dc}}{2}$	$-\frac{V_{dc}}{2}$	$-\frac{V_{dc}}{2}$	$\frac{2V_{dc}}{3}$	$-\frac{V_{dc}}{3}$	$-\frac{V_{dc}}{3}$	$\frac{2V_{dc}}{3}$	0	V_5
1	-1	0	$\frac{V_{dc}}{2}$	$-\frac{V_{dc}}{2}$	0	$\frac{V_{dc}}{2}$	$-\frac{V_{dc}}{2}$	0	$\frac{V_{dc}}{\sqrt{3}}$	-30	V_{26}
1	-1	1	$\frac{V_{dc}}{2}$	$-\frac{V_{dc}}{2}$	$\frac{V_{dc}}{2}$	$\frac{V_{dc}}{3}$	$-\frac{2V_{dc}}{3}$	$\frac{V_{dc}}{3}$	$\frac{2V_{dc}}{3}$	-60	V_{25}
1	0	-1	$\frac{V_{dc}}{2}$	0	$-\frac{V_{dc}}{2}$	$\frac{V_{dc}}{2}$	0	$-\frac{V_{dc}}{2}$	$\frac{V_{dc}}{\sqrt{3}}$	30	V_6
1	0	0	$\frac{V_{dc}}{2}$	0	0	$\frac{V_{dc}}{3}$	$-\frac{V_{dc}}{6}$	$-\frac{V_{dc}}{6}$	$\frac{V_{dc}}{3}$	0	V_4
1	0	1	$\frac{V_{dc}}{2}$	0	$\frac{V_{dc}}{2}$	$\frac{V_{dc}}{6}$	$-\frac{V_{dc}}{3}$	$\frac{V_{dc}}{6}$	$\frac{V_{dc}}{3}$	-60	V_{24}
1	1	-1	$\frac{V_{dc}}{2}$	$\frac{V_{dc}}{2}$	$-\frac{V_{dc}}{2}$	$\frac{V_{dc}}{3}$	$\frac{V_{dc}}{3}$	$-\frac{2V_{dc}}{3}$	$\frac{2V_{dc}}{3}$	60	V_9
1	1	0	$\frac{V_{dc}}{2}$	$\frac{V_{dc}}{2}$	0	$\frac{V_{dc}}{6}$	$\frac{V_{dc}}{6}$	$-\frac{V_{dc}}{3}$	$\frac{V_{dc}}{3}$	60	V_8
1	1	1	$\frac{V_{dc}}{2}$	$\frac{V_{dc}}{2}$	$\frac{V_{dc}}{2}$	0	0	0	0	0	V_2

The inverter output pole voltages and phase voltages, for a sequence of switching functions, are shown in fig. 2.2. In this figure V_{aN} is a single pulse of 150° width. This gives rise to a non zero V_{nN}, as shown in fig. 2.2. The phase voltage V_{an}, in this case has three positive three negative and one zero level. It can be shown that if V_{aN} is square wave of 120° width instead of 150° the voltage, V_{nN}, goes to zero and phase voltage, V_{an}, has only three levels

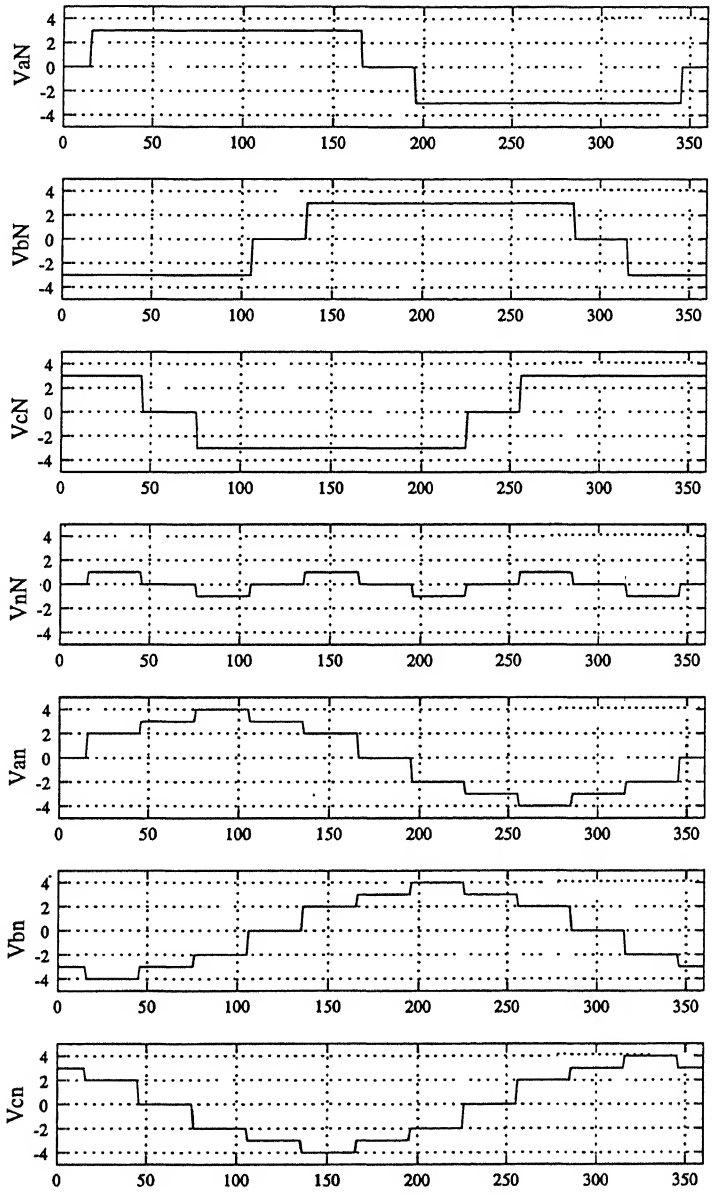

Figure 2.2: Pole voltages, neutral voltage and phase voltages for a switching combination.

2.5 Three Phase Four Wire Load

In the inverter shown in fig. 2.1, the neutral point of the load n is shown to be isolated from point N. However it is possible to physically connect the nodes n and N. For such a case the voltage V_{nN} is zero, therefore from equations 2.4, 2.5 and 2.6 the pole voltages V_{aN}, V_{bN}, V_{cN} are equal to the phase voltages V_{an}, V_{bn}, V_{cn}. The pole voltages and switching functions shown in table 2.2 are valid in this case also. The sum of line currents I_a, I_b, I_c is not zero in this case and each phase operates independently.

2.6 Inverter Output as a Voltage Vector in Complex Plane

The inverter output does not vary smoothly, but varies in steps. There are 27 (3^3) combination of switches, giving 27 possible voltage values as shown in table 2.2.

The pole voltage vector can be defined as

$$\overline{V} = \frac{2}{3}(V_{aN} + aV_{bN} + a^2V_{cN}) \tag{2.11}$$

where $a = e^{j\frac{2\pi}{3}}$.

These 27 voltage values give voltage vectors distributed at different angles in the complex plane. The voltage vectors in the complex plane are shown in fig. 2.3. Table 2.2 shows the possible combination of switches and voltage vectors.

Fig. 2.3 shows the vectors distributed in the space. These can be grouped as follows.

1. Six vectors ($V_5, V_9, V_{13}, V_{17}, V_{21}, V_{25}$) of magnitude $\frac{2V_{dc}}{3}$, are distributed in space with 60° phase difference from each other.

2. Six vectors ($V_6, V_{10}, V_{14}, V_{18}, V_{22}, V_{26}$) of magnitude $\frac{V_{dc}}{\sqrt{3}}$, distributed in space with 60° phase difference from each other and the entire group shifted by 30° from the group of vectors of magnitude $\frac{2V_{dc}}{3}$.

3. Twelve vectors ($V_3, V_4, V_7, V_8, V_{11}, V_{12}, V_{15}, V_{16}, V_{19}, V_{20}, V_{23}, V_{24}$) of magnitude $\frac{V_{dc}}{3}$, in six pairs of coincident vectors of two each, distributed in space with 60° from each other.

4. There are three zero vectors (V_0, V_1, V_2).

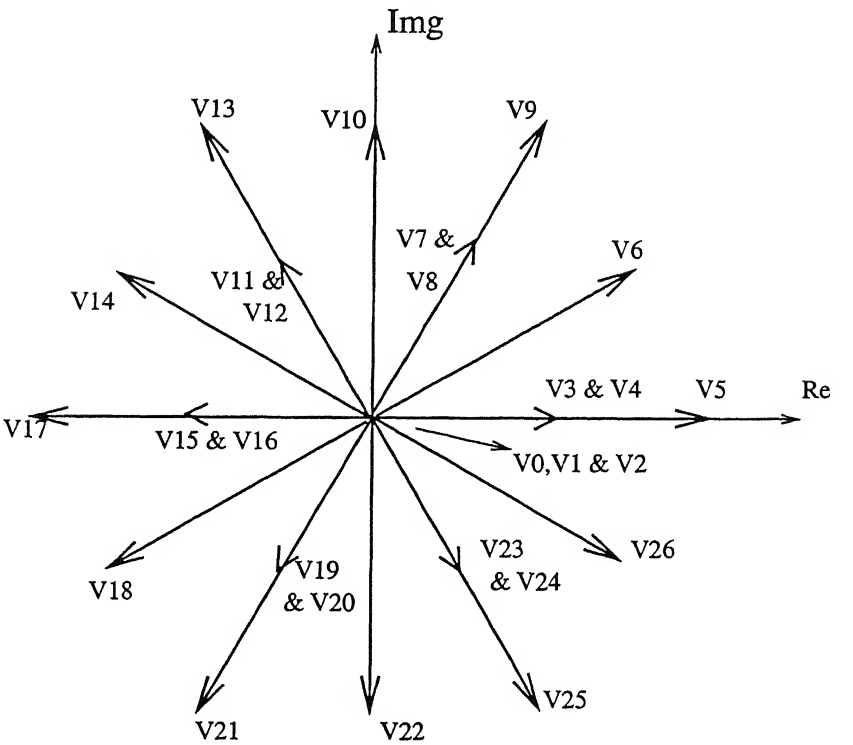

Figure 2.3: Inverter voltage vector in complex plane.

In comparison the standard 2-level inverter has only six vectors distributed in space with 60° phase difference from each other, and two zero vectors.

2.7 Operation as a Current Source Using Hysteresis Controller

This voltage source inverter can be converted to a current source by connecting a large inductor in series with each phase. Current feedback and a hysteresis controller is used to force the output current to follow a reference current waveform by changing the output voltage. Here the three phases are controlled independently and in each phase a reference current, e.g. I_{aref}, is set, and the corresponding inverter output current, e.g. I_a, is forced to follow the reference current. A hysteresis window, h_w, is created around the reference current and the current is regulated to be within the boundary of this window. The switching logic for phase 'a' is as follows [27].

1. If $I_a > I_{aref} + \frac{h_w}{2}$ decrease the output voltage by changing switching function S_a to the next lower level, i.e. if S_a is '1' switch it to '0' and if it is '0' switch it

to $'-1'$.

2. If $I_a < I_{aref} - \frac{h_w}{2}$ increase the output voltage by changing switching function S_a to the next higher level, i.e. if S_a is $'-1'$ switch it to $'0'$ and if it is $'0'$ switch it to $'1'$.

3. If $I_{aref} + \frac{h_w}{2} > I_a > I_{aref} - \frac{h_w}{2}$ the output voltage and the switching function S_a is not changed.

Similar logic can be applied to phases 'b' and 'c'. Thus the current follows the reference current with a peak to peak ripple of h_w.

2.7.1 Method of Simulation

The inverter is simulated for R-L load shown in the fig. 2.1. The circuit can be modeled by the following differential equations.

$$V_{an} = L_l \frac{dI_a}{dt} + R_l I_a \tag{2.12}$$

$$V_{bn} = L_l \frac{dI_b}{dt} + R_l I_b \tag{2.13}$$

$$V_{cn} = L_l \frac{dI_c}{dt} + R_l I_c \tag{2.14}$$

Where V_{an}, V_{bn}, V_{cn} are the inverter phase voltages, and their magnitude depends upon the switching function, as defined in equations 2.8, 2.9 and 2.10.

To act as a current source, inverter current should follow a given reference current. The reference currents for each phases can be given as.

$$I_a^* = I_{sm} \sin(\omega t) \tag{2.15}$$

$$I_b^* = I_{sm} \sin\left(\omega t - \frac{2\pi}{3}\right) \tag{2.16}$$

$$I_c^* = I_{sm} \sin\left(\omega t + \frac{2\pi}{3}\right) \tag{2.17}$$

Now the circuit is simulated with $R = 2\Omega$, $L = .008H$, $V_{dc} = 100V$ and $I_{sm} = 5A$, Max $f = 10khz$.

The inverter currents I_a, I_b, I_c are compared with the reference currents I_a^*, I_b^*, I_c^* respectively. Hysteresis controller is applied, as given in section 2.7, and the values

of switching functions are generated. The values of inverter currents I_a, I_b, I_c at the next sampling instant are calculated by solving the differential equations 2.12, 2.13 and 2.14.

2.7.2 Results

Fig. 2.4(a) shows the current in phase 'a' with the hysteresis band of .5 amp. and a reference current of 5 amps. Thus it can be seen that the current follows the reference within the boundary of hysteresis band. The currents in other phases are similar. Fig. 2.4(b) shows the inverter phase voltage, V_{an}. Thus it is clearly seen that the frequency is not constant.

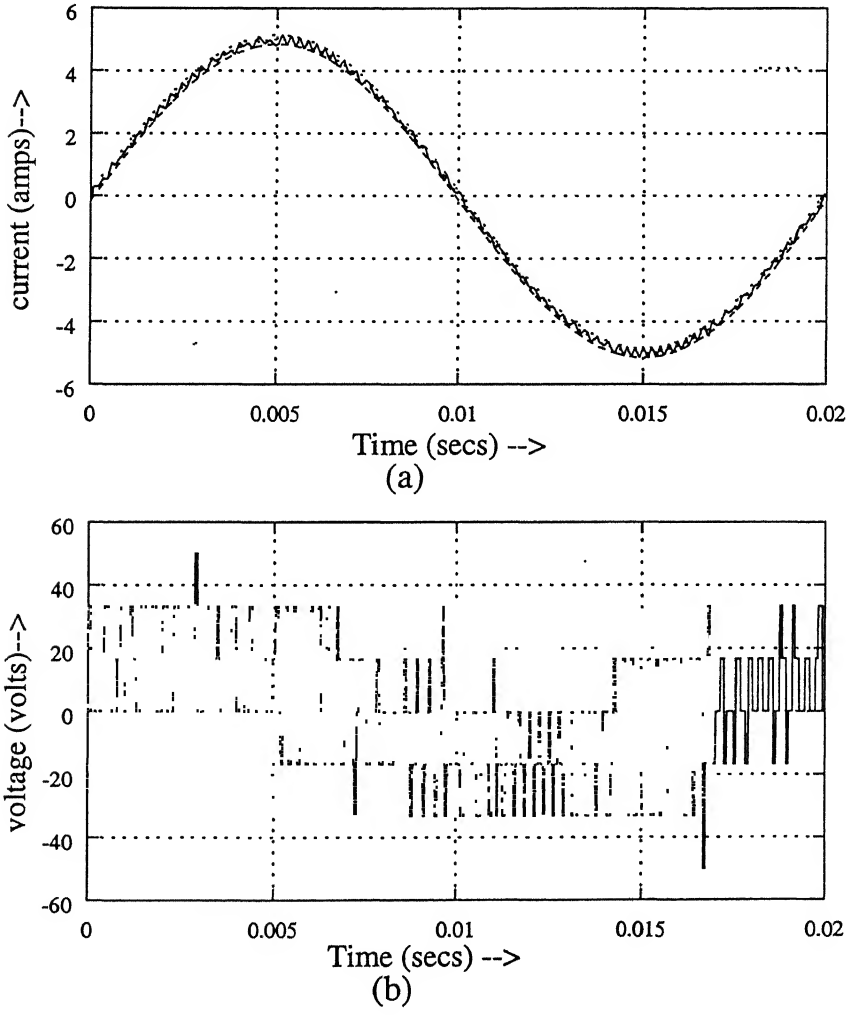

Figure 2.4: (a) Phase 'a' current (b) phase 'a' voltage, using hysteresis controller.

2.8 Operation as a Current Source Using Space Vector Modulation for Voltage Control

Space vector PWM is based on the space vector representation of voltages in the complex plane. The inverter output is represented by 27 voltage vectors as shown in the fig. 2.3 and as discussed earlier. The modulation is based on the selection of the best vector or the combination of the vectors to give the required voltage. Thus in this scheme all the three phases are not controlled independently. There is one and only one best switching combination to obtain the required voltage. Various modulation schemes of three level inverter are given in the literature [22, 28] but here a simple approach is applied as explained below.

A reference current vector, $\overline{I_{ref}}$, is set and the inverter output current vector, $\overline{I}$, is calculated using the currents, I_a, I_b, I_c which are sampled at a constant rate, $\frac{1}{T}$.

$$\overline{I} = \frac{2}{3}(I_a + aI_b + a^2I_c) \tag{2.18}$$

This current is forced to follow $\overline{I_{ref}}$.

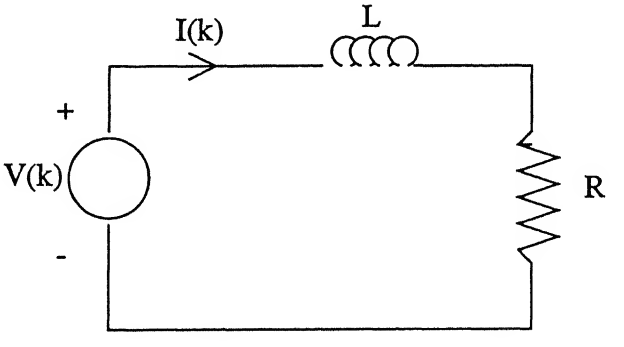

Figure 2.5: The equivalent two phase model.

The equivalent of three phase circuit shown in fig. 2.1, can be represented by a vector equivalent circuit as shown in fig. 2.5. It can be represented by a single equation.

$$\overline{V}(k) = \frac{Ld\overline{I}(k)}{dt} + R\overline{I}(K) \tag{2.19}$$

$\overline{V}(k)$ and $\overline{I}(k)$ are the inverter voltage vector and the inverter current vector at the k^{th} sampling instant. $\overline{V}(k)$, is the required voltage vector that would make the

current error vector ($\overline{I_{ref}}$ - $\overline{I}$) zero. Equation 2.19 can be simplified as.

$$\overline{V}(k) = \frac{L}{T}[\overline{I_{ref}}(k+1) - \overline{I}(k)] + R\overline{I}(k) \tag{2.20}$$

$\overline{V}(k)$, is the voltage vector required, at the kth sampling instant, that forces the current vector to attain the reference current vector $\overline{I_{ref}}(k+1)$ at the next sampling instant.

Space vector modulation is applied to get the required voltage vector $\overline{V}$, as a combination of two inverter voltage vectors. The selection of inverter voltage vectors depends on the magnitude and angle of required voltage vector, $\overline{V}$, as explained below.

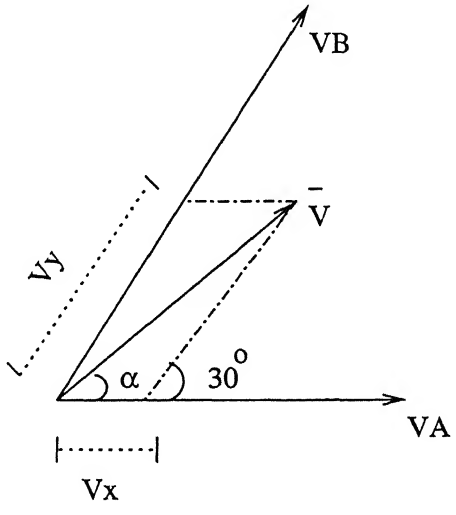

Figure 2.6: Components of voltage vector $\overline{V}$ in the direction $\overline{V_A}$ and $\overline{V_B}$.

Angle, α, and the two inverter voltage vectors, $\overline{V_A}$ and $\overline{V_B}$, between which the voltage vector, $\overline{V}$, lie are found, as shown in fig. 2.6. The conduction times T_A for vector $\overline{V_A}$, T_B for vector $\overline{V_B}$ and T_C for zero vector are calculated, that would approximate the total vector, $\overline{V}$, on an average, during the sampling time T.

$$\overline{V} = \frac{T_A\overline{V_A} + T_B\overline{V_B}}{T} \tag{2.21}$$

Let $\overline{V_x}$ and $\overline{V_y}$ be the components of $\overline{V}$ in the direction of vectors $\overline{V_A}$ and $\overline{V_B}$ respectively, as shown in the fig. 2.6, therefore

$$\overline{V} = \overline{V_x} + \overline{V_y} \tag{2.22}$$

Magnitudes V_x and V_y can be calculated as.

$$V_y = 2\left|\overline{V}\right| \sin\alpha \tag{2.23}$$

$$V_x = \left|\overline{V}\right| \cos\alpha - \frac{\sqrt{3}}{2} V_y \tag{2.24}$$

Thus from equations 2.21 and 2.22.

$$T_A = \frac{V_x}{V_A} T \tag{2.25}$$

$$T_B = \frac{V_y}{V_B} T \tag{2.26}$$

$$T_c = T - T_A - T_B \tag{2.27}$$

The above result can be directly applied to approximation of $\overline{V}$ by inverter vectors in fig. 2.6. However there are multiple vectors in the same direction, e.g. $\overline{V_3}$, $\overline{V_4}$ and $\overline{V_5}$. The selection of appropriate vector can be done by following criteria.

1. The time $T_A + T_B$ should be less than or equal to the sampling time T.
2. The switching of devices in the inverter should be minimum.

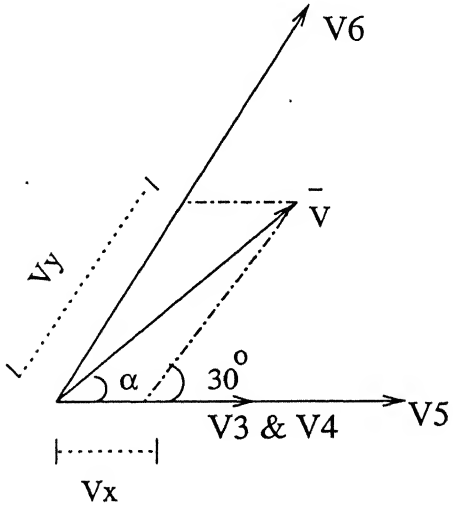

Figure 2.7: Components voltage vector of $\overline{V}$ in the direction V_5 and V_6.

For e.g. The vector lies in between $\overline{V_5}$ and $\overline{V_6}$, as shown in fig. 2.7. There are two more vectors, $\overline{V_3}$ and $\overline{V_4}$, in the direction of $\overline{V_5}$, so only one of these is to be selected.

$\overline{V_x}$ and $\overline{V_y}$ are the components of vector $\overline{V}$ in the direction of $\overline{V_5}$ and $\overline{V_6}$ respectively. Their magnitudes are calculated similarly from the equations 2.23 and 2.24, T_A, T_B and T_C are calculated as.

$$T_A = \frac{V_x}{|\overline{V_3}|}T \tag{2.28}$$

$$T_B = \frac{V_y}{|\overline{V_6}|}T \tag{2.29}$$

$$T_c = T - T_A - T_B \tag{2.30}$$

If $T_A + T_B < T$, $\overline{V_3}$ or $\overline{V_4}$ is to be selected.

If $T_A + T_B > T$, $\overline{V_5}$ is selected, T_B remains the same but T_A is recalculated as.

$$T_A = \frac{V_x}{|\overline{V_5}|}T \tag{2.31}$$

$$T_C = T - T_A - T_B \tag{2.32}$$

$\overline{V_3}$ and $\overline{V_4}$ are equal vectors, so the state corresponding to any of them can be selected. The choice depends upon the minimum switching required to move to the vector $\overline{V_6}$.

Thus for the time T_A, the switching states corresponding to $\overline{V_3}$,$\overline{V_4}$ or $\overline{V_5}$ (as selected from above) is applied to the inverter, for time T_B, switching states corresponding to $\overline{V_6}$ is applied to the inverter and zero state is applied for the time T_C. There are three zero states, the one which requires the minimum switching to come to the zero state is selected.

2.8.1 Method of Simulation

The circuit is simulated with the same parameters as in section 2.7.1, and three phase currents are to be calculated using the differential equations 2.12, 2.13 and 2.14 but this requires the knowledge of switching states. The inverter current vector $\overline{I}$ is calculated using equation 2.18 from samples at k^{th} sampling instant. The reference currents I_a^*, I_b^*, I_c^* are set as in section 2.7.1 and the reference current vector, $\overline{I_{ref}^*}(k+1)$ at the $(k+1)^{th}$ sampling instant is calculated using the vector transformation i.e, $\overline{I_{ref}^*} = I_a^* + aI_b^* + a^2I_c^*$. The voltage vector $\overline{V}(k)$ required to force this inverter current vector $\overline{I}(k)$ to the reference current vector $\overline{I_{ref}^*}(k+1)$ is calculated using the equation 2.20. The voltage vector $\overline{V}(k)$ is realized using space vector modulation. Thus the

times T_A, T_B, T_c and the corresponding inverter switching states are generated as explained above. These are utilized to solve the differential equations 2.12, 2.13 and 2.14.

2.8.2 Results

Fig. 2.8(a) shows the current in phase 'a'. Fig. 2.8(b) shows the inverter phase voltage, V_{an}. Thus it is seen that both the current and voltage waveforms are smoother, as compared to the hysteresis controller and the switching frequency is constant.

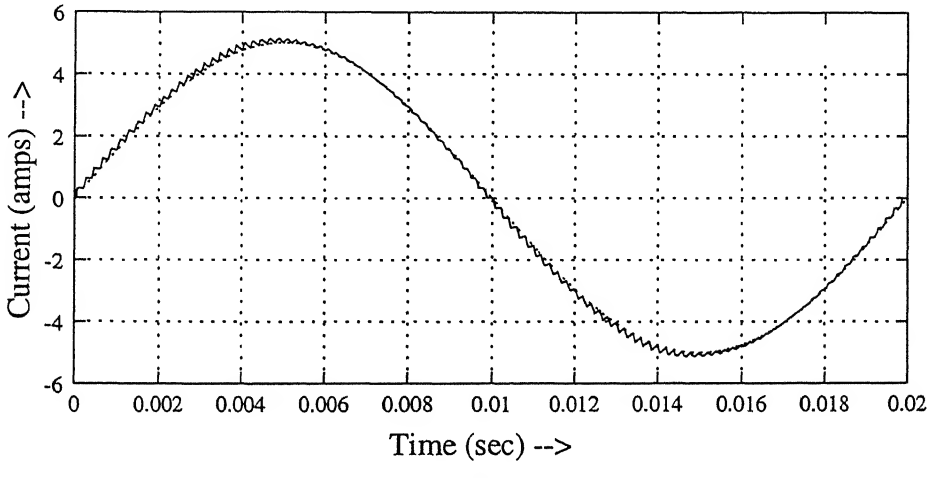

(a)

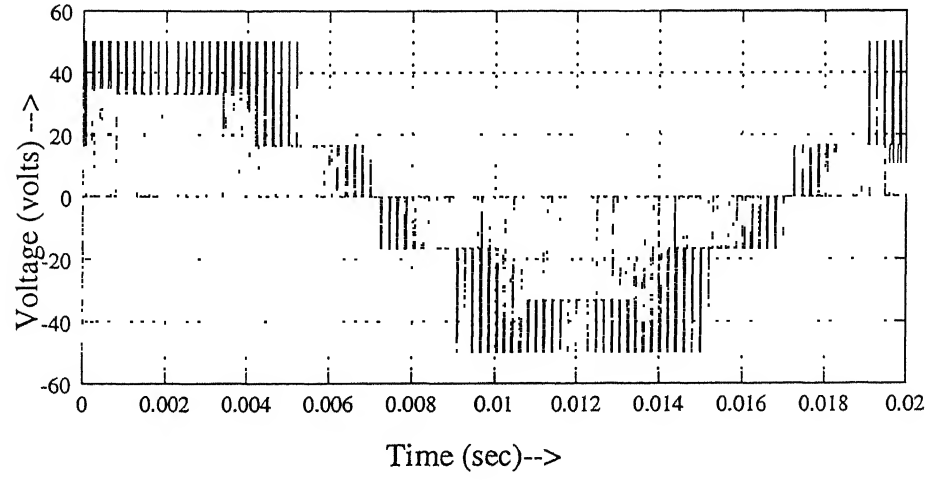

(b)

Figure 2.8: (a) Phase 'a' current (b) phase 'a' voltage, using space vector modulation.

2.9 Conclusion

In three level inverter the switches with lower voltage rating can be used as each switch has to block the voltage equal to half the dc link voltage. Thus low rating and high frequency switches can be used to reduce harmonics. Using the current controllers, 3-level voltage source inverter can be made to act as as current source. Simulation results given above show that, using either hysteresis controller or space vector modulation, the inverter current can be made to follow a 50hz sinusoidal reference current. The bandwidth of the inverter depends upon the value of the load inductance L_l (fig. 2.1).

Chapter 3

3-level Inverter As An Active Filter

3.1 Introduction

In this chapter a detailed study and simulation of active power filter as a compensator for nonlinear loads is is presented. The three level inverter is used as an active power filter for nonlinear loads. The reference currents for the active filter are calculated using the peak source current estimation [14]. The inverter current is forced to follow this reference current using different current controllers. Two controllers, hysteresis current controller [15] and predictive current controller [16, 17] are discussed. The active filter, with the neutral connected to the ground, is also discussed as the compensator for unbalanced loads. Both the compensators are simulated for steady state and transient conditions to prove the validity of the compensators.

3.2 Principle of Active Filter

The basic system for load compensation is shown in fig. 3.1. Active filter consists of a voltage source inverter with a dc capacitor. As the load may be non-linear, the currents I_{la}, I_{lb} and I_{lc} will contain higher order harmonics in addition to the fundamental component. If the source is to provide for these harmonics, the source current also becomes non-sinusoidal. The purpose of active filter is to provide the necessary currents I_{ca}, I_{cb}, I_{cc}, to make the source currents I_{sa}, I_{sb}, I_{sc} sinusoidal and in phase with the corresponding phase voltages. Thus basically active filter is a harmonic generator, which generates the harmonics required by the load.

The load currents I_{la}, I_{lb}, I_{lc} are sensed and the currents to be supplied by the active filter are calculated using an algorithm given in section 3.4.1. These are the

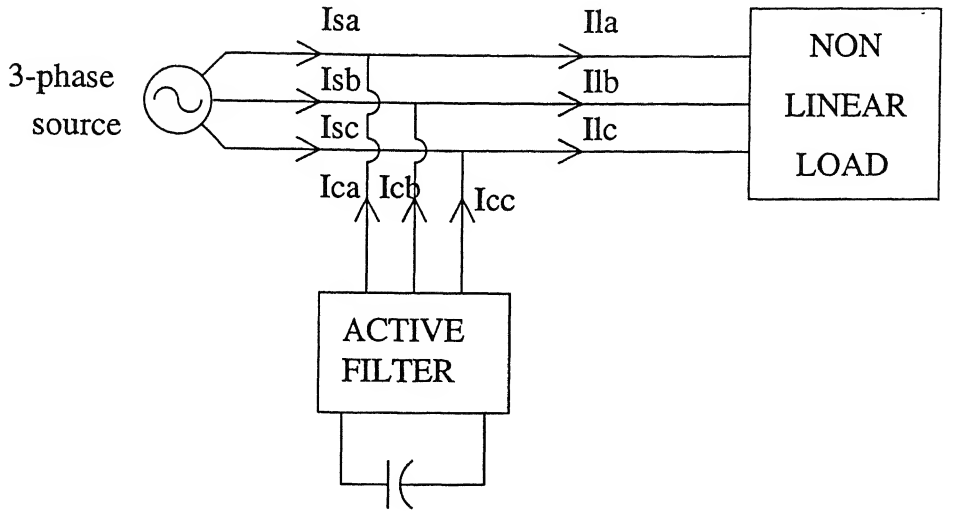

Figure 3.1: Basic compensating system.

reference currents to be generated by the active filter. The active filter is a voltage source inverter operated in the current controlled mode. The output currents of the active filter are controlled to follow these reference currents, using various controllers. Thus with this control structure active filter meets the demand of harmonic and reactive power of the load.

3.3 Active Filter as Compensator for Non-linear Loads

The 3-level inverter as active filter is shown in fig. 3.2. It consists of a dc capacitor instead of the usual battery on the dc side and a large inductor on the ac side. Active filter is to supply only for the harmonics and the reactive power demand of load. The average power drawn or supplied by the inverter is to be zero, so dc battery is not necessary. Only a small capacitor with minimum energy storage is sufficient.

There are two control loops in the active filter. The inner current control loop ensures that the current supplied by the inverter follows the reference current calculated from the samples of load current. The dc capacitor voltage is regulated by an outer voltage control loop, which ensures the transfer of sufficient real power from the ac source to compensate for the inverter losses and to maintain the dc voltage across the capacitor equal to a reference value.

The inverter is modeled by the following differential equations.

$$V_{sa} = -L\frac{dI_{ca}}{dt} - RI_{ca} + V_{an} \tag{3.1}$$

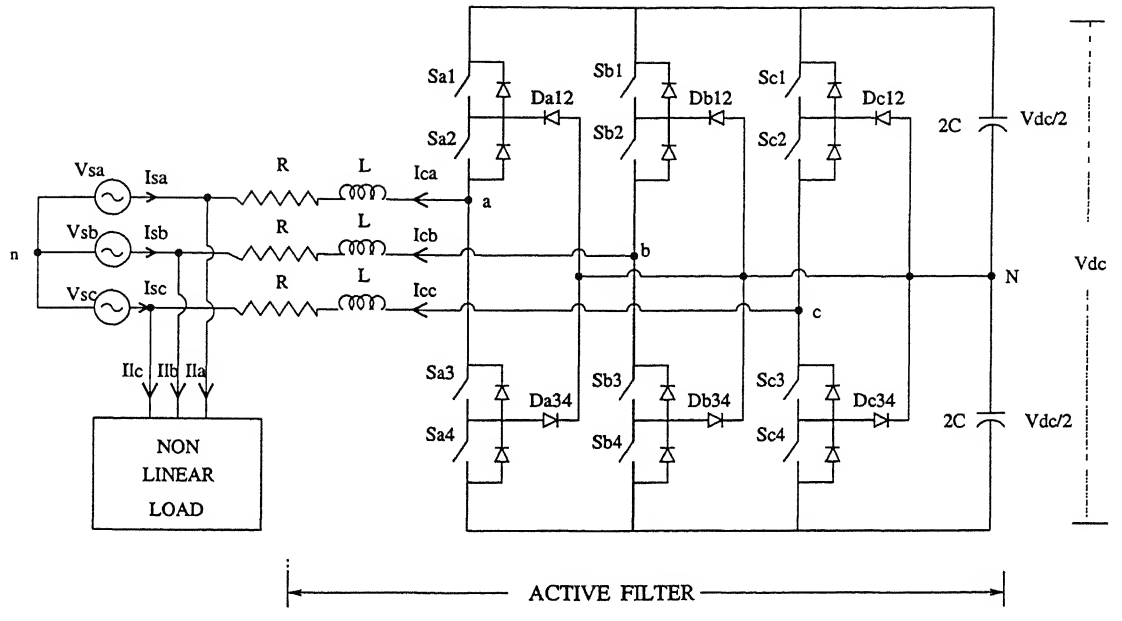

Figure 3.2: 3-level inverter as an active filter.

$$V_{sb} = -L\frac{dI_{cb}}{dt} - RI_{cb} + V_{bn} \tag{3.2}$$

$$V_{sc} = -L\frac{dI_{cc}}{dt} - RI_{cc} + V_{cn} \tag{3.3}$$

$$C\frac{dV_{dc}}{dt} = -\left(S_a I_{ca} + S_b I_{cb} + S_c I_{cc}\right)/2 \tag{3.4}$$

where

$$V_{sa} = V_{sm}\sin\left(\omega t\right) \tag{3.5}$$

$$V_{sb} = V_{sm}\sin\left(\omega t - \frac{2\pi}{3}\right) \tag{3.6}$$

$$V_{sc} = V_{sm}\sin\left(\omega t + \frac{2\pi}{3}\right) \tag{3.7}$$

I_{ca}, I_{cb}, I_{cc} are the currents from the inverter, and S_a, S_b, S_c are the switching functions which depends upon the switches S_{ai}, S_{bi}, S_{ci} Where $i = 1, 2, 3, 4$. The operation of inverter and the switching functions have been defined in detail in section 2.3.

The switches in one leg are fired in such a manner that either S_{a1} is on or S_{a3} is on and either S_{a2} is on or S_{a4} is on, thus giving total four conditions. Here we have

three voltage level in each leg +v , 0 And -v.

S_a , S_b , S_c are defined as in table 3.1

Table 3.1: The switching logic.

$S_a = 1$	if $S_{a1}$and S_{a2} are on
$S_a = 0$	if $S_{a2}$and S_{a3} are on
$S_a = -1$	if $S_{a3}$and S_{a4} are on
$S_b = 1$	if $S_{b1}$and S_{b2} are on
$S_b = 0$	if $S_{b2}$and S_{b3} are on
$S_b = -1$	if $S_{b3}$and S_{b4} are on
$S_c = 1$	if $S_{c1}$and S_{c2} are on
$S_c = 0$	if $S_{c2}$and S_{c3} are on
$S_c = -1$	if $S_{c3}$and S_{c4} are on

V_{an}, V_{bn}, V_{cn} are the 3-phase PWM voltages reflected on the AC side of the active filter and are expressed in terms of the instantaneous dc bus voltages and switching function, as given in section 2.4, as follows.

$$V_{an} = \frac{V_{dc}}{6}(2S_a - S_b - S_c) \tag{3.8}$$

$$V_{bn} = \frac{V_{dc}}{6}(-S_a + 2S_b - S_c) \tag{3.9}$$

$$V_{cn} = \frac{V_{dc}}{6}(-S_a - S_b + 2S_c) \tag{3.10}$$

3.4 The Control Circuit

It is the heart of AF and has three stages.

1. Sensors for the essential voltages and currents.

2. Reference current generation - It is the command current which inverter should generate so as to make the source current sinusoidal and in phase with the voltage.

3. The current controller - It should control the current so that the current follows the command current. It basically generates the signals for the inverter circuit.

3.4.1 Reference Current Generation

The calculation of the reference current is very important as this is the current which has to be supplied by the active filter to make the source current sinusoidal. The AC source has to supply only the fundamental component of the load current and some additional current which accounts for the losses in the inverter. The additional current is required to maintain the capacitor voltage constant under conditions of varying load.

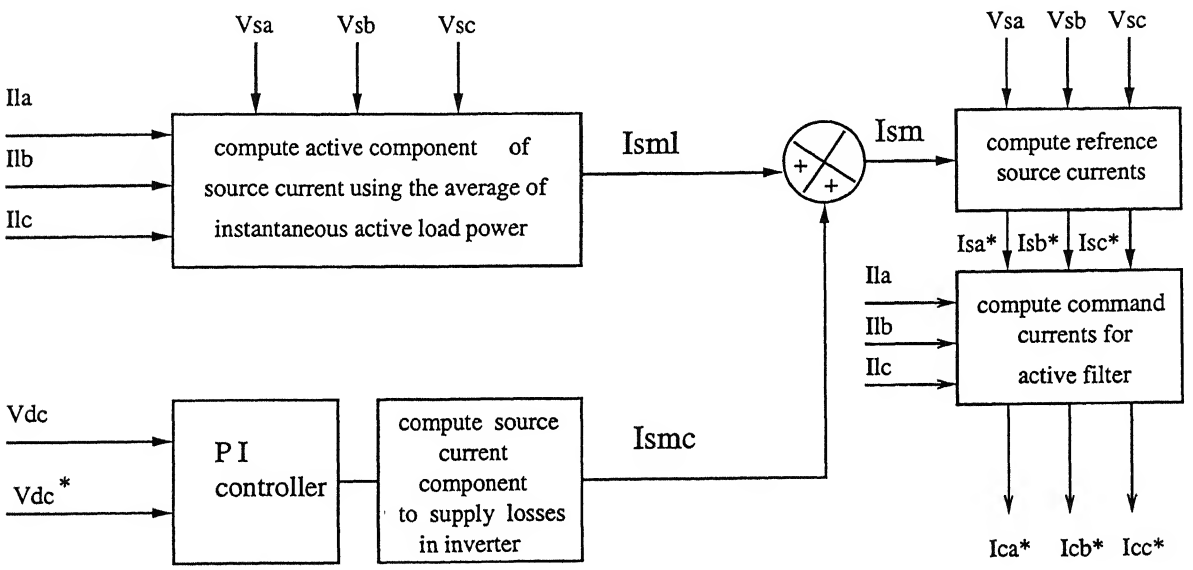

Figure 3.3: Block diagram for reference current generation.

Reference currents are calculated in the time domain with the peak source current estimation I_{sm} [14]. It has two component I_{sml} and I_{smc}. The block diagram is shown in fig. 3.3.

I_{sml} is the peak of the fundamental component of load current and is calculated using the average active power of the load.

$$P_l = V_{sa}I_{la} + V_{sb}I_{lb} + V_{sc}I_{lc} \tag{3.11}$$

where I_{la} , I_{lb}, I_{lc} are the load currents

The waveform of P_l is averaged over a suitable period of the supply frequency to get the average power, P_{av}. The averaging period is dependent on the nature of the load. For any balanced linear load the value of P_l is constant. Therefore an averaging period of half cycle (10 ms) is adequate. For non-linear loads a smaller value needs

to be used. For three phase rectifier load the waveform of power has a 300 Hz ripple, Therefore an averaging period of one-sixth of a cycle is used.

The peak value of source current is given by.

$$I_{sml} = \frac{2P_{av}}{3V_{sm}} \tag{3.12}$$

Second component I_{smc}, which is the magnitude of the fundamental current accounting for the losses in the active filter, is calculated using the outer voltage control loop. The DC capacitor voltage V_{dc} is measured and is subtracted from the reference voltage V_{dc}^*. The error voltage $(V_{dc}^* - V_{dc})$ is fed into the PI controller. The output u of the PI controller is also averaged over the same period as that used for calculation of the average power, P_{av}. This output signal, u_{av}, is added to the value of P_{av} to obtain additional power to compensate losses in the inverter. Thus

$$I_{smc} = \frac{2u_{av}}{3V_{sm}} \tag{3.13}$$

and total peak source current is.

$$I_{sm} = I_{sml} + I_{smc} \tag{3.14}$$

For unity power factor source current, the current should be in phase with the respective voltage. So the reference three phase currents should be.

$$I_{sa}^* = I_{sm}\frac{V_{sa}}{V_{sm}} \tag{3.15}$$

$$I_{sb}^* = I_{sm}\frac{V_{sb}}{V_{sm}} \tag{3.16}$$

$$I_{sc}^* = I_{sm}\frac{V_{sc}}{V_{sm}} \tag{3.17}$$

The three phase A.F. currents are.

$$I_{ca}^* = I_{la} - I_{sa}^* \tag{3.18}$$

$$I_{cb}^* = I_{lb} - I_{sb}^* \tag{3.19}$$

$$I_{cc}^* = I_{lc} - I_{sc}^* \tag{3.20}$$

Now using the current controller the active filter current is forced to track the reference current to ensure that the source current is sinusoidal and in phase of the source voltage.

3.4.2 Current Controller

Function of the current controller, is to give the switching logic to the inverter so that the current given by inverter is equal to the reference current. Thus it basically generates the switching logic for the three switching functions, S_a, S_b, S_c. Various current controllers have been discussed in literature. Two controller, hysteresis current controller and predictive current controller, are discussed here in detail.

3.4.2.1 Hysteresis current controller

Hysteresis current controller is very simple to implement without any complex calculations, but has a drawback that the switching frequency is not constant and the ripple may be high in steady state although it provides fast transient response.

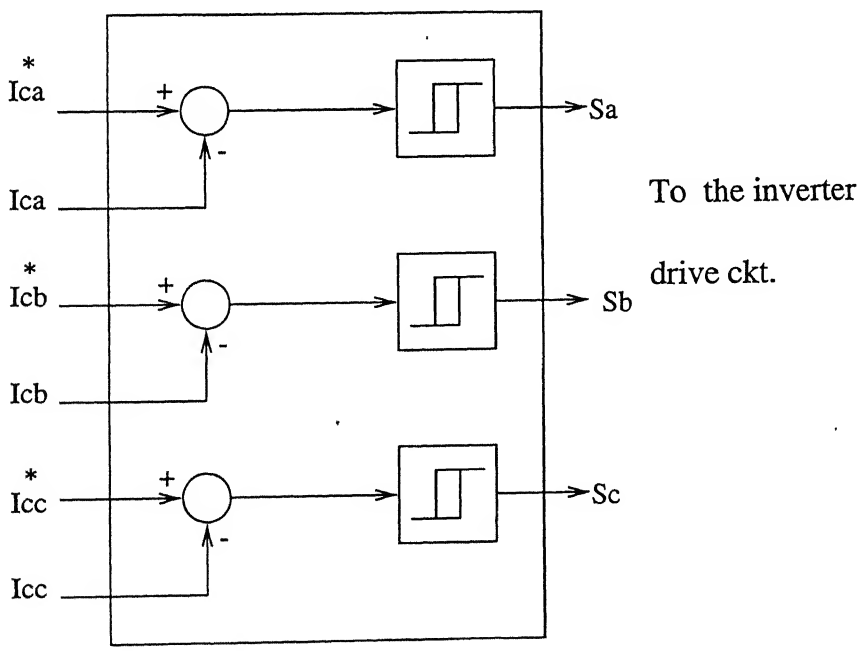

Figure 3.4: Hysteresis current controller.

A typical hysteresis controller is shown in the fig. 3.4. Each controller controls the current in each phase. There are three switching level for each leg '1', '0' and $'-1'$. The switching logic is simple. A hysteresis window, h_w, is created around the

reference current, and current error, ϵ_a, ϵ_b and ϵ_c can be defined as $\epsilon_a = I^*_{ca} - I_{ca}$, $\epsilon_b = I^*_{cb} - I_{cb}$, $\epsilon_c = I^*_{cc} - I_{cc}$. Now the switching logic for phase 'a' can be defined as.

1. If $\epsilon_a > \frac{h_w}{2}$ increase the switching function, S_a, to the next higher level, i.e. if it is $'-1'$ switch it to '0' and if it is '0' switch it to '1'.

2. If $\epsilon_a < -\frac{h_w}{2}$ decreases the switching function, S_a, to the next lower level, i.e. if it is '1' switch it to '0' and if it is '0' switch it to $'-1'$.

3. If $\frac{h_w}{2} > \epsilon_a > -\frac{h_w}{2}$ the switching function, S_a, is not changed.

The same logic is applied for switching functions S_b and S_c in phases 'b' and 'c' respectively.

3.4.2.2 Predictive Current Controller

Predictive controller produces smooth current with constant switching frequency. In predictive current controller the reference currents at the next sampling instant are predicted and the inverter currents are forced to follow these predicted currents. Thus the inverter currents become equal to the reference currents in the next sampling instant. Reference currents are non-sinusoidal, so these cannot be predicted easily. The currents at the next sampling instant are predicted using the samples of currents in the previous instants. The controller is shown in the fig. 3.5. The various methods

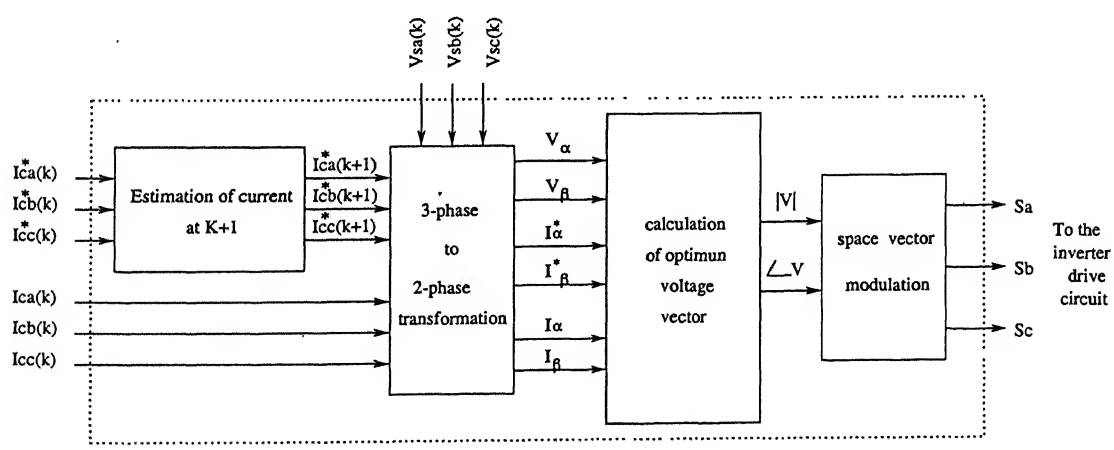

Figure 3.5: The predictive controller.

of predicting the currents are discussed below.

1. Predicting the current with a delay of one cycle. - This method can be used if the load is constant, i.e. the current waveform is similar in each cycle. The samples of currents are taken and used for the next cycle. The current $I^*(k+1)$ of the previous cycle is used as $I^*(k+1)$ for the present cycle. This works only in steady state, if the current changes in each cycle this cannot be used.

2. Predicting the currents with a delay of one sampling time. - The reference current $I^*(k)$ in the k^{th} sampling instant is known. The inverter current $I(k-1)$, in the previous $(k-1)^{th}$ sampling instant, is forced to follow the this reference current $I^*(k)$ instead of the reference current, $I^*(k+1)$ in the $(k+1)^{th}$ sampling instant. Thus the inverter current lags the reference current by one sampling time T. If rate of change of reference current is high then the inverter current will have spikes.

3. Predicting current using the samples of current in last two sampling instants. - The current at $(k+1)^{th}$ sampling instant is estimated using the samples of current at k^{th} and $(k-1)^{th}$ sampling instants. As the sampling time is small the current at $(k-1)^{th}$, $(k)^{th}$ and $(k+1)^{th}$ can be fairly assumed to be in a straight line. Thus the current $I^*(k+1)$ can be estimated using $I^*(k-1)$ and $I^*(k)$.

The control scheme

In this scheme current vector is controlled using a unique controller instead of three controllers. The concept of space voltage vector is used. The inverter voltage vector $\overline{V}$, source voltage vector $\overline{V_s}$, inverter current vector $\overline{I}$ and the reference current vector $\overline{I^*}$, can be defined in terms of respective three phase quantities as follows

$$\overline{V} = \frac{2}{3}\left(V_{an} + aV_{bn} + a^2V_{cn}\right) \tag{3.21}$$

$$\overline{V_s} = \frac{2}{3}\left(V_{sa} + aV_{sb} + a^2V_{sc}\right) \tag{3.22}$$

$$\overline{I} = \frac{2}{3}\left(I_{ca} + aI_{cb} + a^2I_{cc}\right) \tag{3.23}$$

$$\overline{I^*} = \frac{2}{3}\left(I^*_{ca} + aI^*_{cb} + a^2I^*_{cc}\right) \tag{3.24}$$

where $a = e^{j\frac{2\pi}{3}}$.

Inverter conduction state is represented by three logic variables, S_a, S_b, S_c, as defined in section 2.3. For the different combination of these three switches there are 27 operating states and there are 27 voltage space vectors as shown in the table 2.3 and fig 3.6.

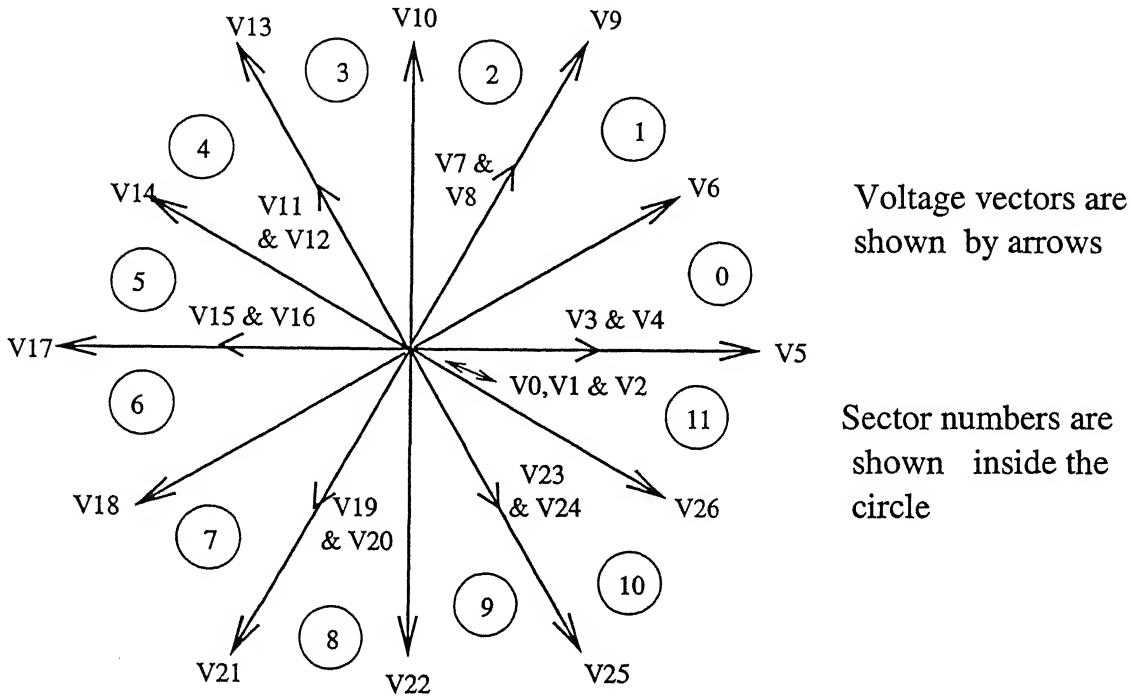

Figure 3.6: The inverter voltage vector.

Predictive current controller selects the best combination from these 27 vectors so that the voltage of the inverter forces the error current vector, $\Delta i = \overline{I^*} - \overline{I}$, zero. The current is sampled with the sampling time T. The current vector $\overline{I}$ is calculated and compared with the reference vector $\overline{I^*}$. The appropriate voltage vector, $\overline{V}$ is calculated that would make the error current vector to zero .

$$\overline{V}(k) = \overline{V_s}(k) + L\frac{d\overline{I}(k)}{dt} + R\overline{I}(k) \tag{3.25}$$

or

$$\overline{V}(k) = \overline{V_s}(k) + \frac{L}{T}\left[\overline{I^*}(k+1) - \overline{I}(k)\right] + R\overline{I}(k) \tag{3.26}$$

This calculation is essentially based on the difference between the actual current $\overline{I}(k)$ at k^{th} sampling instant and the reference current vector $\overline{I^*}(k+1)$ at the next sampling instant. $\overline{V_s}(k)$ is the source voltage vector, $\overline{V}(k)$ is the inverter voltage

vector, T is the sampling interval, R and L are the active filter parameters.

$\overline{V}(k)$ can be expressed in real and imaginary parts.

$$Re[\overline{V}(k)] = V_{sa}(k) + \frac{L}{T}[I^*_{ca}(k+1) - I_{ca}(k)] + RI_{ca}(K) \tag{3.27}$$

$$Im[\overline{V}(k)] = \frac{1}{\sqrt{3}}[V_{sa}(k) + 2V_{sb}(k)] + \frac{L}{\sqrt{3}T}[I^*_{ca}(k+1) + 2I^*_{cb}(k+1) - I_{ca}(k) - 2I_{cb}(k)] +$$

$$\frac{1}{\sqrt{3}}R[I_{ca}(k) + 2I_{lb}(k)] \tag{3.28}$$

$$\left|\overline{V}(k)\right| = \sqrt{(Re[\overline{V}(k)])^2 + (Im[\overline{V}(k)])^2} \tag{3.29}$$

$$\angle\overline{V}(k) = arctg[\frac{Im[\overline{V}(k)]}{Re[\overline{V}(k)]}] \tag{3.30}$$

The voltage vector $\overline{V}(k)$ lies in one of the sectors as shown in the fig. 3.6. To obtain the required vector, the conduction time of the inverter switches are modulated according to the amplitude and the angle of $\overline{V}(k)$.

$$\alpha = \angle\overline{V}(k) - (n-1)\frac{\pi}{6} \tag{3.31}$$

Where n is the sector number as identified in fig. 3.6 and α is the modulation angle shown fig. 3.7. The inverter is switched from one active vector to the other active vector with the duty cycle determined by the values of vectors $\overline{V_x}$ and $\overline{V_y}$. Referring the fig. 3.7, V_x and V_y can be calculated as

$$V_y = \frac{2}{\sqrt{3}}\left|\overline{V}(k)\right|\sin\alpha \tag{3.32}$$

$$V_x = \left|\overline{V}(k)\right|\cos\alpha - 0.5V_y \tag{3.33}$$

The vector $\overline{V}(k)$ can lie in any of the 12 sectors. If it falls in the even numbered sector then there are three vectors in the direction of $\overline{V_x}$ and one in the direction of $\overline{V_y}$. And if it falls in the odd numbered sector then there are three vectors in the direction of $\overline{V_y}$ and one in the direction of $\overline{V_x}$. Among these three only one is to be selected.

If vector is in the even numbered sector, for eg. the vector lies in the sector number

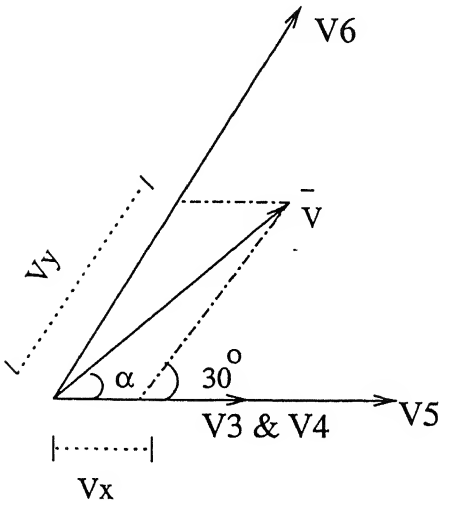

Figure 3.7: Components voltage vector $\overline{V}(k)$.

0 as in fig. 3.7, $\overline{V_x}$ is in the directions of $\overline{V_3}$, $\overline{V_4}$ and $\overline{V_5}$, thus only one of these is to be selected, and $\overline{V_y}$ is in the direction of $\overline{V_6}$. V_y and V_x are calculated from equations 3.32 and 3.33 respectively. The conduction times T_A (for $\overline{V_3}$, $\overline{V_4}$ or $\overline{V_5}$), T_B (for V_6) and T_C (for zero vector) are calculated as.

$$T_A = \frac{V_x}{|\overline{V_3}|}T \tag{3.34}$$

$$T_B = \frac{V_y}{|\overline{V_6}|}T \tag{3.35}$$

$$T_C = T - T_A - T_B \tag{3.36}$$

If $T_A + T_B < T$ then, either $\overline{V_3}$ or $\overline{V_4}$ is selected. $\overline{V_3}$ and $\overline{V_4}$ are equal vectors, so the state corresponding to any of them can be selected. But the choice depends upon the minimum switching required to move to the vector $\overline{V_6}$.

If $T_A + T_B > T$ then $\overline{V_5}$ is selected and T_A and T_C are recalculated

$$T_A = \frac{V_x}{|\overline{V_5}|}T \tag{3.37}$$

$$T_C = T - T_A - T_B \tag{3.38}$$

Thus for the time T_A, the switching states corresponding to $\overline{V_3}$, $\overline{V_4}$ or $\overline{V_5}$ (as selected from above) is applied to the inverter, for time T_B, switching states corresponding

to $\overline{V_6}$ is applied to the inverter and zero state is applied for the time T_C. There are three zero states, the one which requires the minimum switching to come to the zero state is selected.

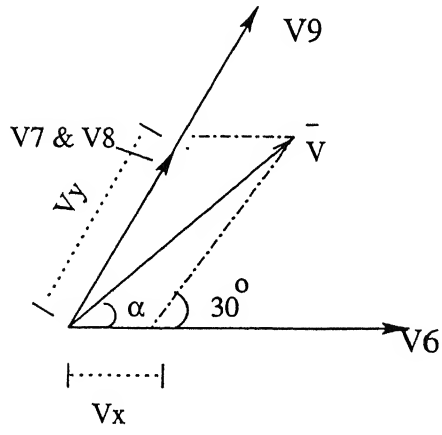

Figure 3.8: Components of voltage vector $\overline{V}(k)$.

And If vector is in the odd numbered sector, for eg. vector lies in sector 1 as in fig. 3.8 and 3.6, V_y is in the directions of $\overline{V_7}$, $\overline{V_8}$ and $\overline{V_9}$, thus only one of these is to be selected, and V_x is in the direction of V_6. V_y and V_x are calculated from equations 3.32 and 3.33 respectively. Thus the conduction times T_A (for V_6) T_B (for $\overline{V_7}$, $\overline{V_8}$ or $\overline{V_9}$), and T_C (for zero vector) are calculated as.

$$T_A = \frac{V_x}{|\overline{V_6}|}T \tag{3.39}$$

$$T_B = \frac{V_y}{|\overline{V_7}|}T \tag{3.40}$$

$$T_C = T - T_A - T_B \tag{3.41}$$

If $T_A + T_B < T$ then, either $\overline{V_7}$ or $\overline{V_8}$ is selected. $\overline{V_7}$ and $\overline{V_8}$ are equal vectors, so the state corresponding to any of them can be selected. But the choice depends upon the minimum switching required to move from the vector $\overline{V_6}$.

If $T_A + T_B > T$ then $\overline{V_9}$ is selected and T_B and T_C are recalculated

$$T_B = \frac{V_y}{|\overline{V_9}|}T \tag{3.42}$$

$$T_C = T - T_A - T_B \tag{3.43}$$

Thus for the time T_A, the switching states corresponding to $\overline{V_6}$ is applied to the inverter, for time T_B switching states corresponding to $\overline{V_7}$, $\overline{V_8}$ or $\overline{V_9}$ (as selected from above) is applied to the inverter and zero state is applied for the time T_C. There are three zero states, one which requires the minimum switching to come to the zero state is selected.

3.5 Simulation results

The active filter is tested for the balanced three phase thyristor load. The circuit is shown in fig. 3.9. Load currents I_{la}, I_{lb}, I_{lc} are calculated by simulating the load circuit. The details of this simulation is given in appendix. Load parameters are $R_l = 10\Omega$, $L_l = .02H$, $R_c = .1\Omega$, $L_c = .003H$ and the source voltage $V_{sm} = 230V$. Now using these load currents, the reference compensator currents, I^*_{ca}, I^*_{cb}, I^*_{cc} for the active filter, are calculated as explained in section 3.4.1. Various current controllers have been described in section 3.4.2. One of the current controllers is used to generate the switching logic for the switching functions S_a, S_b, S_c and the inverter is fired accordingly. The model of the inverter is given by the differential equations 3.1, 3.2, 3.3 and 3.4. These equations are solved using Runge-Kutta method to get the actual compensator currents, I_{ca}, I_{cb}, I_{cc}, for the switching determined above. This process is repeated with a time step of 1.1μsec. The active filter parameters are $R = .1\Omega, L = .02H, 2C = 1000\mu F$, $V_{dc} = 1200V$ and the stitching frequency f_s of the inverter switches is kept at $20Khz$. However it is constant at $20Khz$ for predictive controller but varies for the hysteresis controller with the maximum limit of $20Khz$.

3.5.1 Performance of Active Filter in Steady State Using Different Controllers

Active filter current is controlled using different current controllers. Fig.3.10 to 3.13 shows, for phase 'a', (a) load current, (b) compensator current, (c) source current with source voltage, (d) source current vector, (e) harmonic spectrum of the source and (f) harmonic spectrum load, for the firing angle of 30°, using different controllers.

- Fig. 3.10 shows waveforms using hysteresis controller.

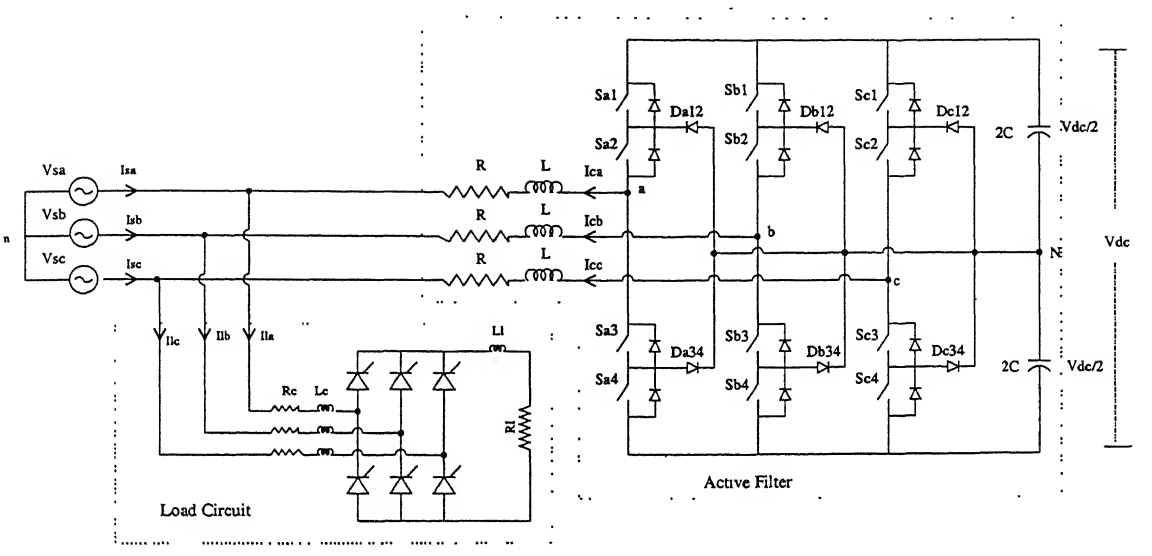

Figure 3.9: Active filter compensating for balanced load.

- Fig. 3.11 shows waveforms using predictive current controller, by predicting the current with a delay of one cycle.
- Fig. 3.12 shows waveforms using predictive current controller, by predicting the current with a delay of one sampling time.
- Fig. 3.13 shows waveforms using predictive current controller, by predicting the current from the last two samples of current.

From the figs. 3.10 to 3.13 it is seen that the source current is sinusoidal and is in phase with the source voltage. The peak of the source current is always less than the load current. It can be seen that the current is smoother in all the three predictive controllers compared to the hysteresis controller. The advantage of using predictive controller is that the switching frequency is constant.

Fig. 3.10(f) shows harmonic spectrum of load current, and figs. 3.10(e), 3.11(e), 3.12(e), and 3.13(e), shows the harmonic spectra of the source current using different controllers. Table 3.2 shows TDH and p.f. of load current and source currents using different controllers. THD of the source current is 17.56% without any controller, which is reduced to less than 1.5% (between 0.53% to 1.47% for different controllers) using active filter. P.f. is also improved from 0.67 to nearly 1 in all the cases.

Table 3.2: THD and p.f. using various controllers.

controller used	THD in load	p.f of load	THD in source	P.f. of source
No controller	17.56%	0.67	17.56%	0.67
Hysteresis controller	17.56%	0.67	0.59%	0.99
Predictive controller[1]	17.56%	0.67	0.52%	0.99
Predictive controller[2]	17.56%	0.67	1.42%	0.99
Predictive controller[3]	17.56%	0.67	0.86%	0.99

[1] with a delay of one cycle
[2] with a delay of one sampling time
[3] with estimation of current using the last two samples of current

3.5.2 Performance of Active Filter During the Transients

Active filter is also tested for transient conditions. The firing angle is changed to 60° , from 0°, after 0.1 sec. and then again changed to 30° after 0.2 sec.

- Fig. 3.14 shows current waveforms of phase 'a' and fig. 3.15 shows the output of PI controller and the recovery of DC capacitor voltage during the transients using hysteresis controller.
- Fig. 3.16 shows current waveforms of phase 'a' and fig. 3.17 shows the output of PI controller and the recovery of DC capacitor voltage during the transients using predictive controller by predicting the current from the last two samples of current.

For transient conditions the active filter adjusts itself to make the source current sinusoidal. As seen in the fig. 3.14(c) and fig. 3.16(c) the source current settles to steady state in less than a cycle, thus showing fast transient response of the active filter. As firing angle is changed load current changes, so as to settle the source current instantaneously the extra energy is supplied or stored by the capacitor, as shown by the output of the PI controller in figs.3.15(a) and 3.17(a). Thus capacitor voltage rises or falls, and settles to the reference value in about 0.015 sec as shown in fig. 3.15(b) and fig. 3.17(b).

From the fig. 3.18 it is clearly seen that for transient loads predictive current controller with one sampling delay cannot be used, as the source current settles to steady state after a long time, approximately 2 cycles.

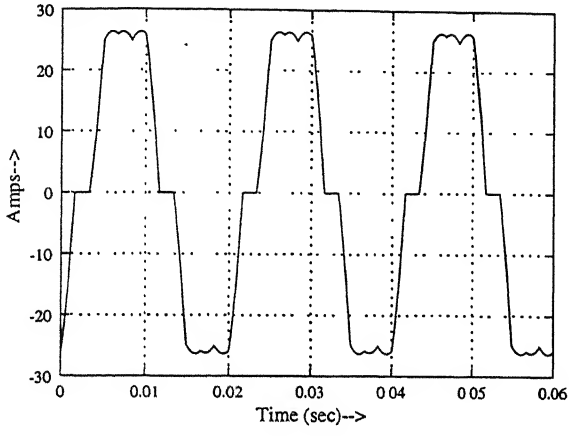

(a) Load current

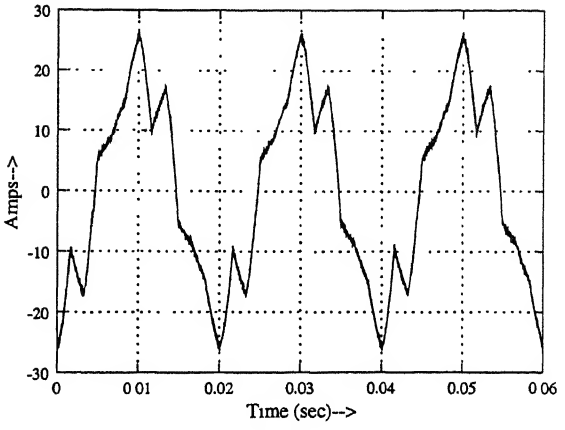

(b) Compensator current

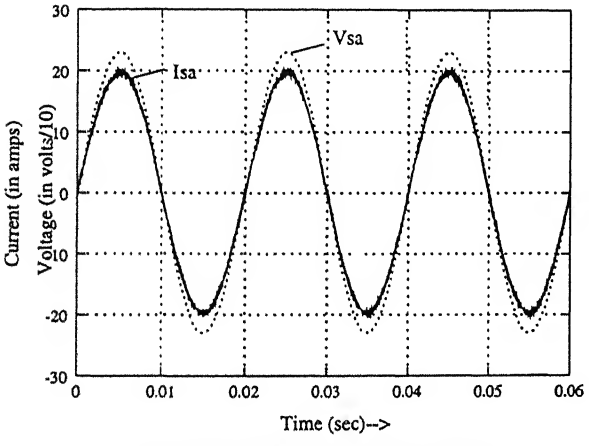

(c) Source current and Source voltage

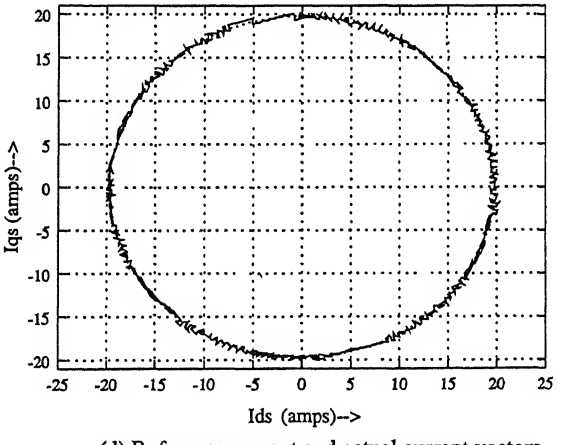

(d) Reference current and actual current vectors

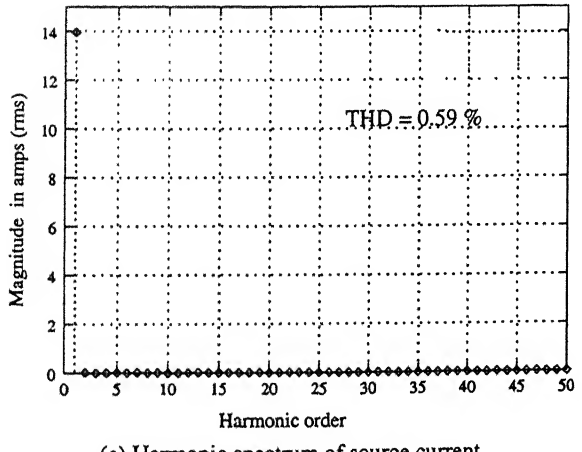

(e) Harmonic spectrum of source current

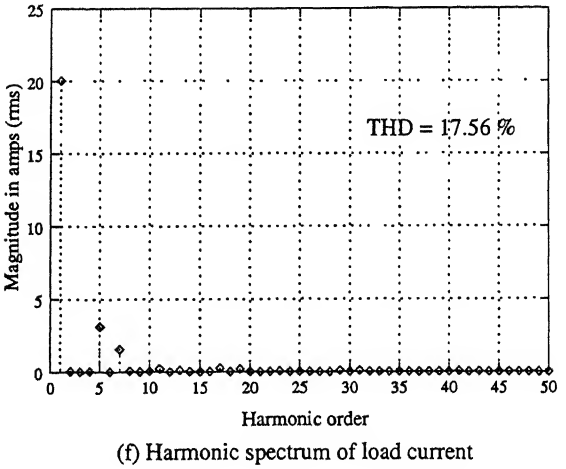

(f) Harmonic spectrum of load current

Figure 3.10: Simulated results for phase 'a' using hysteresis controller.

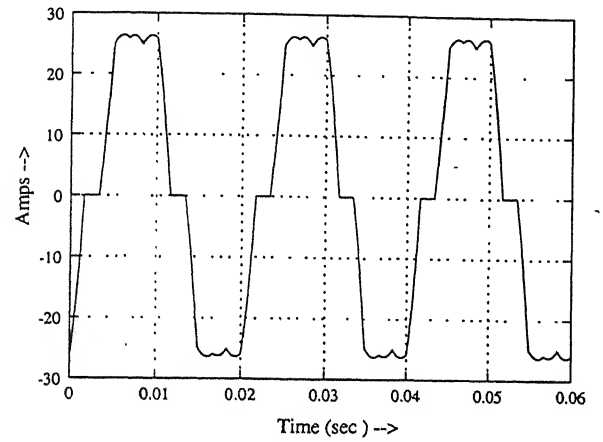

(a) Load current

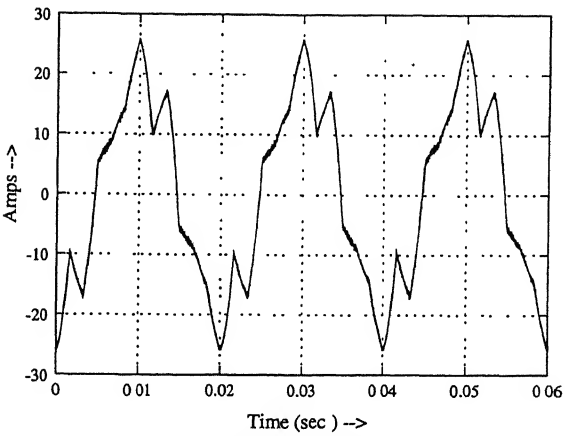

(b) Compensator current

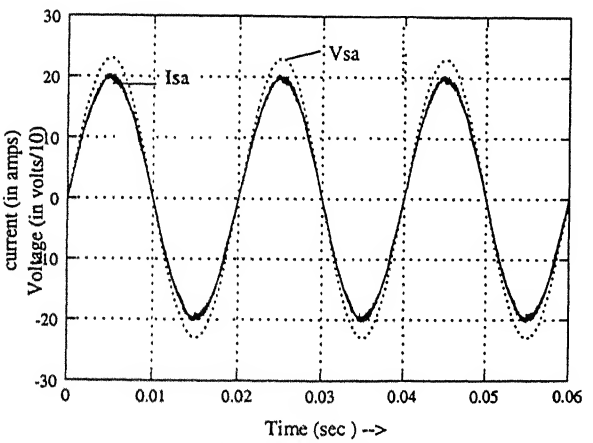

(c) Source current and Source voltage

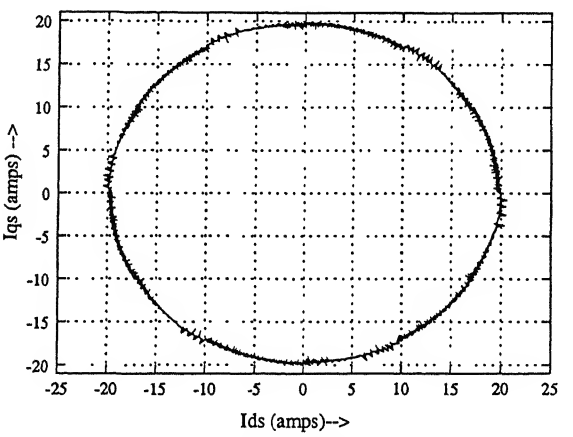

(d) Reference current and actual current vectors

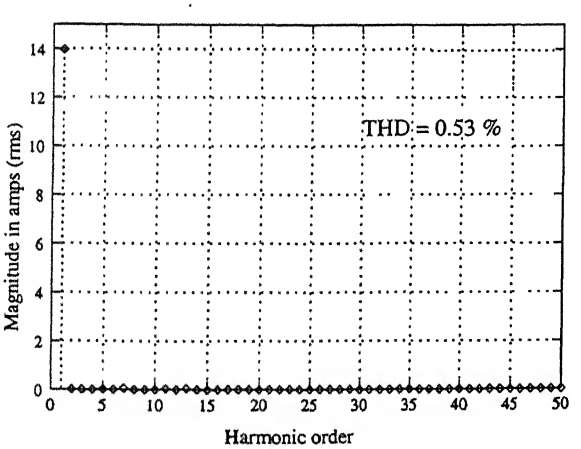

(e) harmonic spectrum of source current

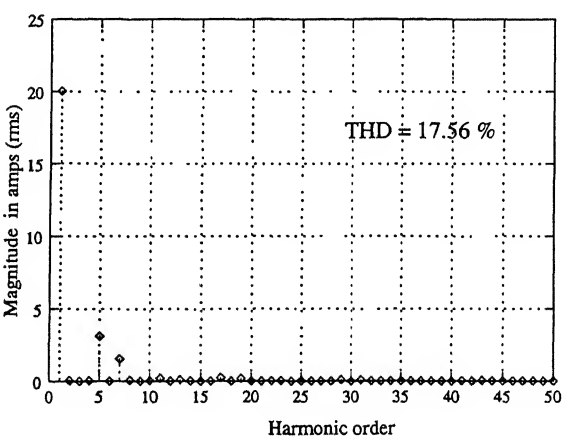

(f) Harmomic spectrum of load current

Figure 3.11: Simulated results for phase 'a' by predicting the current with one cycle delay.

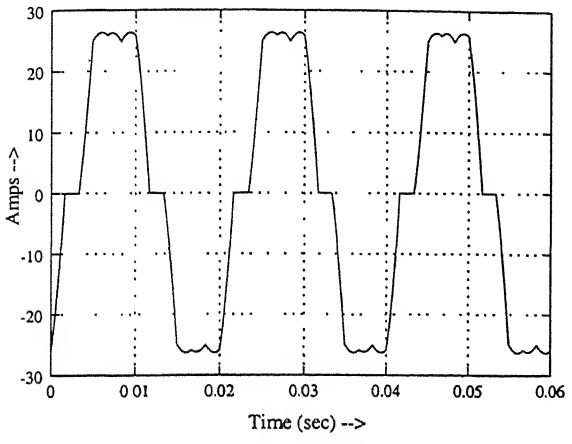

(a) Load current

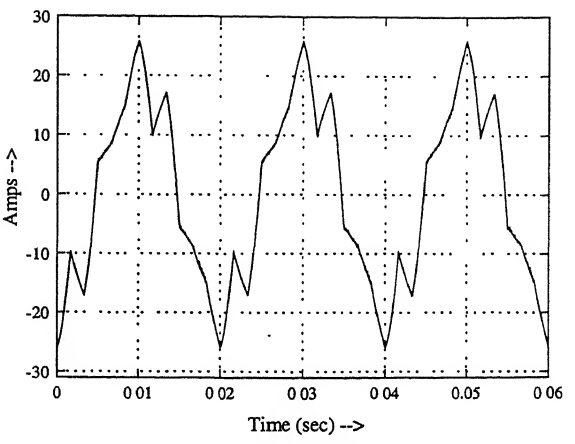

(b) Compensator current

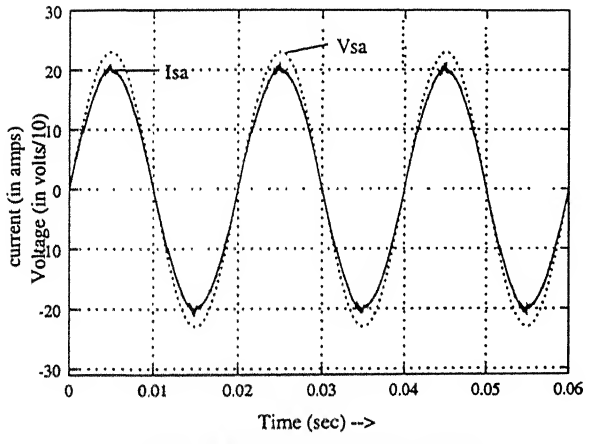

(c) Source current and source voltage

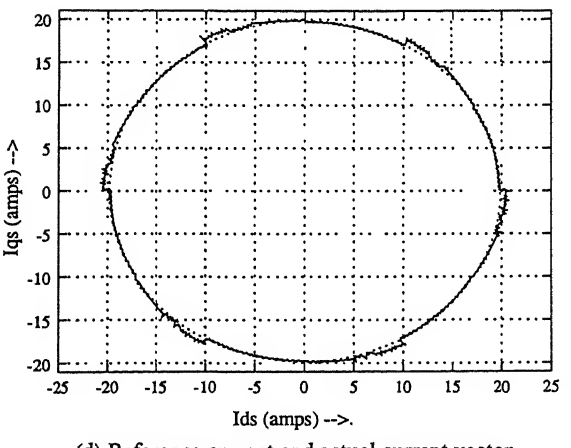

(d) Reference current and actual current vector

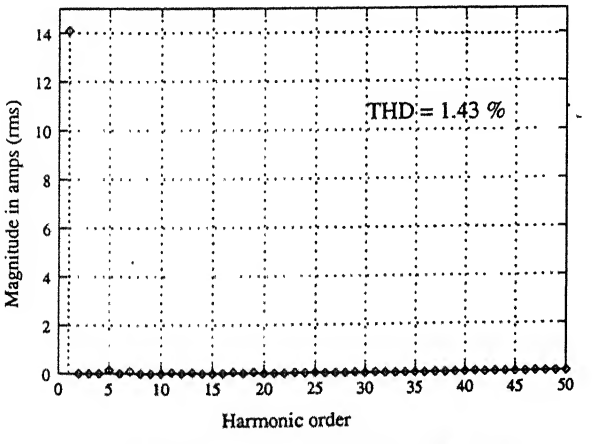

(e) Harmonic spectrum of source current

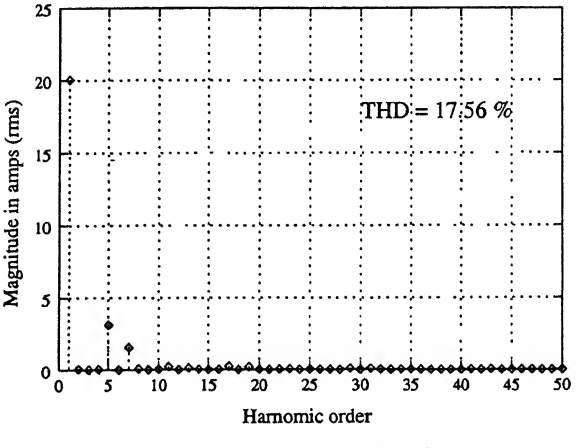

(f) Harmonic spectrum of load current

Figure 3.12: Simulated results for phase 'a' by predicting the current with a delay of one sampling time.

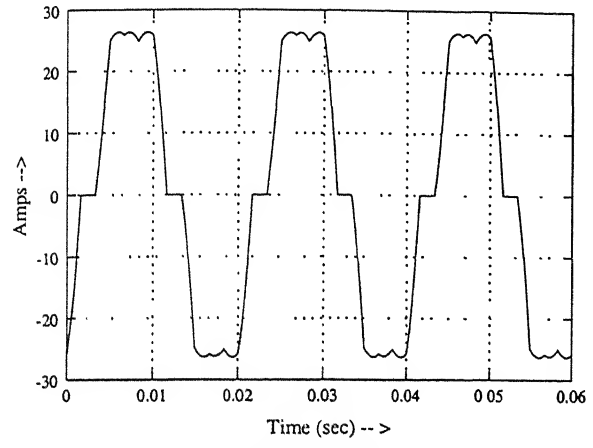

(a) Load current

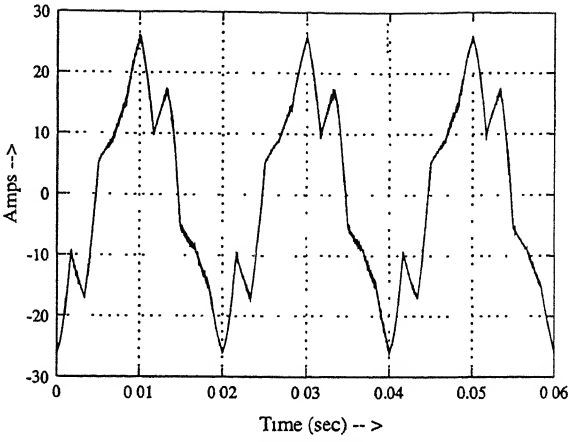

(b) Compensator current

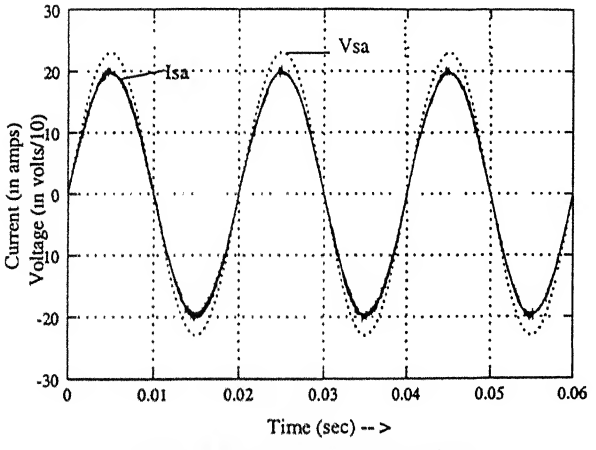

(c) Source current and Source voltage

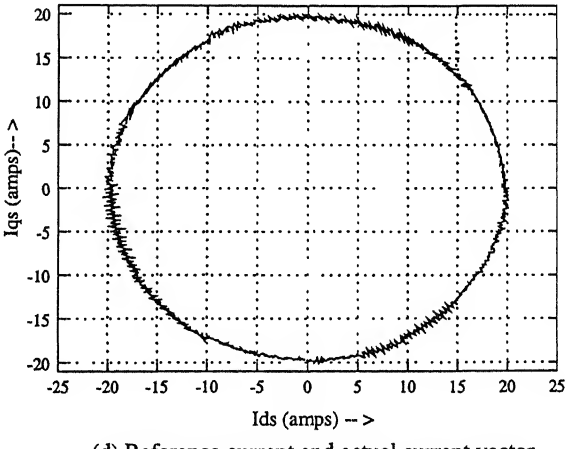

(d) Reference current and actual current vector

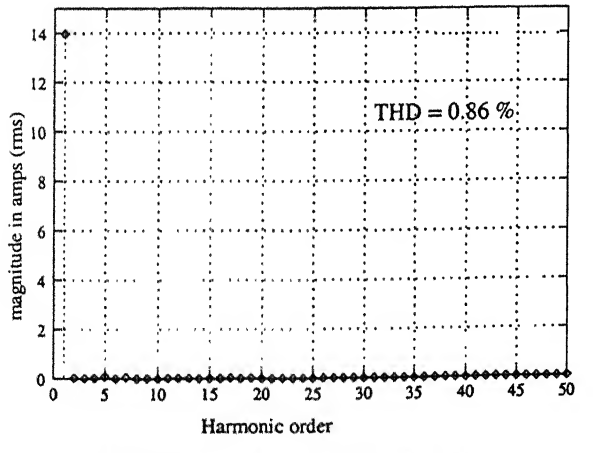

(e) Harmonic spectrum of source current

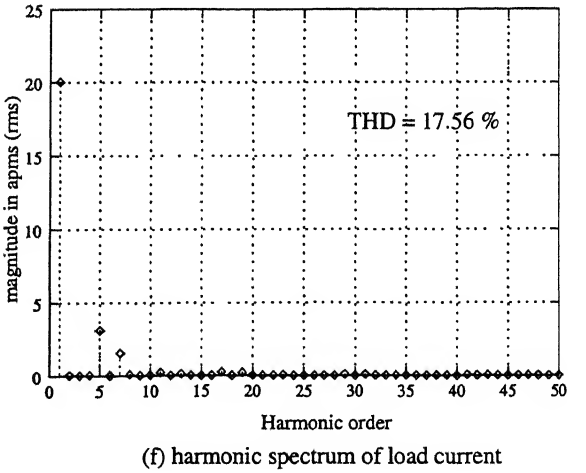

(f) harmonic spectrum of load current

Figure 3.13: Simulated results for phase 'a' by predicting the current from the last two samples of currents.

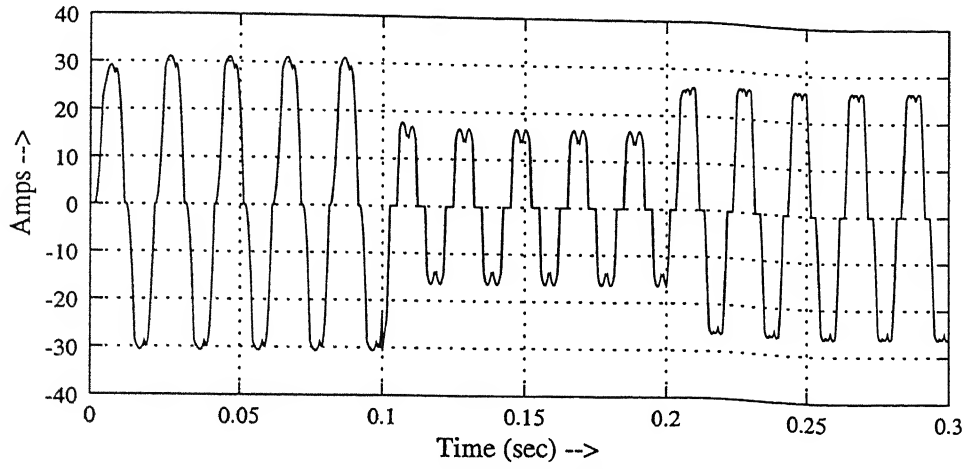

(a) Load current

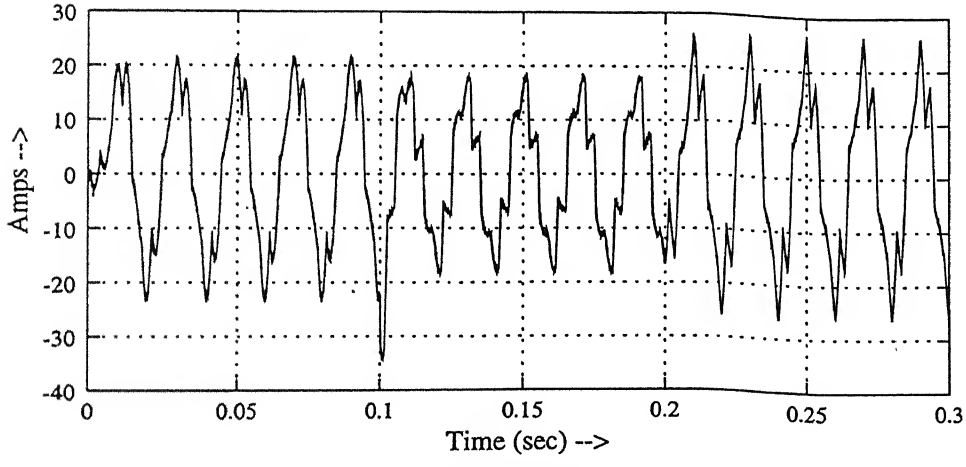

(b) Compensator current

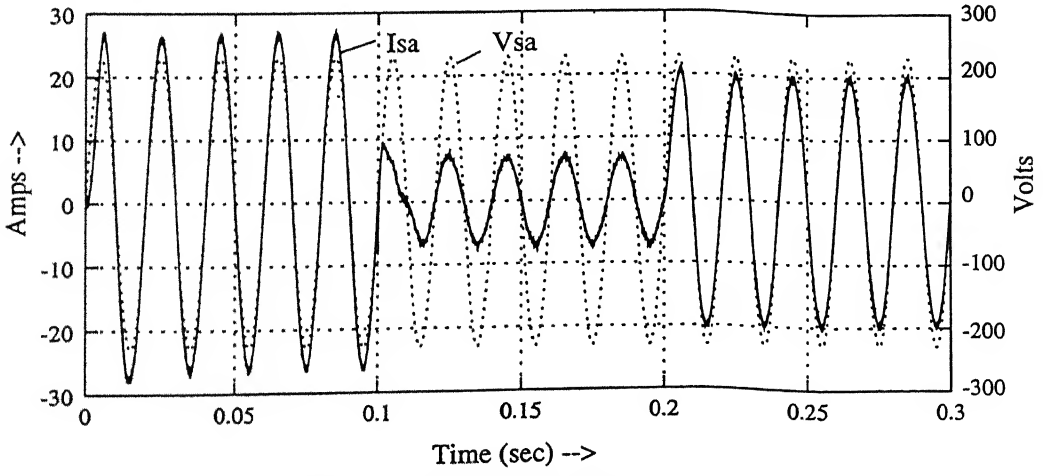

(c) Source current and source voltage

Figure 3.14: The transient response of phase 'a' currents when the load firing angle is changed from 0° to 60° and then again to 30°, using hysteresis controller.

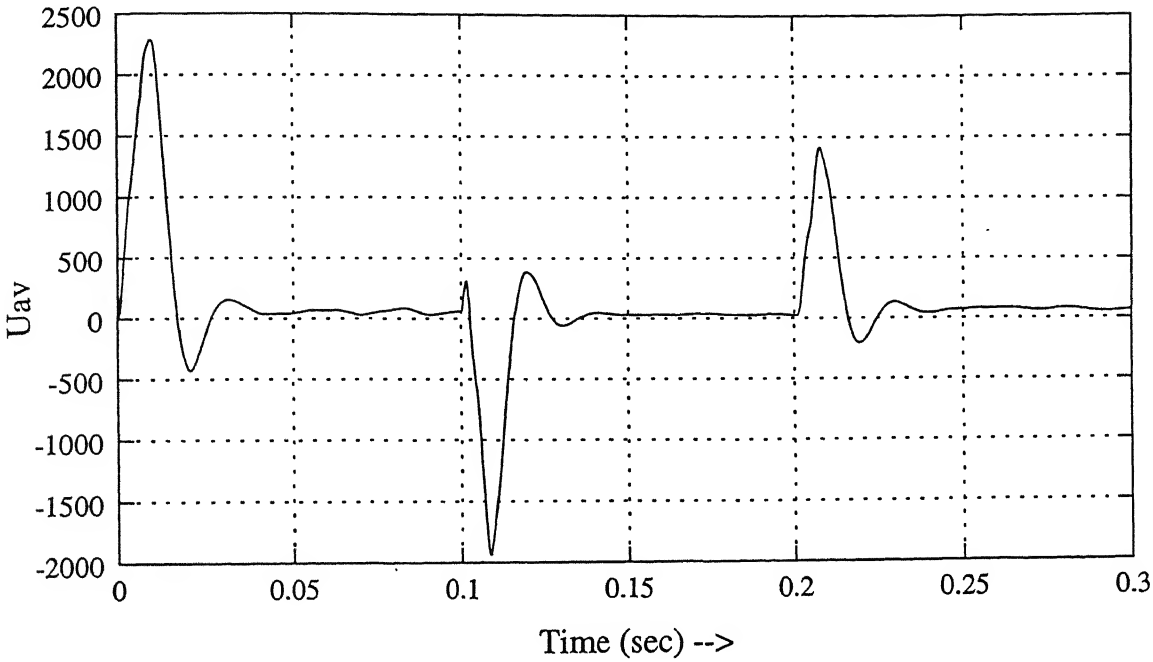

(a) Output of PI controller

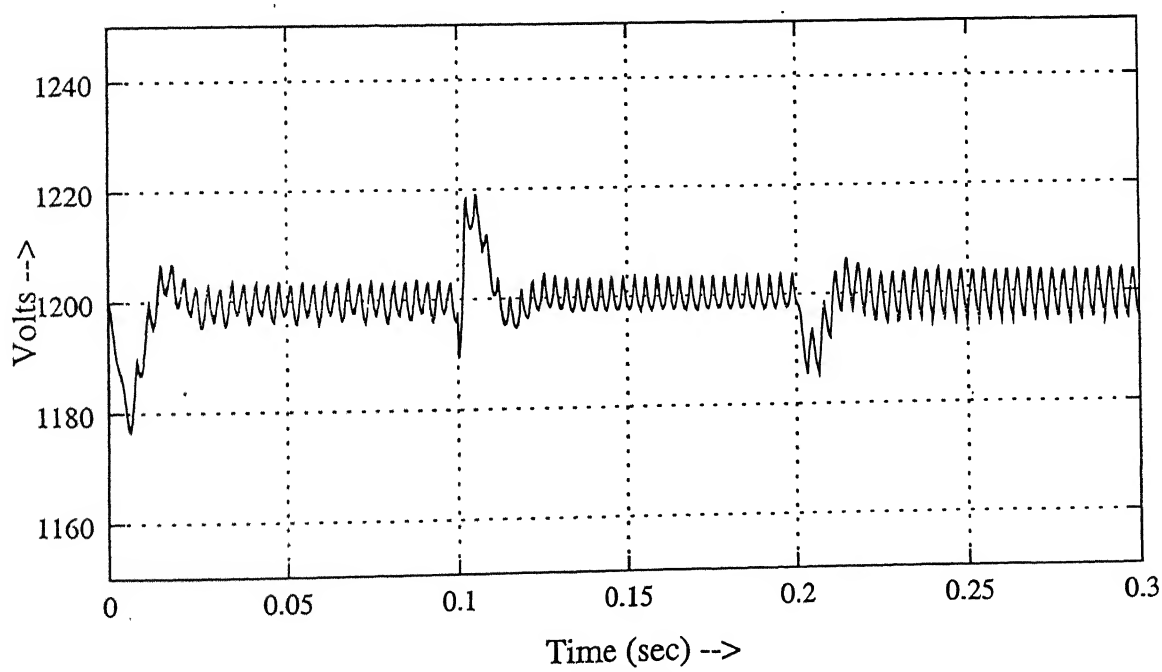

(b) DC capacitor voltage

Figure 3.15: The transient response when the load firing angle is changed from 0° to 60° and then again to 30°, using hysteresis controller.

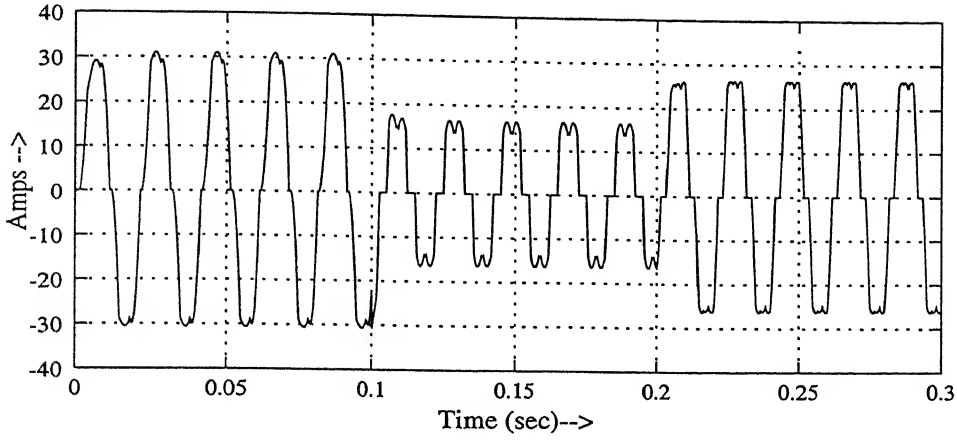

(a) Load current

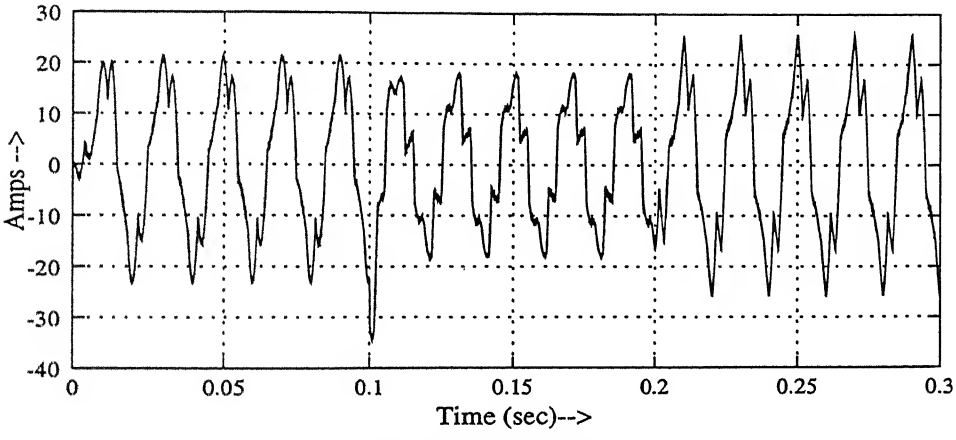

(b) Compensator current

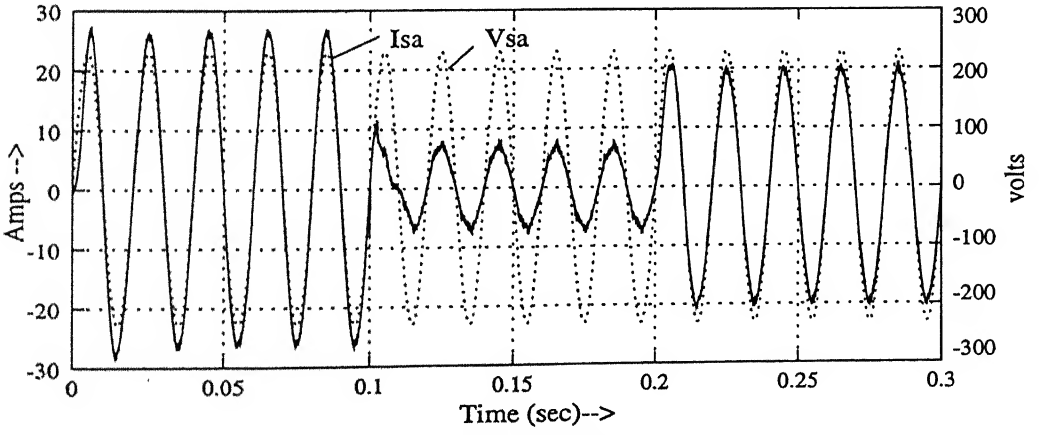

(c) Source current and source voltage

Figure 3.16: The transient response of phase 'a' currents when the load firing angle is changed from 0° to 60° and then again to 30° , using predictive controller.

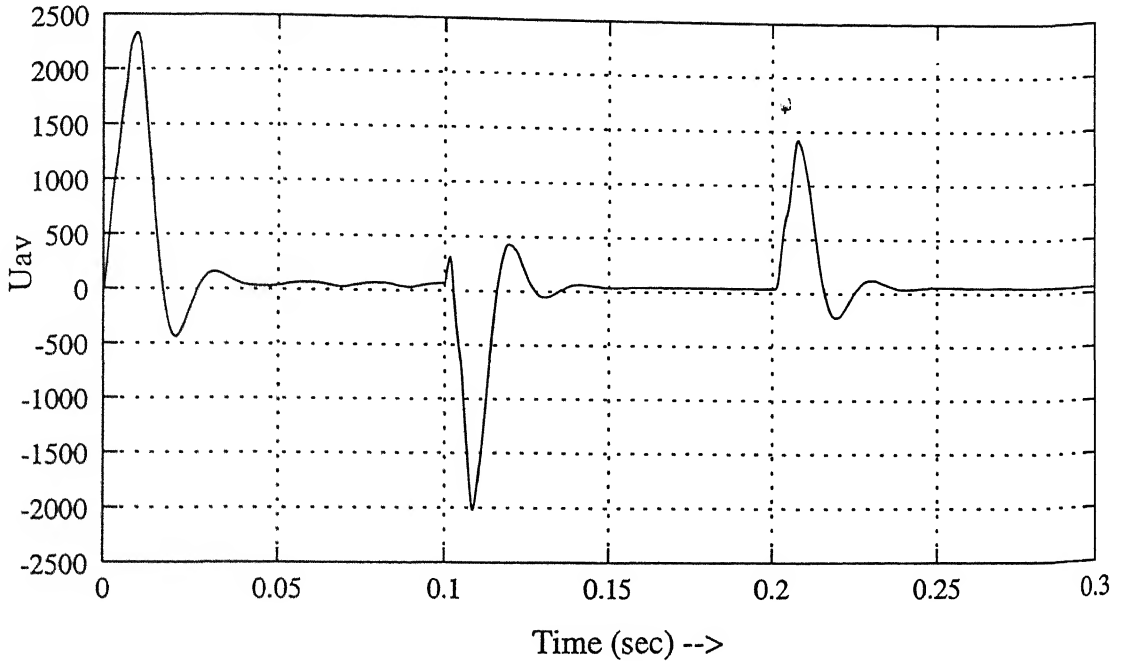

(a) Output of PI controller

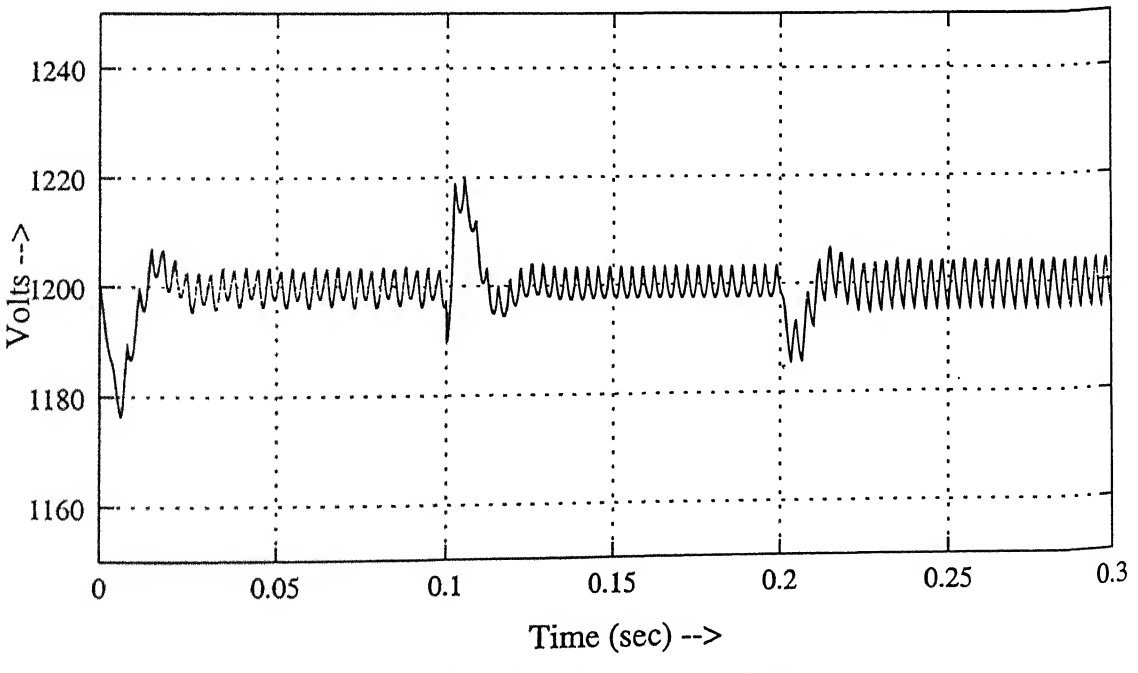

(b) DC capacitor voltage

Figure 3.17: The transient response when the load firing angle is changed from 0° to 60° and then again to 30°, using predictive controller.

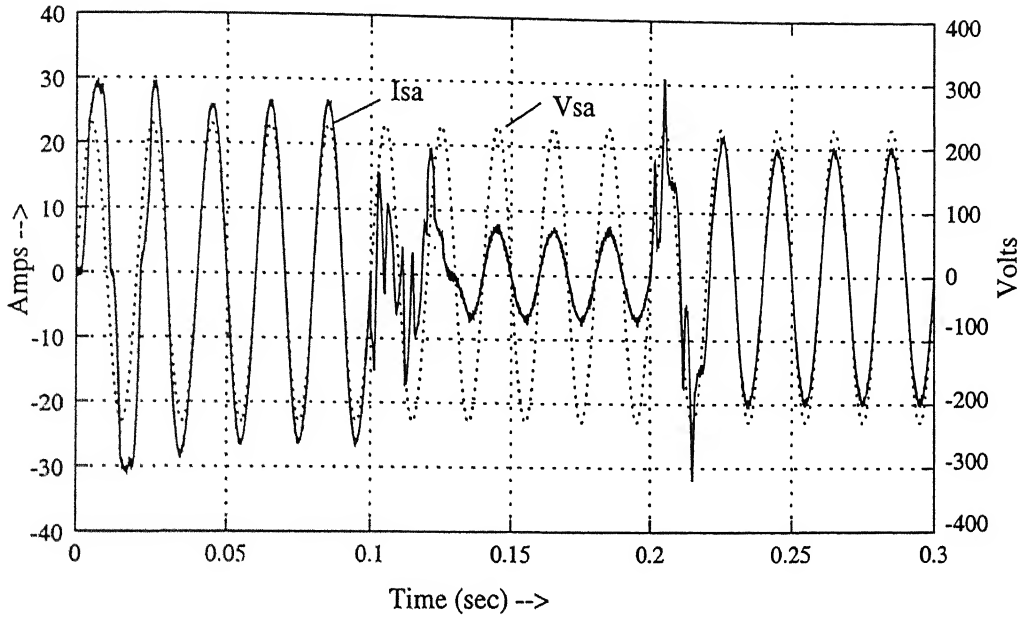

Figure 3.18: The transient response of source current when the load firing angle is changed from 0° to 60° and then again to 30° , using predictive controller with a delay of one cycle.

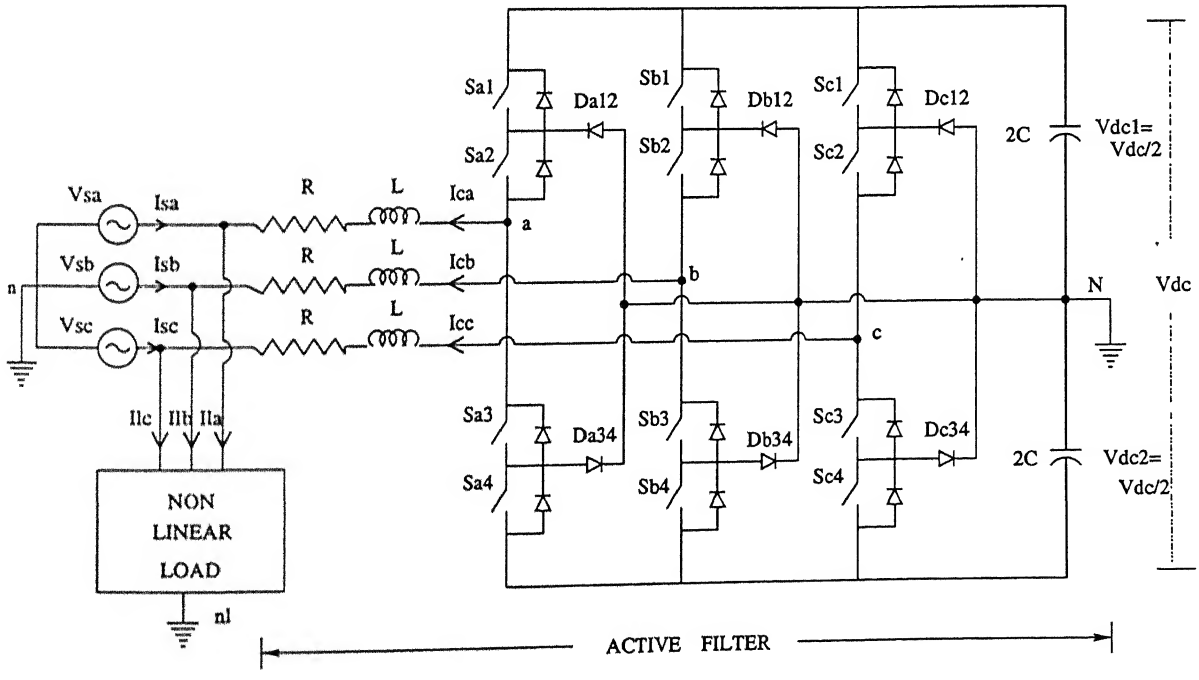

Figure 3.19: Active filter for unbalanced loads..

3.6 Active Filter as Compensator for Unbalanced Loads

Loads connected to the source can be unbalanced or they may be connected through a neutral wire. To get the balanced three phase supply currents the active filter is to supply this neutral current. Thus the neutral of the inverter is to be grounded. The circuit is shown in fig. 3.19.

As the nodes n and N are grounded, the phase voltages become equal to pole voltages as discussed in section 2.5. Thus $V_{an} = V_{aN}$,$V_{bn} = V_{bN}$ and $V_{cn} = V_{cN}$. The inverter can be modeled by the following differential equations.

$$V_{sa} = -L\frac{dI_{ca}}{dt} - RI_{ca} + S_a\frac{V_{dc}}{2} \tag{3.44}$$

$$V_{sb} = -L\frac{dI_{cb}}{dt} - RI_{cb} + S_b\frac{V_{dc}}{2} \tag{3.45}$$

$$V_{sc} = -L\frac{dI_{cc}}{dt} - RI_{cc} + S_c\frac{V_{dc}}{2} \tag{3.46}$$

$$C\frac{dV_{dc}}{dt} = -\left(S_aI_{ca} + S_bI_{cb} + S_cI_{cc}\right)/2 \tag{3.47}$$

Where S_a, S_b, S_c are the switching functions as discussed in section 2.3 .

3.6.1 The control circuit

Reference currents I^*_{ca}, I^*_{cb} and I^*_{cc} are calculated similarly as in section 3.4.1. The current is controlled using the hysteresis controller described in section 3.4.2.1. Inverter phase voltages are depend only on the switching function of their respective phases, so the current can be controlled independently in each phases. Predictive controller is not used here. The neutral point is grounded, so phase voltages are not balanced and there are zero sequence voltages. The model described above (in section 3.4.2.2) is not defined for zero sequence voltages. Thus while calculating the switching states the zero sequence voltages are not taken account and the currents do not follow the reference. Predictive controller is applied for the circuit shown in figure 3.21, and results are shown in fig. 3.28. Thus it is seen from the fig. 3.28 given in section 3.7, that while the current vector follows the reference but the actual three phase currents

do not follow their respective references.

3.6.2 DC Capacitor Voltage Control Loop

As the loads are unbalanced, it may happen that one of the capacitor gets charged and the other gets discharged. The total voltage will be constant as the voltage control loop is there. So to get rid of this unbalance a chopper circuit is used as shown in the fig. 3.20.

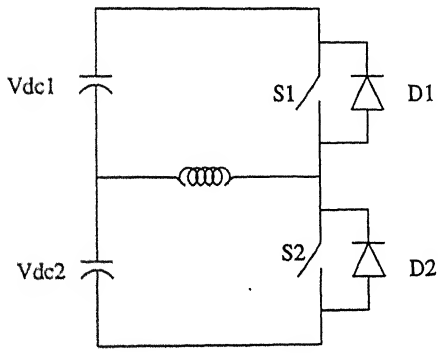

Figure 3.20: DC capacitor voltage balanced circuit.

The charging and discharging can be controlled by the duty cycle of the switches S_1 and S_2. Thus the energy can be transfered from one capacitor to the other through an inductor. As the voltage of a capacitor rises its corresponding switch is switched on to discharge its energy to the other capacitor through the inductor. As the voltage of the upper capacitor rises above the set reference S_1 is switched on, so the energy from the capacitor is discharged to inductor through switch S_1. And as the voltage level falls below the set level the switch S_1 is turned off and the energy stored in inductor now charges the lower capacitor through the diode D_2. Thus by controlling the switch S_1 the charge of the upper capacitor can be transfered to the lower capacitor. Similarly if the voltage level of the lower capacitor rises above the set reference S_2 is turned on and it charges the inductor in the opposite direction. As S_2 is turned off inductor charges the upper capacitor through the upped diode D_1. Thus maintains the voltage of both the capacitors.

3.7 Simulation Results

The active filter is tested for three types of unbalanced loads.

Case 1

Balanced three phase controlled rectifier, with unbalanced three phase R load, each connected to ground. The circuit is shown in fig. 3.21. Various load parameters are, $R_l = 20$, $L_l = .02H$, $R_c = .1\Omega$, $L_c = .003H$, for controlled rectifier and $R_{la} = 20$, $R_{lb} = 50$, $R_{lc} = 30$ for three phase resistive load.

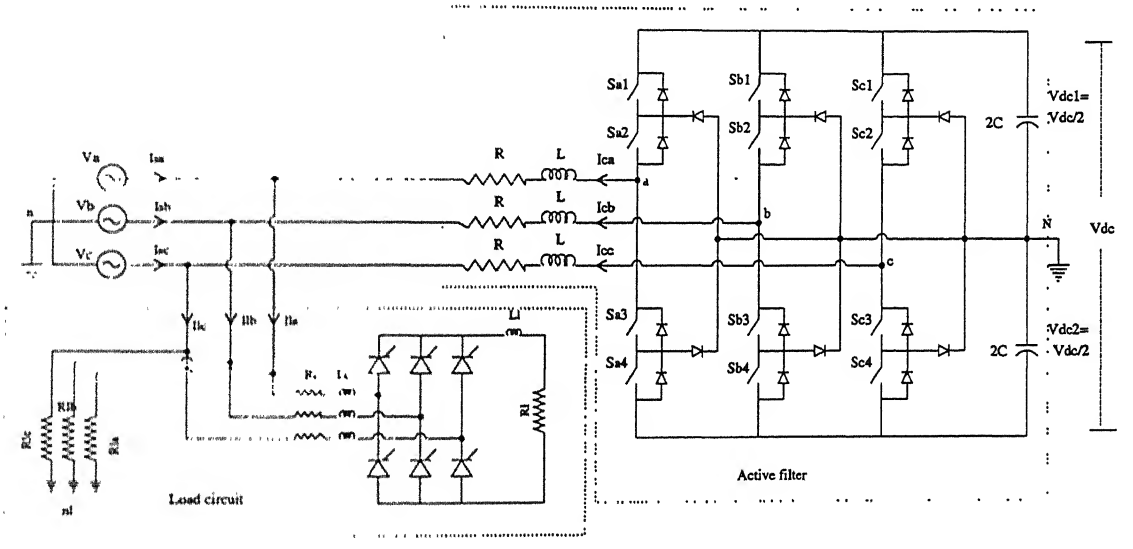

Figure 3.21: Circuit for case 1.

Case 2

Balanced three phase controlled rectifier, with full wave bridge diode rectifier connected to phase 'a' through ground. The circuit is shown in fig. 3.22. Various load parameters are $R_l = 15$, $L_l = .02H$, $R_c = .1\Omega$, $L_c = .003H$, for controlled rectifier and $R_f = 20\Omega$, $L_f = .02H$, $R_{cf} = .01\Omega$, $L_{cf} = .0035H$ for full wave rectifier.

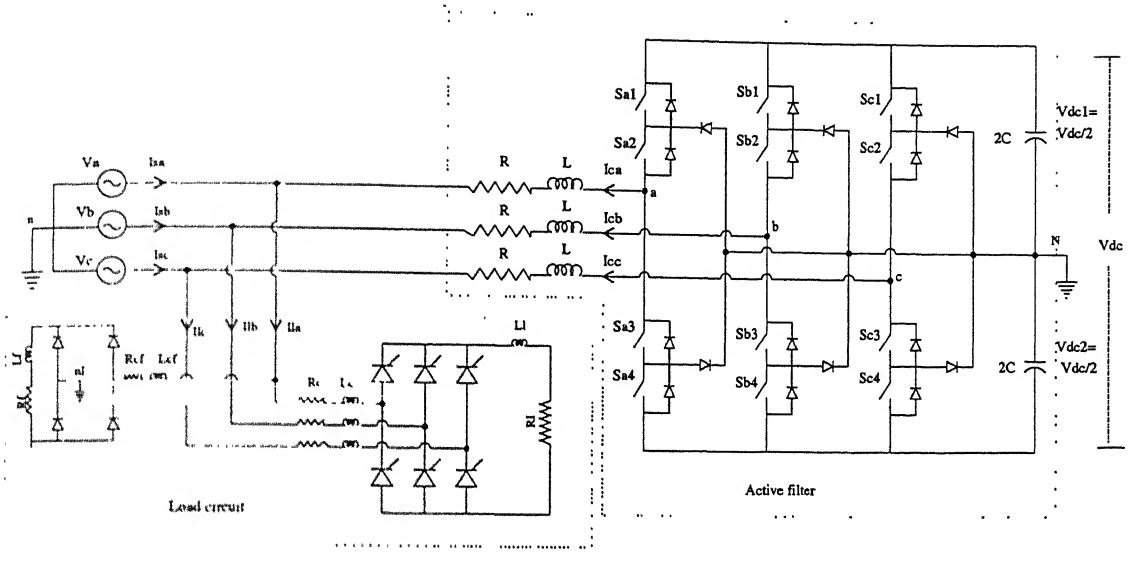

Figure 3.22: Circuit for case 2.

Case 3

Balanced three phase controlled rectifier, with half wave diode rectifier, supplying a R-L load, connected to phase 'a' through ground. The circuit is shown in fig. 3.23. Various load parameters are $R_l = 20$, $L_l = .02H$, $R_c = .1\Omega$, $L_c = .003H$, for controlled rectifier and $R_{ah} = 30\Omega$, $L_{ah} = .02H$ for half wave rectifier.

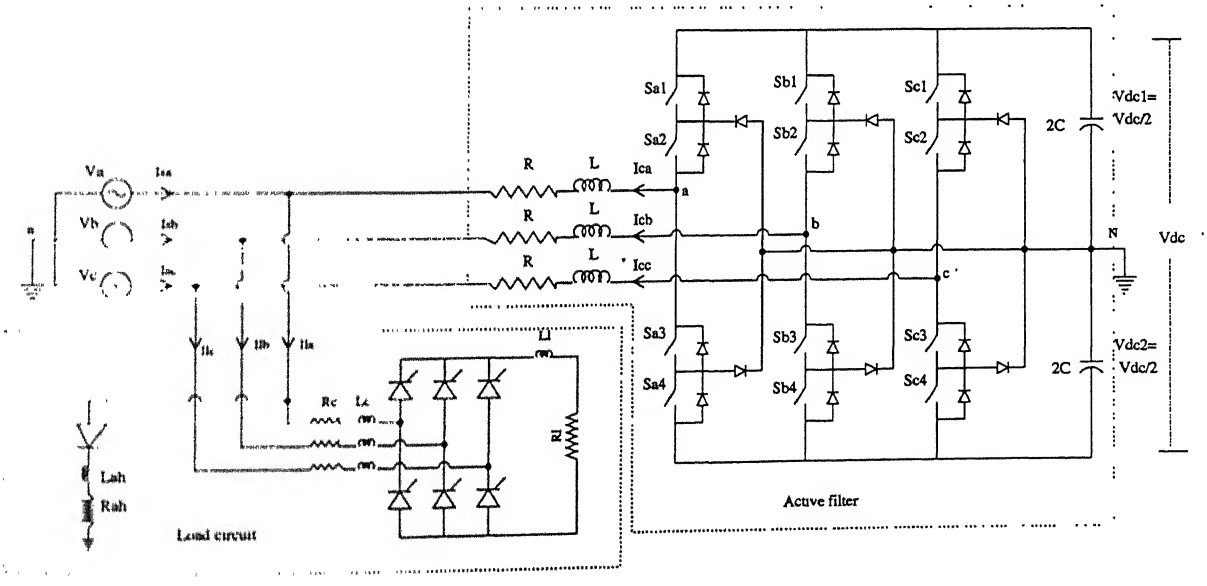

Figure 3.23: Circuit for case 3.

Case 4

The circuit shown in fig 3.21 is also simulated using predictive current controller.

3.7.1 Simulation Method

Load circuit is simulated as described in appendix, and load currents I_{la}, I_{lb}, I_{lc} are calculated solving various differential equations of the load circuit given in the appendix. Using these load currents, reference compensator currents I^*_{ca}, I^*_{cb}, I^*_{cc} for active filter are calculated as explained in section 3.4.1. Hysteresis current controller, as described in section 3.4.2.1, is used to generate the switching logic for the switching functions S_a, S_b, S_c and the inverter is fired accordingly. The model of the inverter is given by the differential equations 3.44, 3.45, 3.46 and 3.47. These equations are solved using Runge-Kutta method to get the actual compensator currents, I_{ca}, I_{cb}, I_{cc}, for the switching determined above. This process is repeated with a time step of 1.1μsec. Active filter parameters are $R = .1\Omega, L = .02H, 2C = 1000\mu F$, $V_{dc} = 1200V$, and maximum frequency f_{max} is limited to $20Kkz$.

3.7.2 Performance of Filter in Steady State

Active filter is tested for all the above cases, with firing angle of thyristor bridge to be 30°.

Case 1

Respective source voltages, load currents, compensator currents and source currents for the phases 'a', 'b' and 'c' are shown in fig. 3.24(a),(b),(c); fig 3.24(d),(e),(f); fig 3.24(g),(h),(i); fig 3.24(j),(k),(l). Thus it is seen from the figure that however the load current is non-sinusoidal and unbalanced in each phases but the source current is, sinusoidal, balanced and in phase with its respective voltages. Table 3.3 shows the THD of load currents and the source current. Table also shows the power factor of load and source. Thus as seen from the table, using the active filter the THD of the source current is reduced and the power factor is improved.

Table 3.3: THD and p.f for case 1.

Current	THD	P.F
load current of phase 'a', I_{la}	14.86 %	0.91
load current of phase 'a', I_{lb}	19.33 %	0.84
load current of phase 'a', I_{lc}	17.03 %	0.88
Source current	0.29%	0.99

Case 2

Respective source voltages, load currents, compensator currents and source currents for the phases 'a', 'b' and 'c' are shown in fig 3.25(a),(b),(c); fig 3.25(a),(b),(c); fig 3.25(a),(b),(c); fig 3.25(a),(b),(c). Thus it is seen from the figure that however the load current is non-sinusoidal and unbalanced in each phases but the source current is, sinusoidal, balanced and in phase with its respective voltage. Table 3.4 shows the THD of load currents and the source current. Table also shows the power factor of load and source. Thus as seen from the table, using the active filter the THD of the source current is reduced and the power factor is improved.

Table 3.4: THD and p.f. for case 2.

Current	THD	P.F
load current of phase 'a', I_{la}	14.99 %	0.8231
load current of phase 'a', I_{lb}	20.24 %	0.71
load current of phase 'a', I_{lc}	20.24 %	0.71
Source current	1.14%	0.99

Case 3

Respective source voltages, load currents, compensator currents and source currents for the phases 'a', 'b' and 'c' are shown in fig 3.26(a),(b),(c); fig 3.26(a),(b),(c); fig 3.26(a),(b),(c); fig 3.26(a),(b),(c). Thus it is seen from the figure that however the

load current is non-sinusoidal and unbalanced in each phases but the source current is, sinusoidal, balanced and in phase with its respective voltage. Table 3.5 shows the THD of load currents and the source current. Table also shows the power factor of load and source. Thus as seen from the table, using the active filter the THD of the source current is reduced and the power factor is improved. In this case the load current in phase 'a' also contains the dc value which is equal to 2.4 amps.

Table 3.5: THD and p.f. for case 3.

Current	THD	P.F
load current of phase 'a', I_{la}	20.42 %	0.79
load current of phase 'a', I_{lb}	22.42 %	0.74
load current of phase 'a', I_{lc}	22.42 %	0.74
Source current	1.56%	0.99

It is seen that the load current also contain DC value of 2.4 Amps. Thus due to this dc value one of the capacitor gets charged and the other gets discharged. So using the capacitor balance loop a described in section 3.6.2 the voltages of capacitors are regulated. Figs. 3.27(a),(b) and (c), show the capacitor voltages when the control loop is not used, thus it is seen that however the total voltage is approximately constant but the voltages of individual capacitors rises or decreases. Figs. 3.27(d),(e) and (f) show the capacitor voltages when the control loop is used. Thus it shows that the voltages of both the capacitor is within a limited peak to peak ripple.

Case 4

Figure 3.28 shows the (a) reference current and (b) actual current for phase 'a'. This figure also shows (c) reference current vector and (d) actual current vector. Thus is is clear from the figure 3.28 that while the actual current vector follows reference current vector but the actual current in phases do not follow their reference. Thus for unbalanced loads predictive current controller cannot be used.

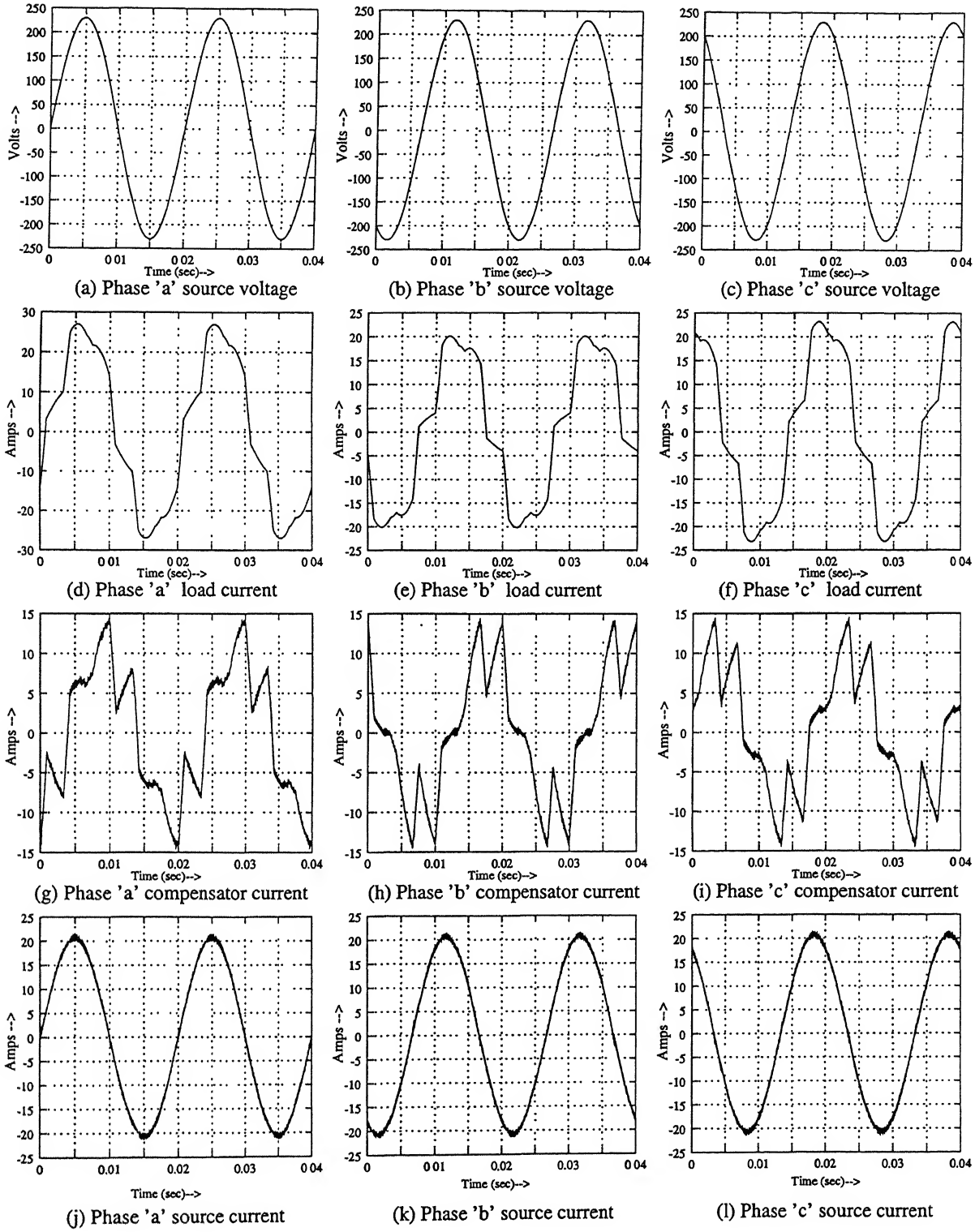

Figure 3.24: Simulated waveforms for case1.

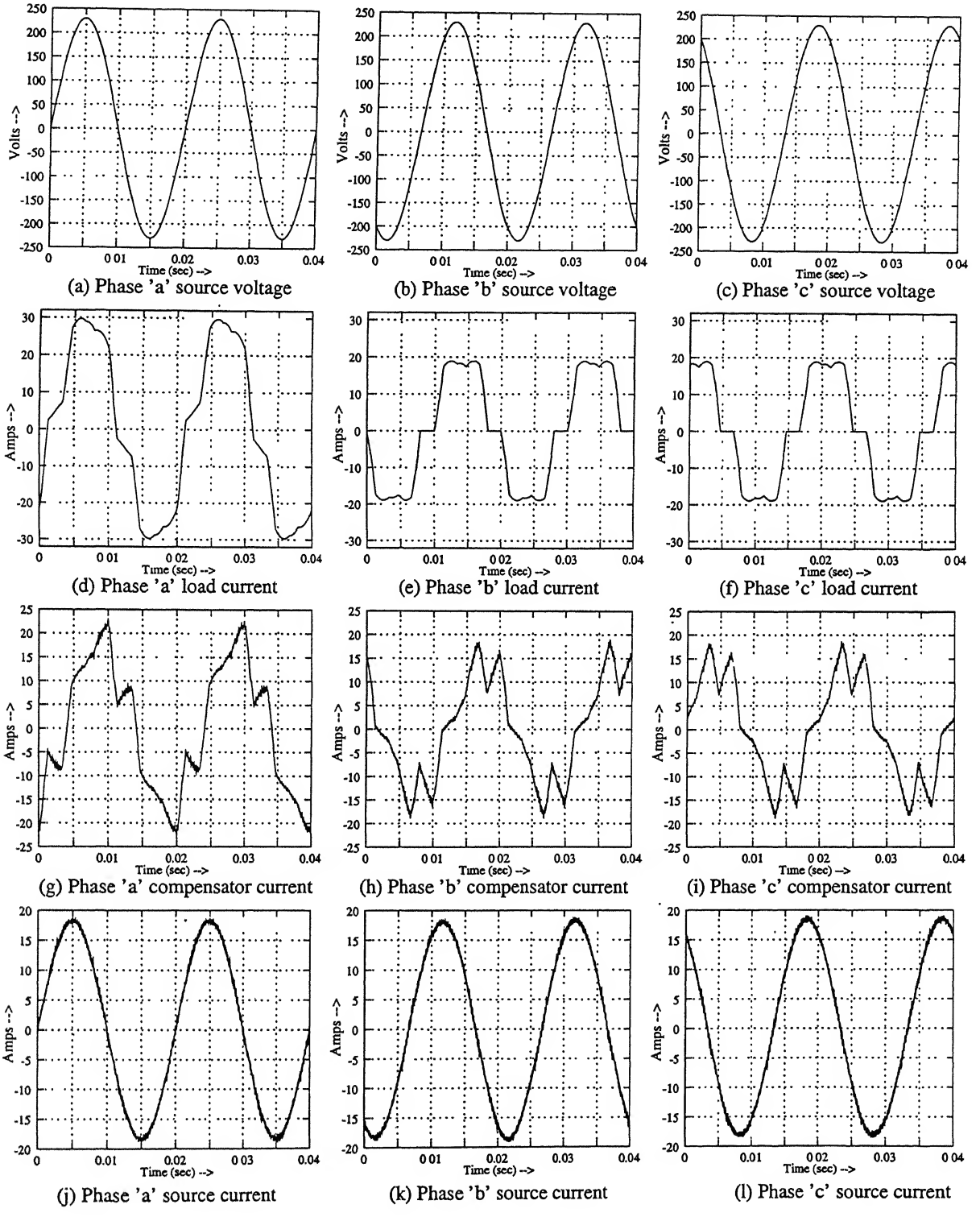

Figure 3.25: Simulated waveforms for case2.

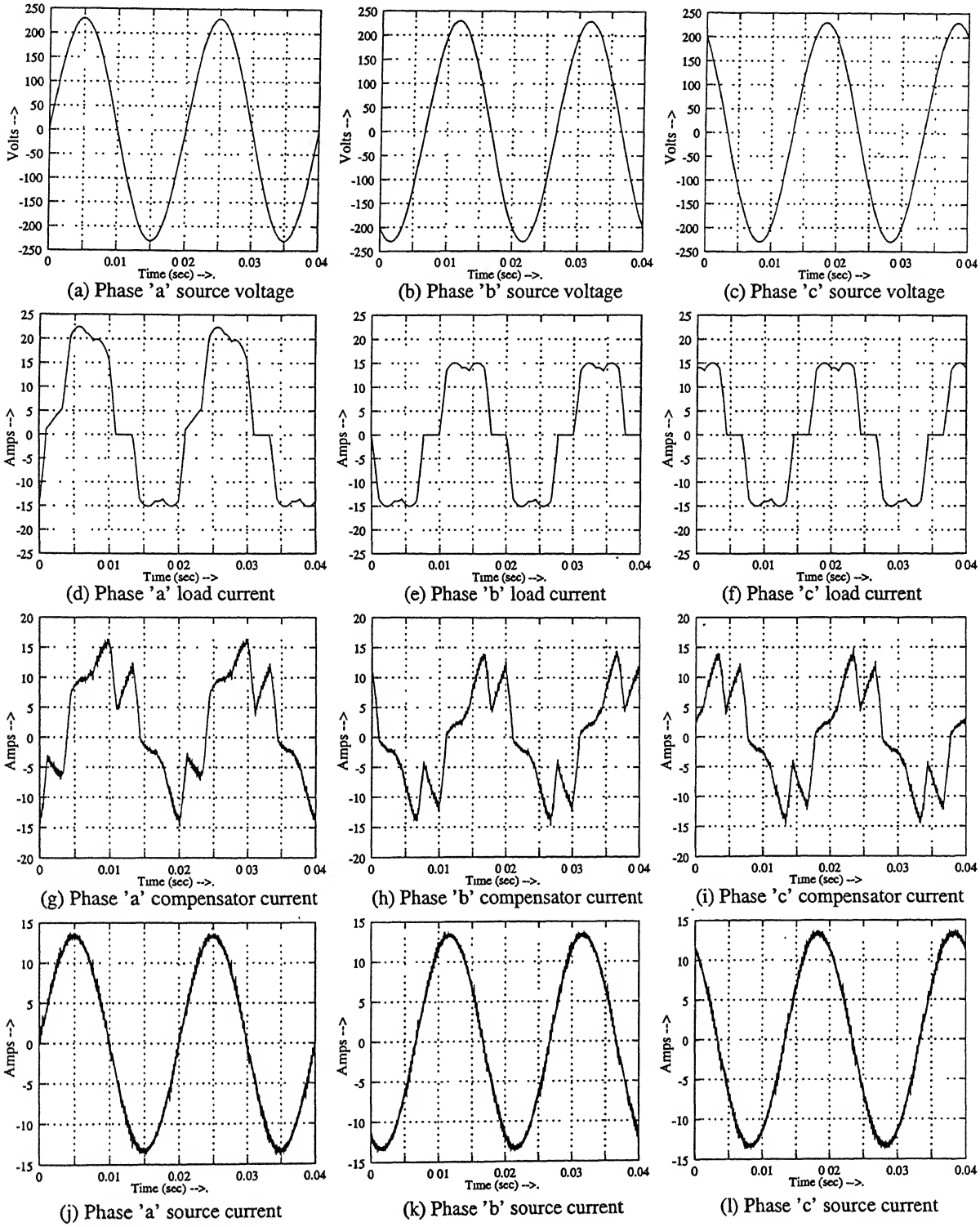

Figure 3.26: Simulated waveforms for case3.

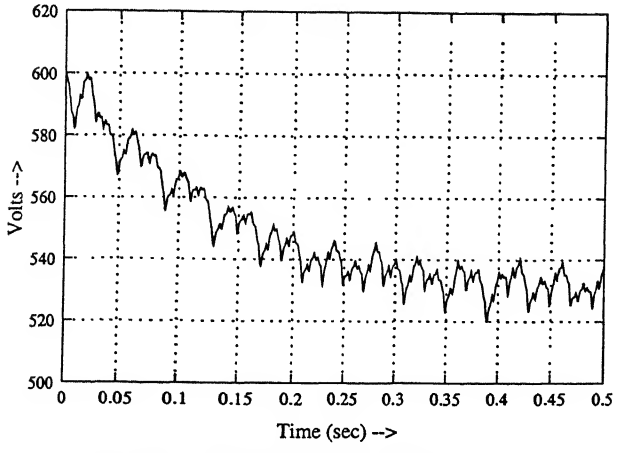

(a) Vdc1 without capacitor voltage control loop

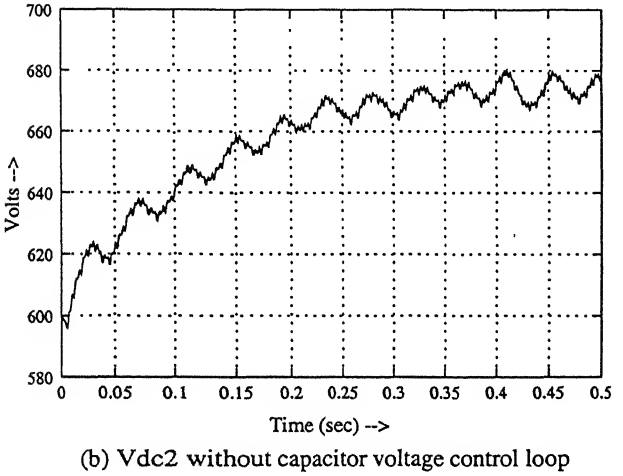

(b) Vdc2 without capacitor voltage control loop

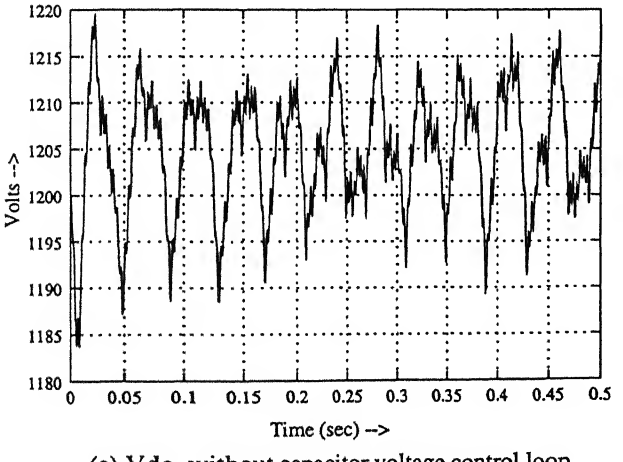

(c) Vdc without capacitor voltage control loop

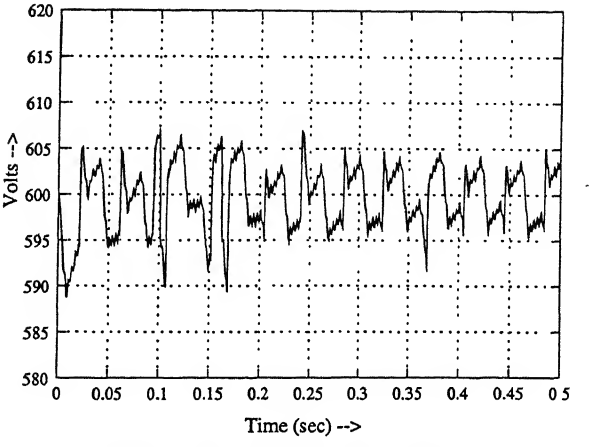

(d) Vdc1 with capacitor control voltage loop

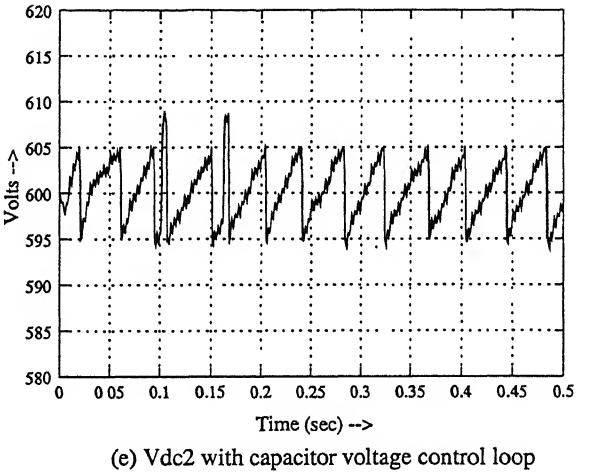

(e) Vdc2 with capacitor voltage control loop

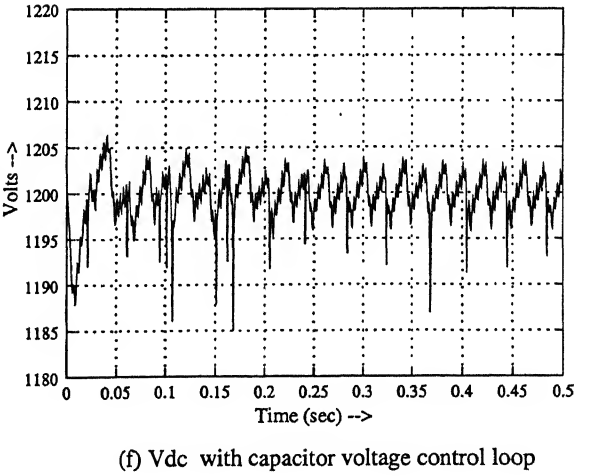

(f) Vdc with capacitor voltage control loop

Figure 3.27: Capacitor voltage with and without capacitor voltage balance loop.

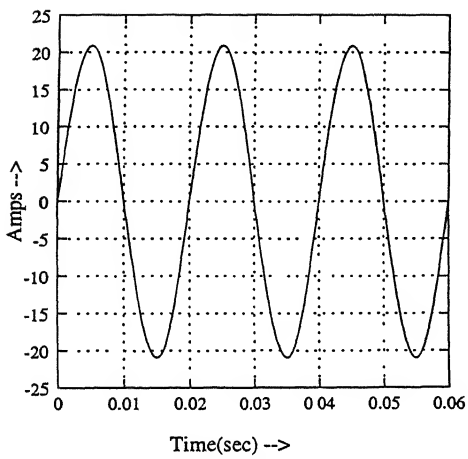

(a) The reference current for phase 'a'

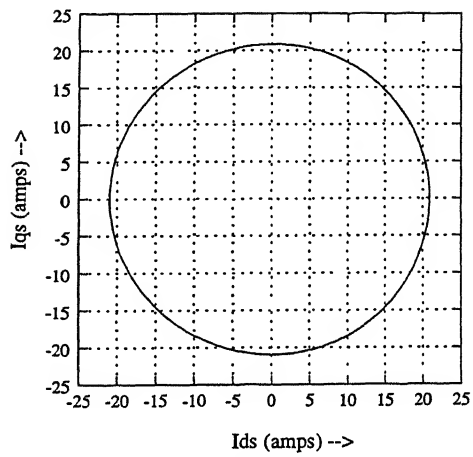

(c)The reference current vector

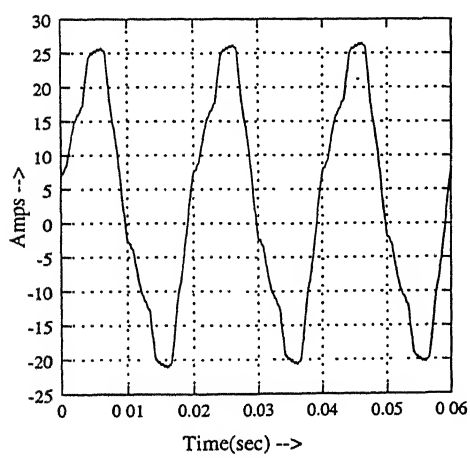

(b) Phase 'a' actual current

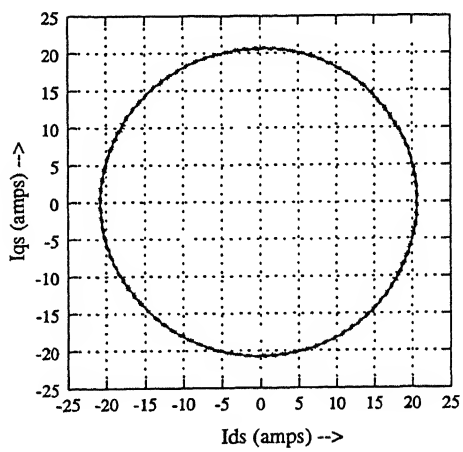

(d) The actual current vector

Figure 3.28: Currents using predictive controller.

3.7.3 Performance of Filter During the Transient Conditions

Active filter is simulated for transients also. Load firing angle is changed to 60°, from 0°, after 0.1 sec. and then again changed to 30° after 0.2 sec. The waveforms for all the three cases are shown.

Case 1

The (a) load current, (b) compensator current and (c) source current with the source voltage for all the three phases are shown in fig. 3.29, 3.30 and 3.31. It is seen from the figs. 3.29(c), 3.30(c), 3.31(c) that source current is always in phase with the source voltage during the transients also. The source current settles to the steady state in less than one cycle.

The capacitor voltages, shown in fig. 3.32, V_{dc1} and V_{dc2} are constant within the peak to peak ripple. During the transients the voltages rises or falls accordingly and settle to the reference within one cycle.

Case 2

The (a) load current, (b) compensator current and (c) source current with the source voltage for all the three phases are shown in fig. 3.33, 3.34 and 3.35. It is seen from the figs. 3.33(c), 3.34(c), 3.35(c) that source current is always in phase with the source voltage even during the transients. The source current settles to the steady state in about one and a half cycle.

The capacitor voltages, shown in fig. 3.36, V_{dc1} and V_{dc2} are constant within the peak to peak ripple. During the transients the voltages rises or falls accordingly and settle to the reference within two cycles.

Case 3

The (a) load current, (b) compensator current and (c) source current with the source voltage for all the three phases are shown in fig. 3.37, 3.38 and 3.39. It is seen from the figs. 3.37(c), 3.38(c), 3.39(c) that source current is always in phase with the source voltage. The source current settles to the steady state within two cycles.

The capacitor voltages, shown in fig 3.40, V_{dc1} and V_{dc2} are constant within the peak to peak ripple. During the transients the voltages rises or falls accordingly and settle to the reference within two and a half cycle.

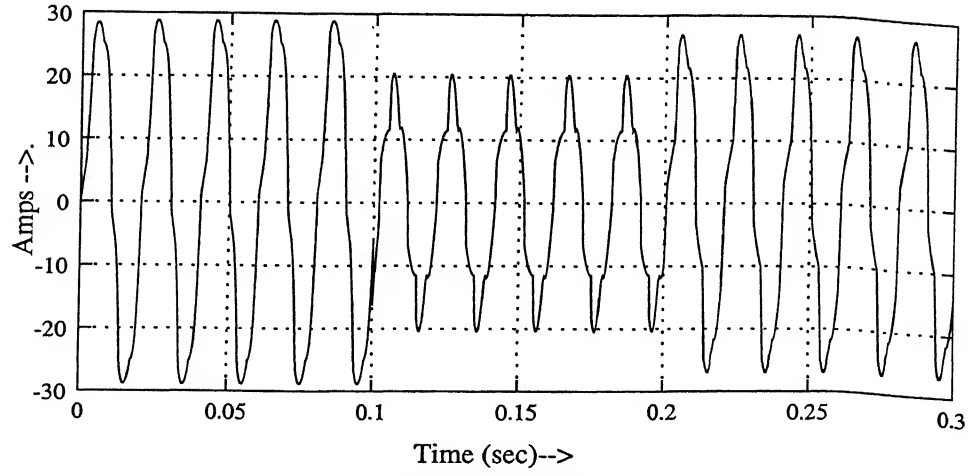

(a) Load current

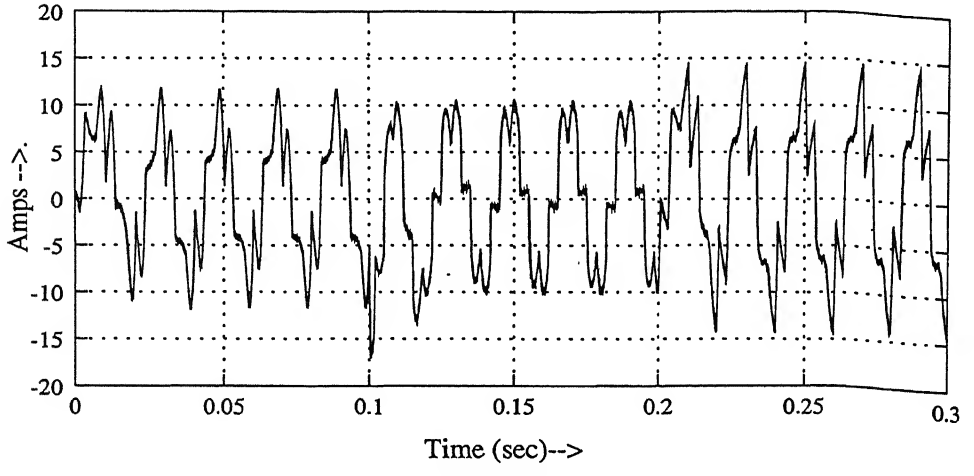

(b) Compensator current

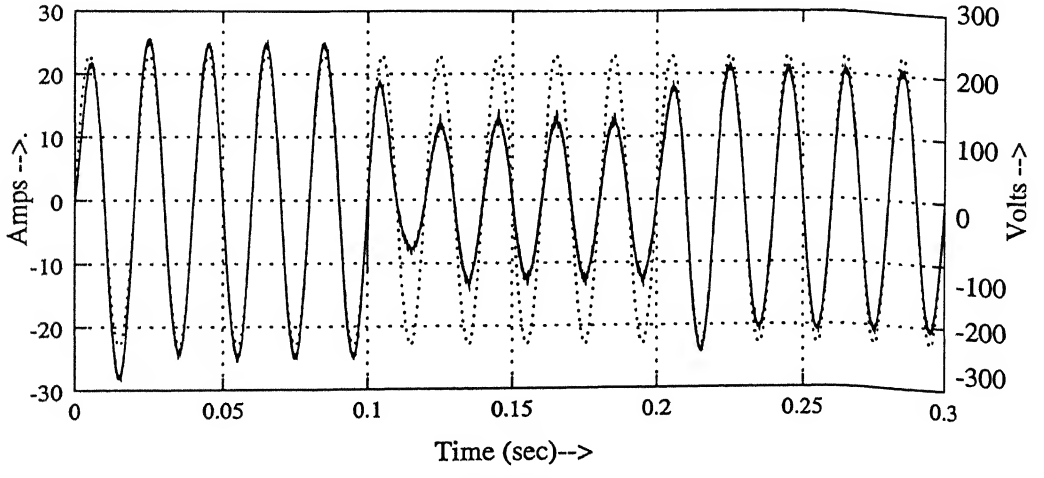

(c) Source current with source voltage

Figure 3.29: Phase 'a' currents during transients for case 1.

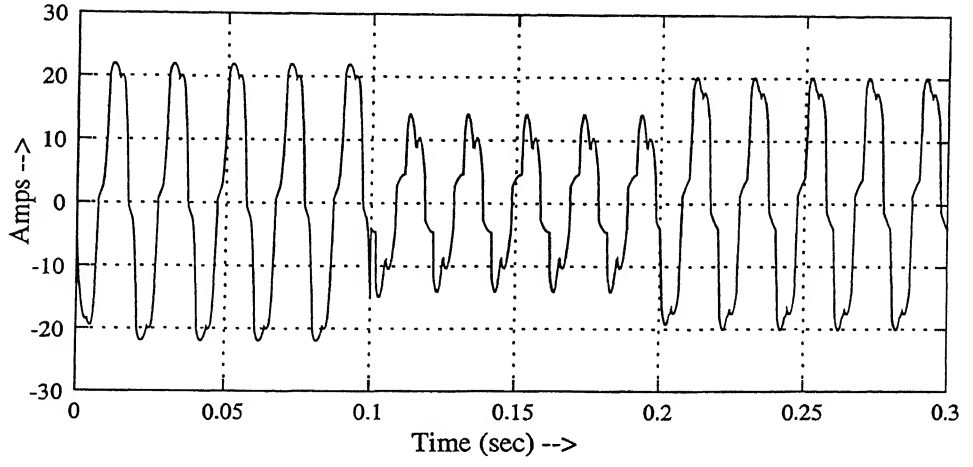

(a) Load current

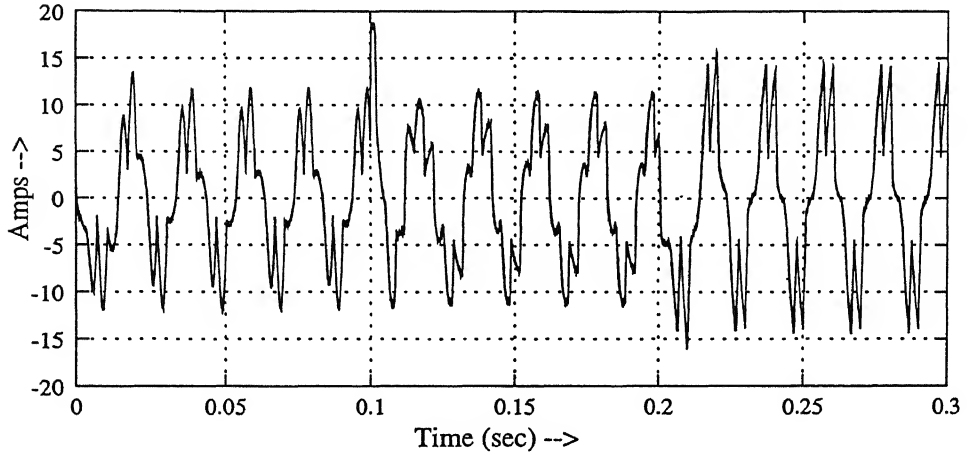

(b) Compensator current

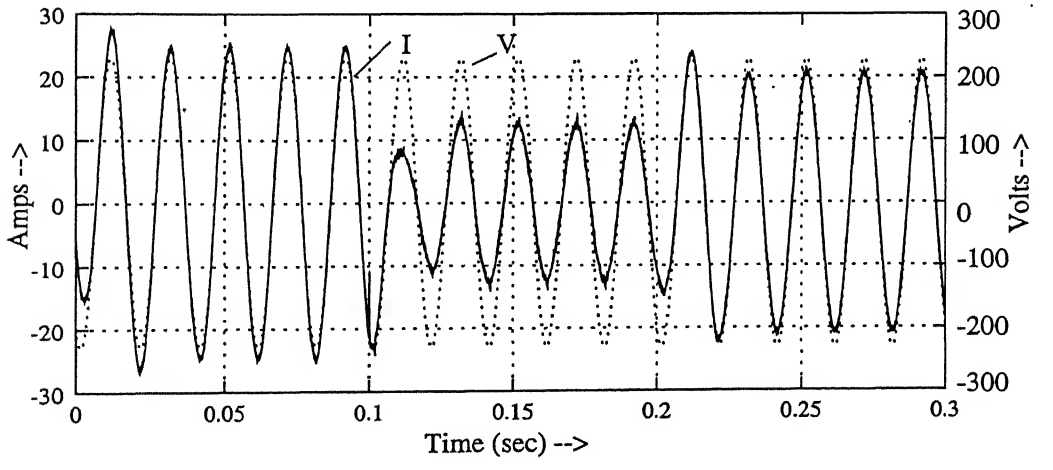

(c) Source current with source voltage

Figure 3.30: Phase 'b' currents during transients for case 1.

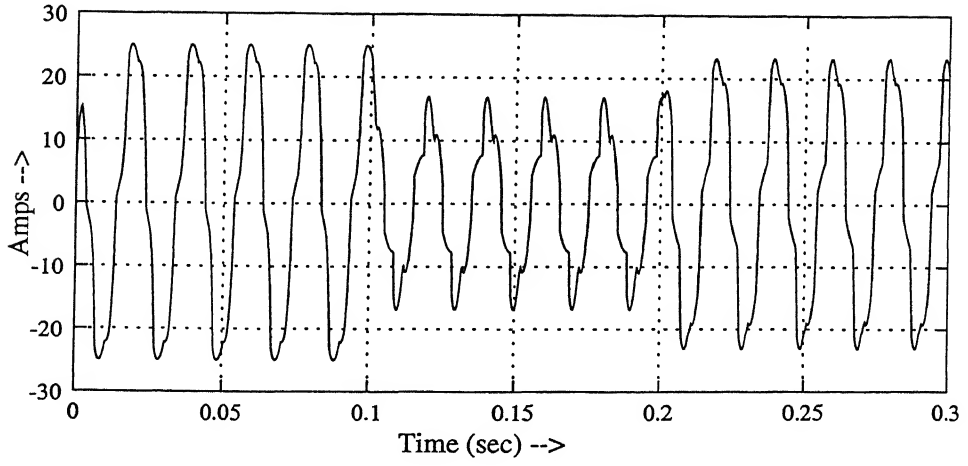

(a) Load current

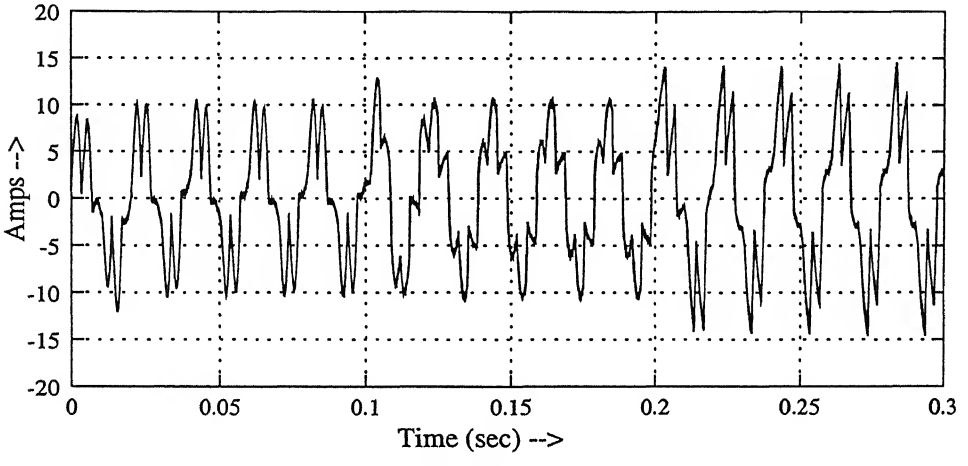

(b) Compensator current

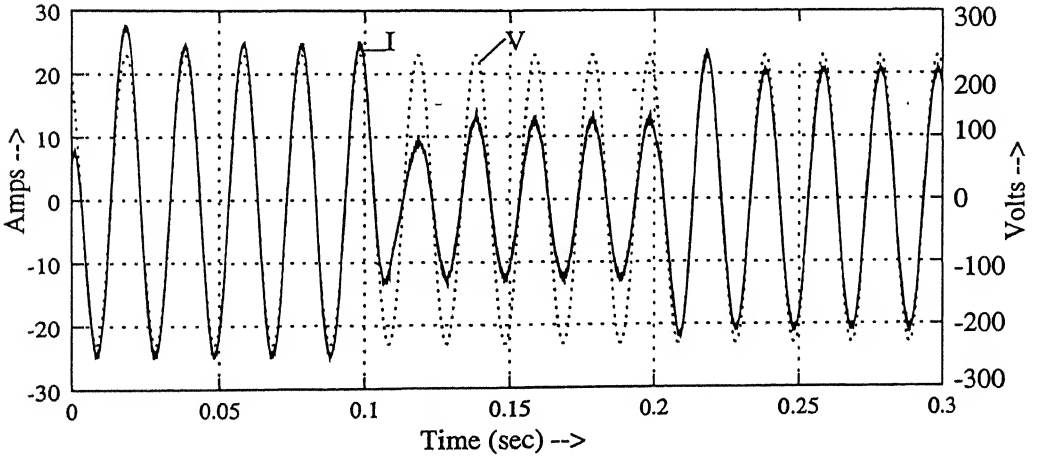

(c) Source current with source voltage

Figure 3.31: Phase 'c' currents during transients for case 1.

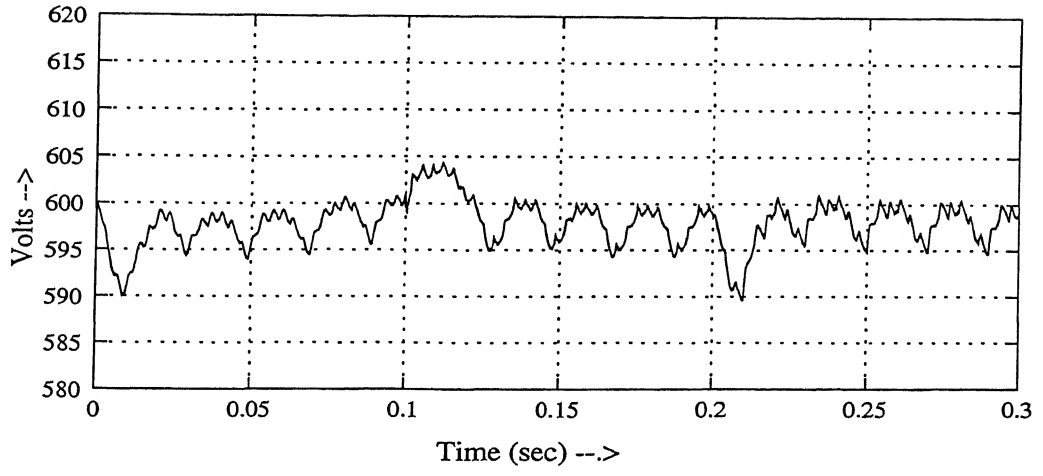

(a) Vdc1 Voltage of upper capacitor

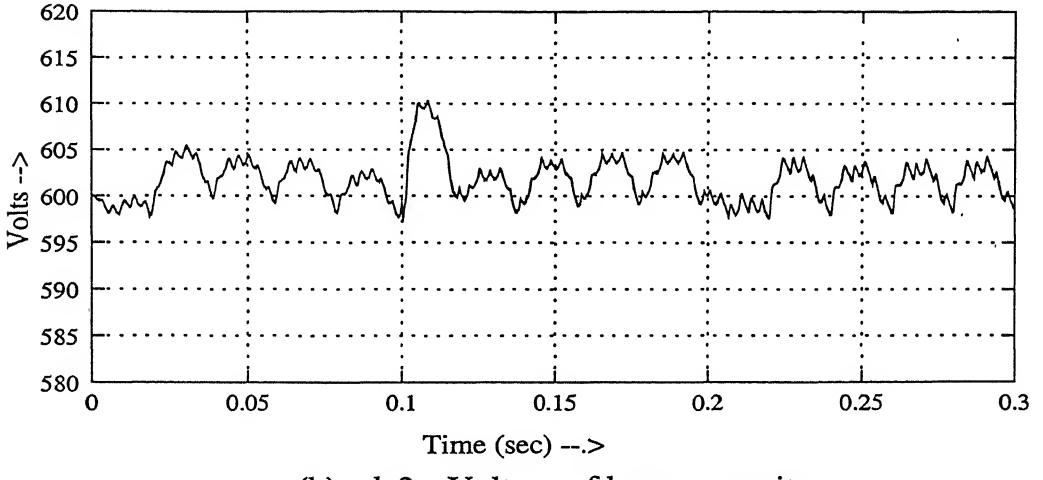

(b) vdc2 Voltage of lower capacitor

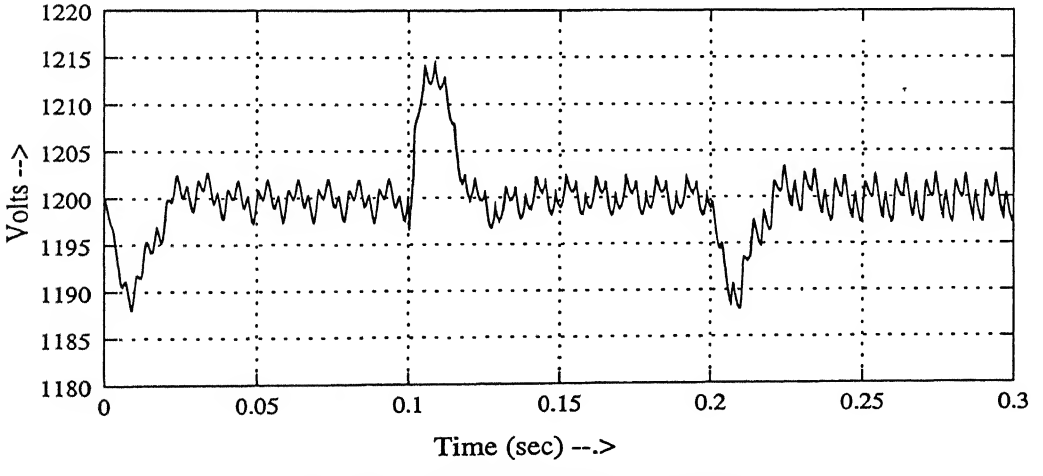

(c) Vdc Total capacitor voltage

Figure 3.32: Capacitor voltages during the transients for case 1.

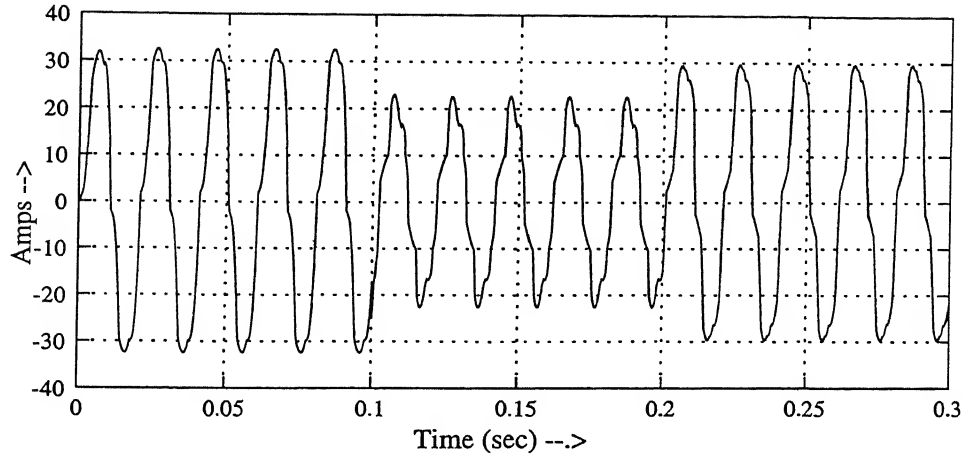

(a) Load current

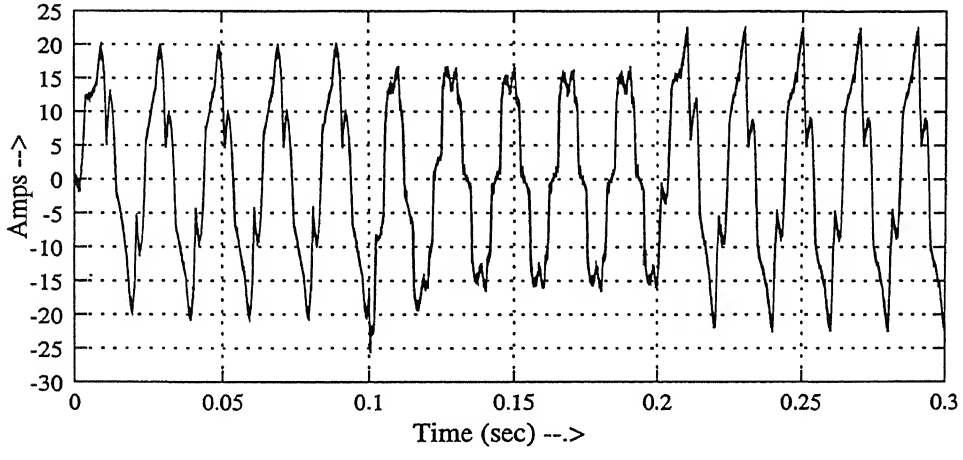

(b) Compensator current

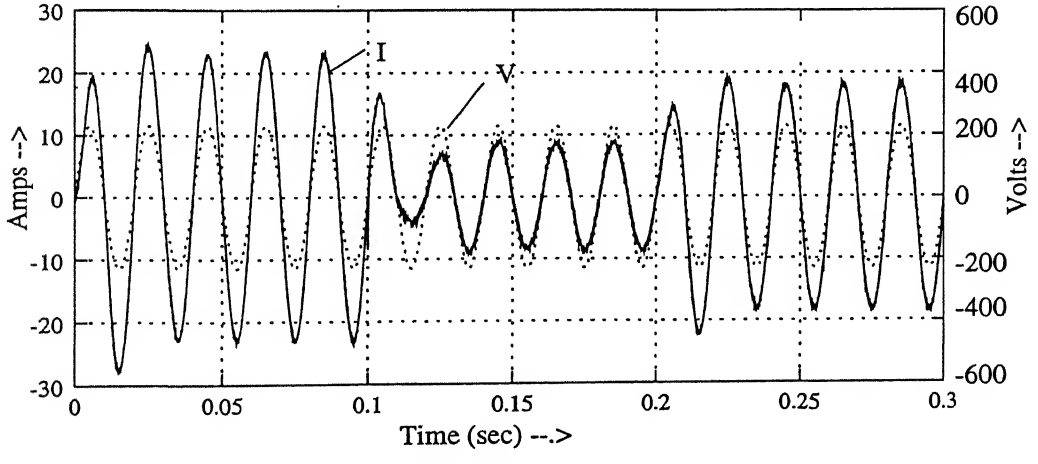

(c) Source current with source voltage

Figure 3.33: Phase 'a' currents during the transients for case 2.

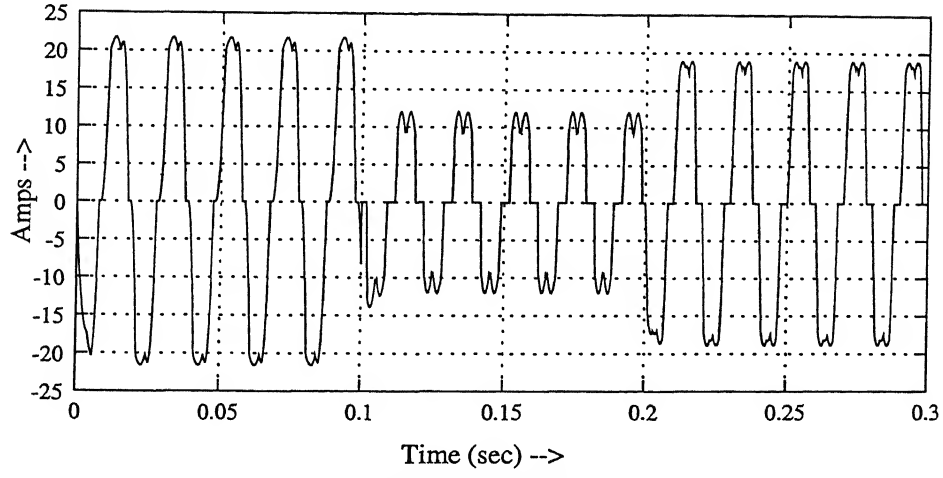

(a) Load current

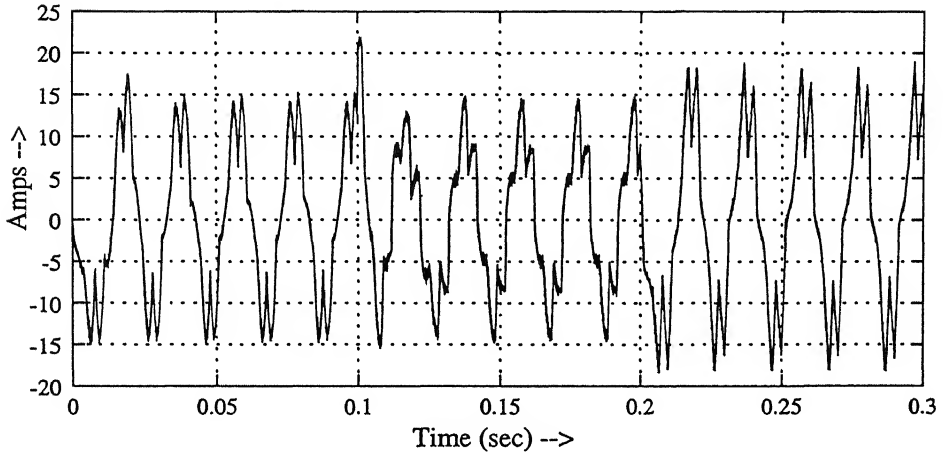

(b) Compensator current

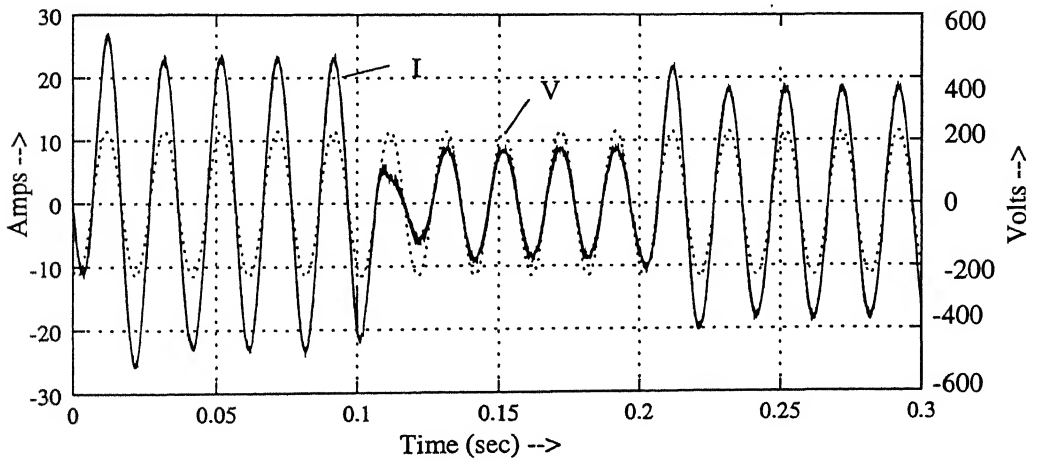

(c) Source current and source voltage

Figure 3.34: Phase 'b' currents during the transients for case 2.

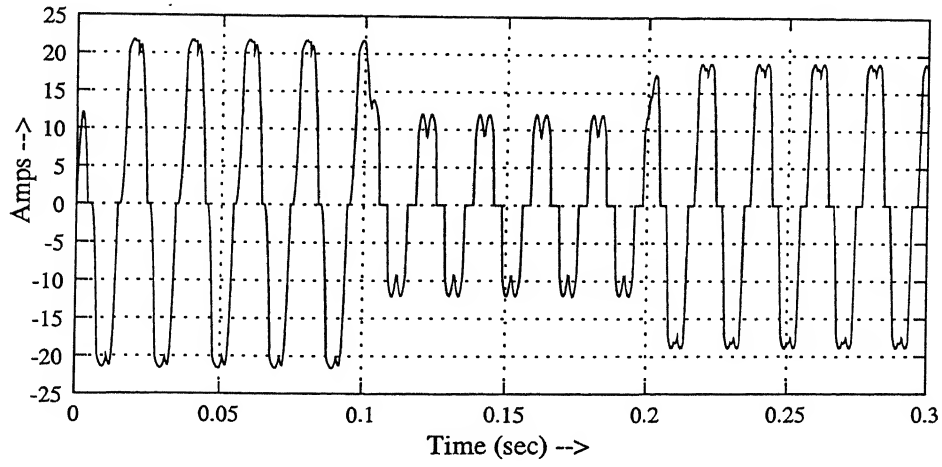

(a) load current

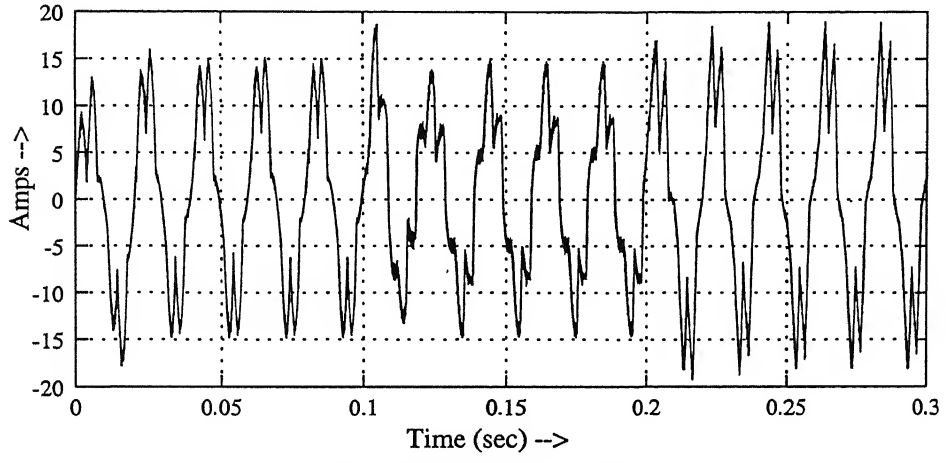

(b) Compensator current

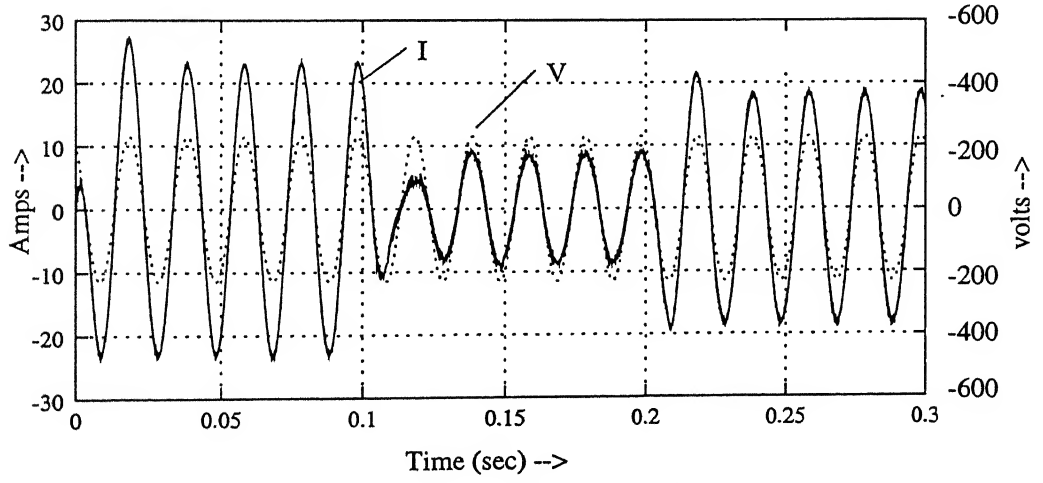

(c) Source current with source voltage

Figure 3.35: Phase 'c' currents during the transients for case 2.

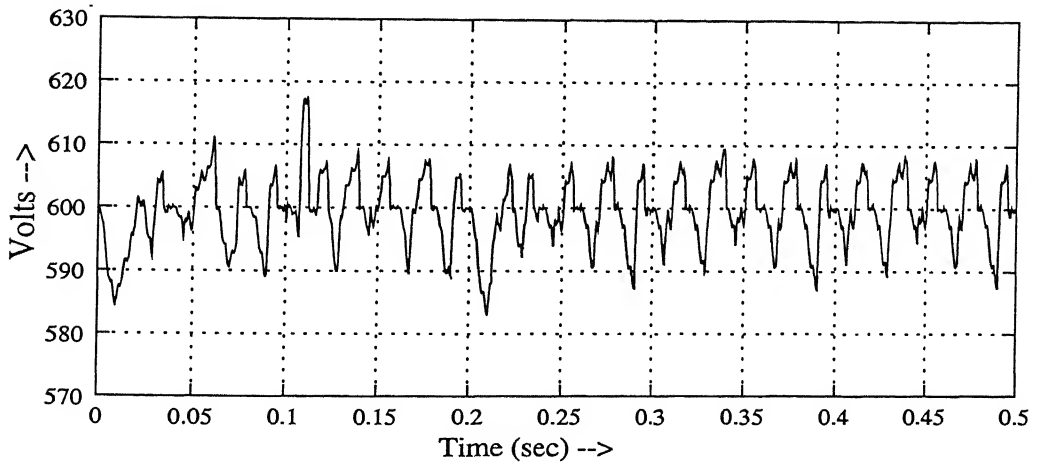

(a) Vdc1 Voltage of upper capacitor

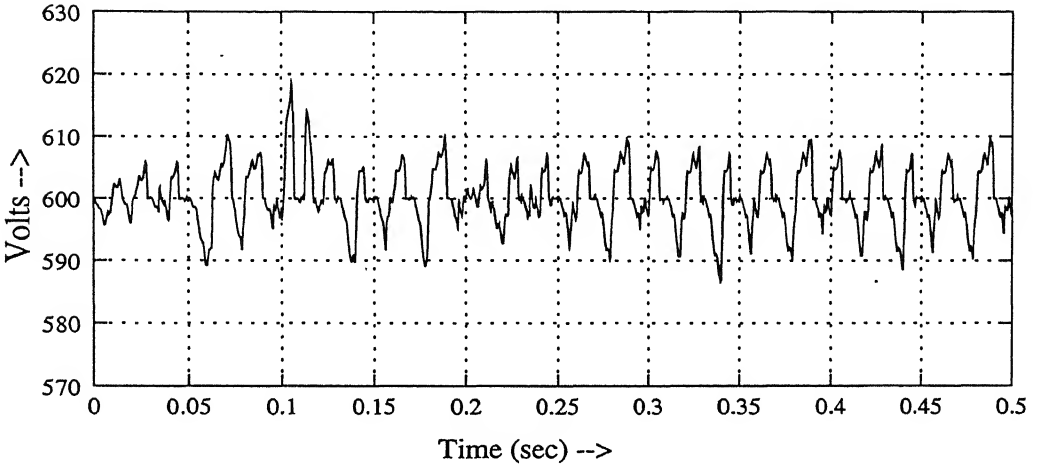

(b) Vdc2 Voltage of lower capacitor

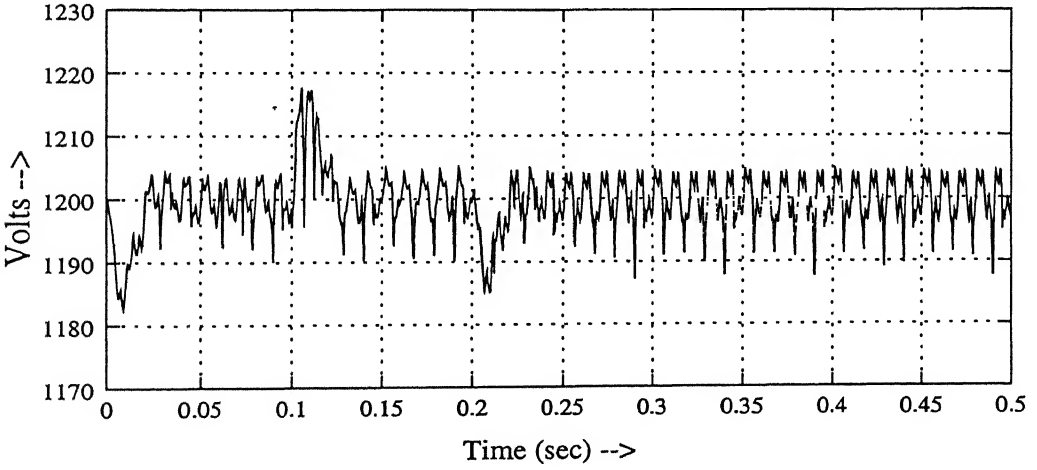

(c) Vdc Total capacitor voltage

Figure 3.36: Capacitor voltages during the transients for case 2.

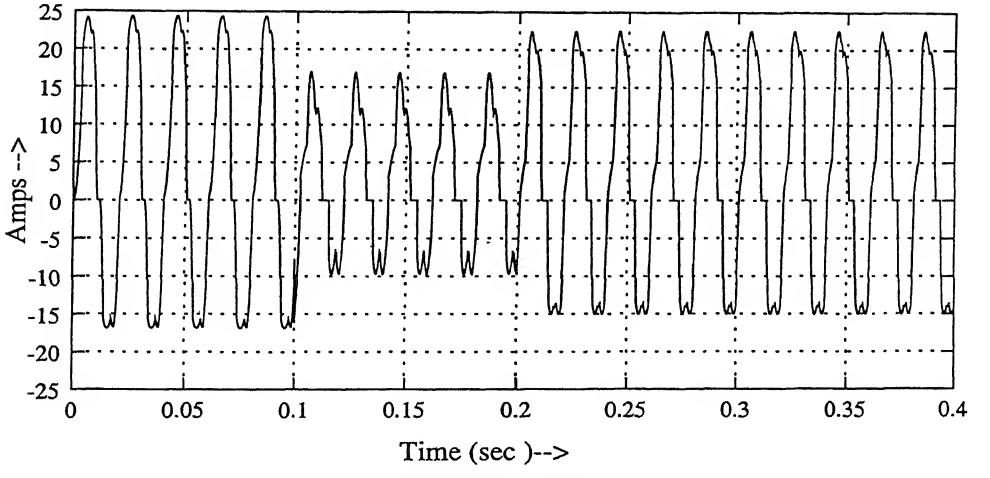

(a) Load current

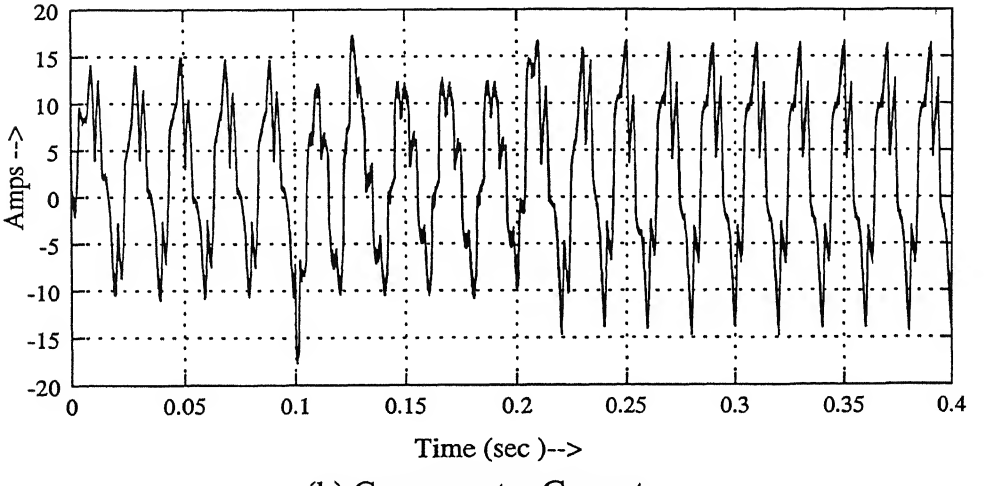

(b) Compensator Current

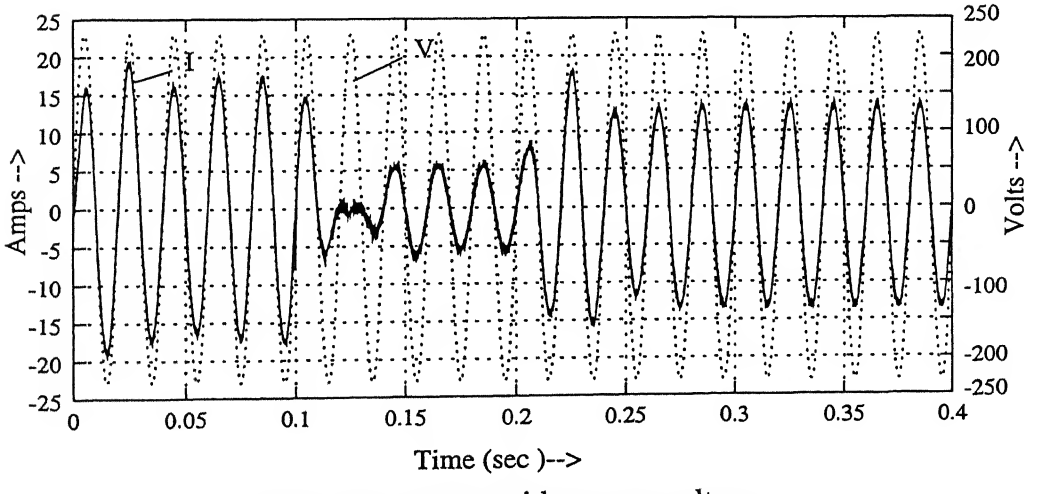

(c) Source current with source voltage

Figure 3.37: Phase 'a' currents during the transients for case 3.

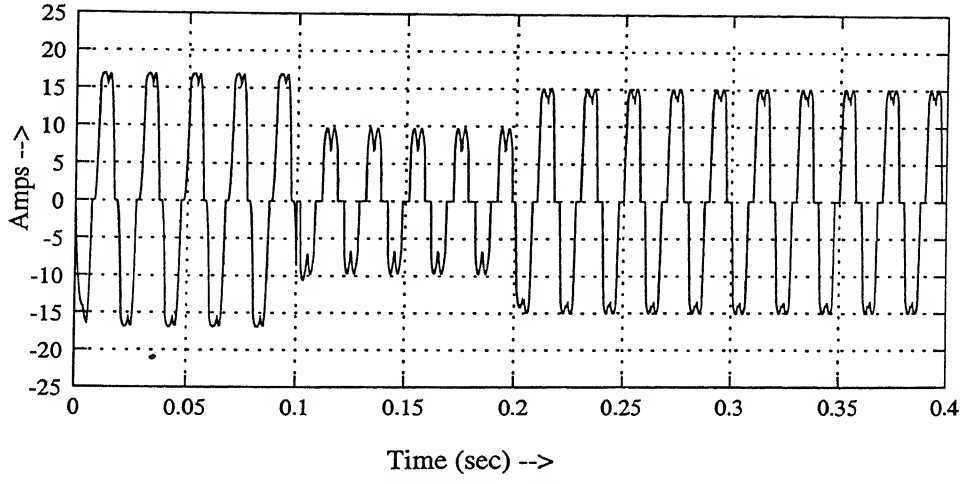

(a) Load current

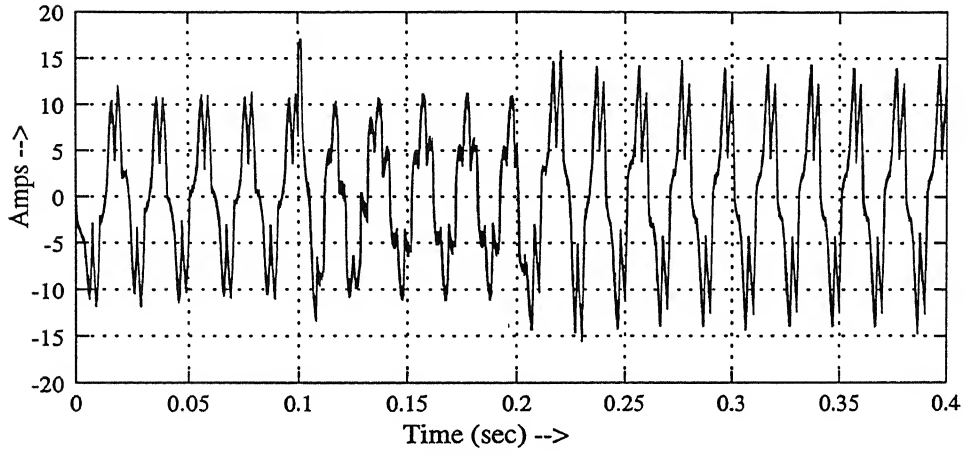

(b) Compensator current

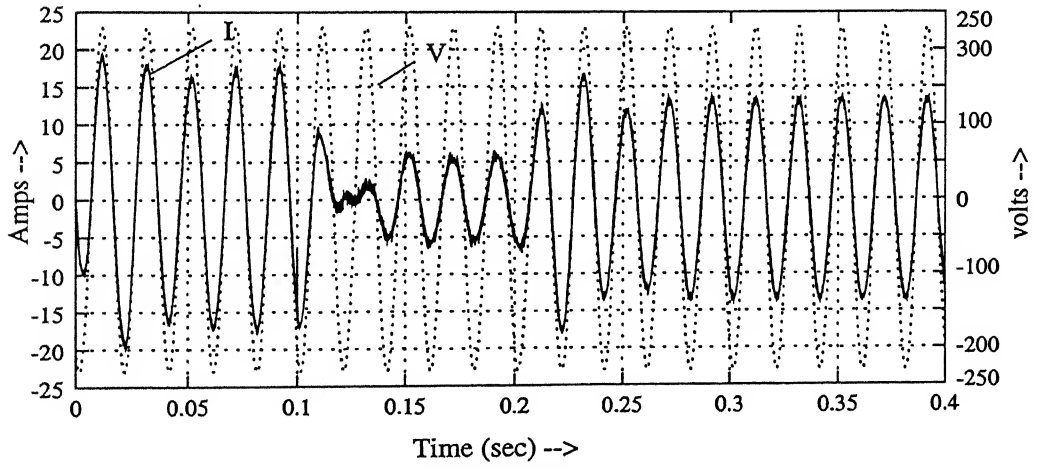

(c) Source current with source voltage

Figure 3.38: Phase 'b' currents during the transients for case 3.

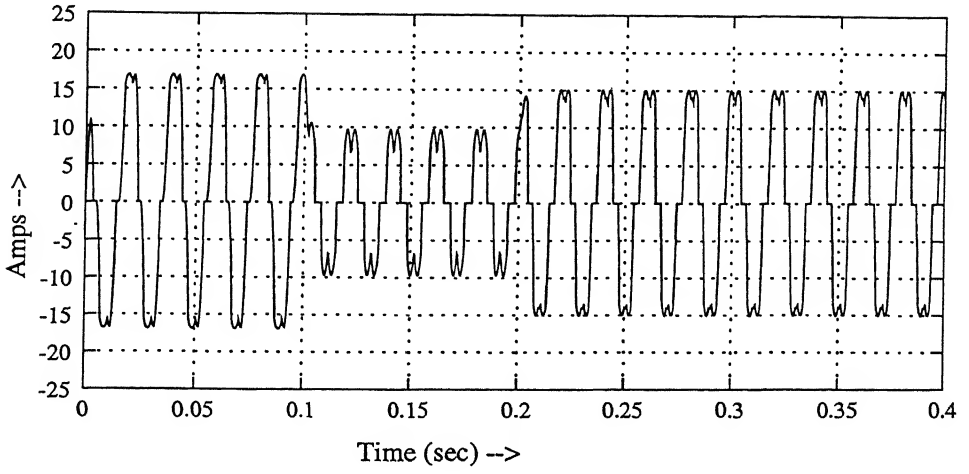

(a) Load current

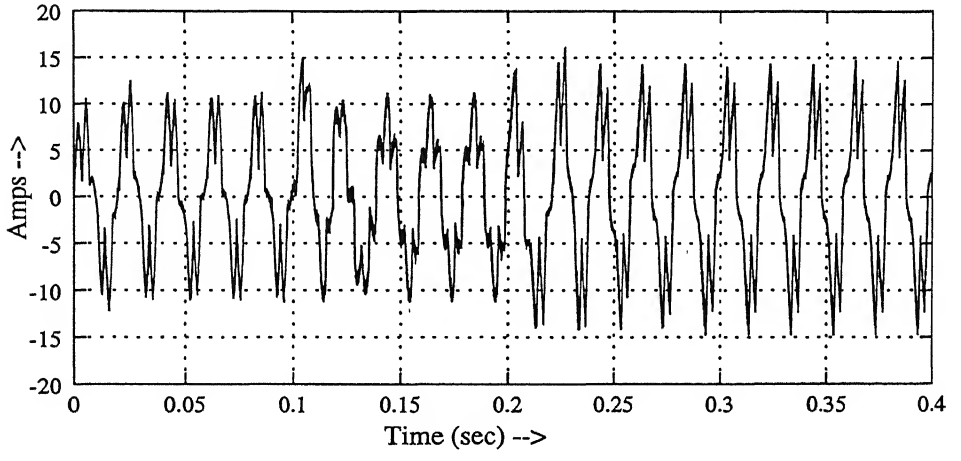

(b) Compensator current

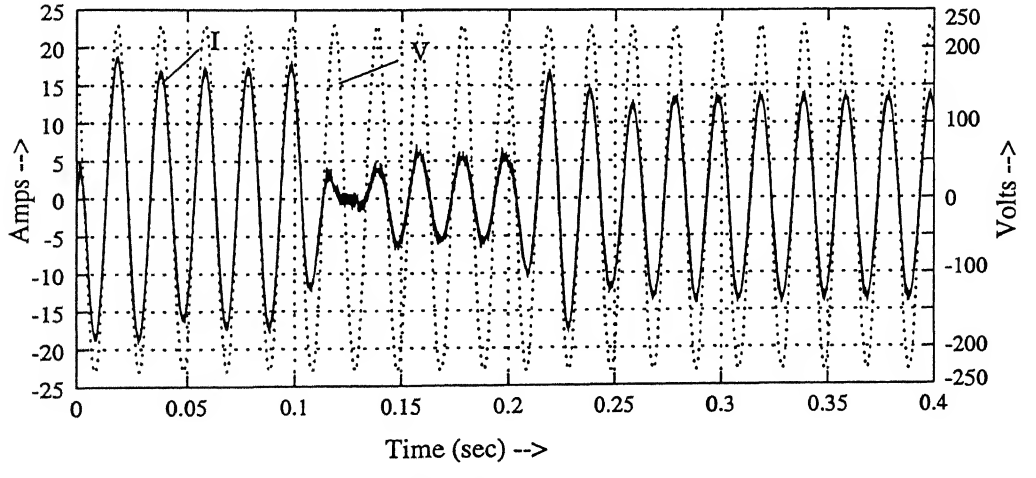

(c) Source current with source voltage

Figure 3.39: Phase 'c' currents during the transients for case 3.

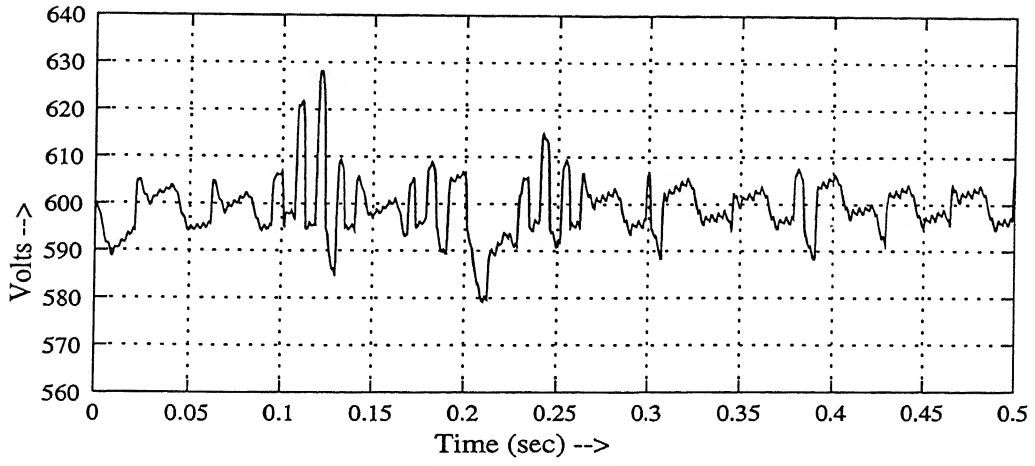

(a) Vdc1 voltage of upper capacitor

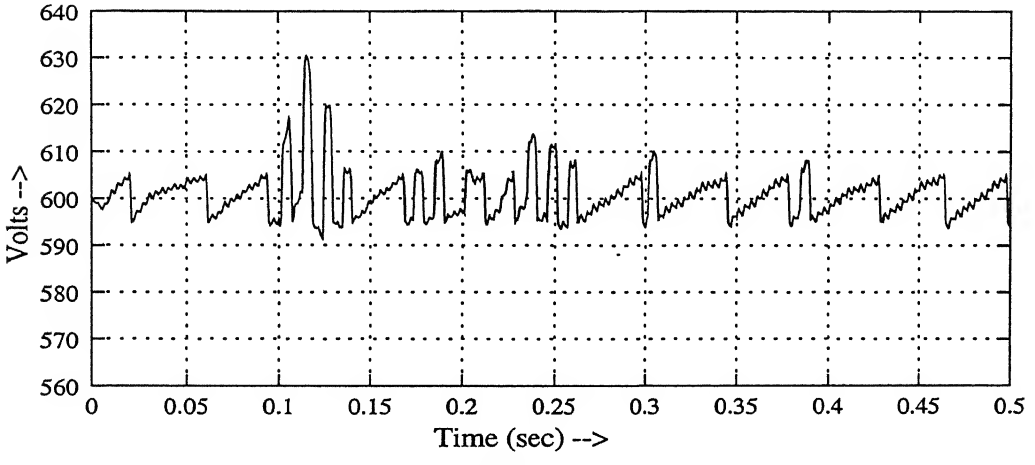

(b) Vdc2 Voltage of lower capacitor

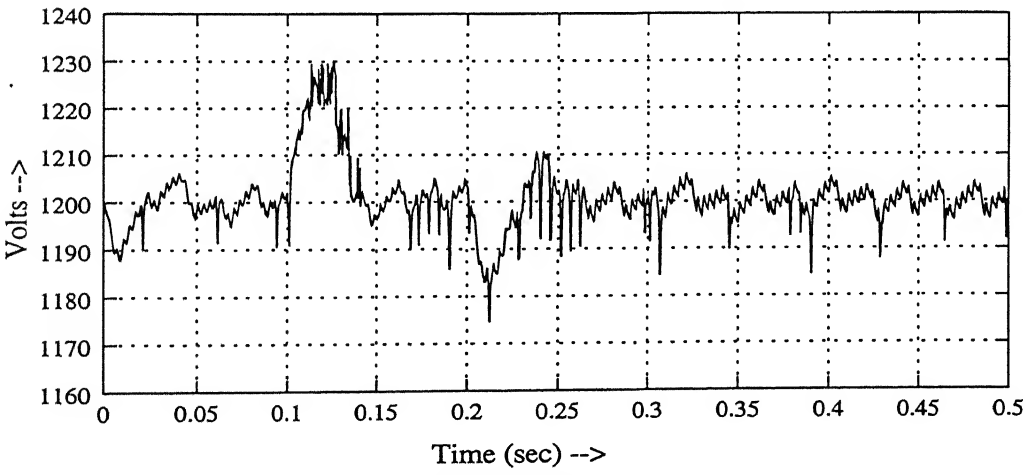

(c) Vdc Total capacitor voltage

Figure 3.40: Capacitor voltages during the transients for case 3.

3.8 Conclusion

The proposed active filter works for both steady state and transient conditions. It adjusts itself to make the source current sinusoidal. The filter proposed in section 3.3 has a disadvantage that it cannot compensate for unbalanced loads. So the active filter with neutral connected to the ground is proposed in section 3.6. This filter is able to compensate for unbalance loads, and makes the source current distortion free.

From the simulation results following conclusions can be made.

1. Source current is sinusoidal and always in phase with the source voltage.
2. The peak of the source current is less than the load current in all the cases.
3. For balanced loads the active filter, without the grounded neutral, can be used with predictive controller to make the source current smooth and the switching frequency constant.
4. The active filter, with neutral grounded, is capable of compensating any type of unbalance in the load. In this case predictive controller cannot be used as it is not capable of computing zero sequence current. The hysteresis controller must be employed in this case.
5. The dc capacitor voltage control loop is used to balance the unbalanced voltage of each capacitor in the dc link.

Chapter 4

Conclusion And Recommendation For Further Work

4.1 Conclusion

In this thesis the operation of an active filter using 3-level voltage source inverter has been studied. The entire system has been modeled using differential equations and its operation has been studied for various types of loads. The hysteresis controller and controller using space vector modulation have been employed. The steady state and transient of the system have been studied. The following conclusions can be made from the simulation results in chapter 2 and 3.

1. The 3-level inverter can be made to act as current source using hysteresis controller or predictive controller.

2. Hysteresis controller is simple to implement without any large calculations. On the other hand the implementation of predictive controller depends on large calculations but the switching frequency is constant.

3. The predictive controller, using space vector modulation fails to work for unbalance loads. In this method, the required voltage vector is predicted from the system model. Reverse transformation is used to determine the time durations for individual inverter states. This step cannot account for the zero sequence components in the phase voltages. Therefore while the current vector is correctly tracked the individual currents do not follow their references.

4. The harmonic correction is done in time domain, thus the response of filter is fast correction is obtained within one cycle.

5. The active filter is able to compensate for reactive power of load and the source current is sinusoidal and always in phase with the source voltage even during transients.

6. The usual dc capacitor voltage control loop fails to correct any unbalance in the voltages of individual capacitors due to unbalances in load. To overcome this problem a chopper circuit has been proposed. It is shown that with the addition of this circuit capacitor voltages can be balanced even when load current contains dc component.

7. During the transients the dc capacitor supplies or stores the energy to instantaneously adjust the source current for any change in the load current.

8. The active filter simulated for different types of loads, gave satisfactory results.

4.2 Recommendation for Further Work

1. A higher level (eg. 5-level) inverter can be used, as an active filter, instead of 3-level inverter to obtain better performance.

2. The 3-level inverter can be studied in detail for the harmonic contents in the voltage and current.

3. The predictive controller, using space vector modulation can be modified to compensate unbalanced loads correctly.

4. The active filter is simulated assuming ideal switches, a detailed analysis can be done with non-ideal switches.

5. Performance of the system, when a combination of passive and active filters is used, can be studied.

Bibliography

[1] Bimal K. Bose, "*Recent advances in power electronics,*" IEEE Transactions on Power Electronics, Vol. 7, No. 1, Jan. 1992, pp. 2-16.

[2] Sikyung Kim, Prasad N. Enjeti, Paul Packebush and Ira J. Pitel, "*A new approach to improve power factor and reduce harmonic in a three-phase diode rectifier type utility interface,*" IEEE Transactions on I.A., vol. 30, No. 6, Nov./Dec. 1994, pp. 1557-1563.

[3] W. M. Grady, M. J. Samotgj and A. H. Noyola, "*Survey of active power line conditioning methodologies,*" IEEE Transactions on Power Delivery, vol. 5, No. 3, July 1990, pp. 1536-1542.

[4] Luis A., Juan W. Dixon and Rogel R. Wallace, "*A three-phase active power filter operating with fixed switching frequency for reactive power and current harmonic compensation,*" IEEE Transactions on I.E., vol. 42, No. 4, Aug. 1995, pp. 402-408.

[5] Richard M. Duke and Simon D. Round, "*The steady-state performance of a controller current active filter,*" IEEE Transactions on P.E., vol. 8, No. 3, April 1993, pp. 140-146.

[6] Hirofumi Akagi, "*New trends in active filters for power conditioning,*" IEEE Transactions on I.A., vol. 32, No. 6, Nov./Dec. 1996, pp. 1312-1321.

[7] Hirofumi Akagi, Akira Nabae and Satoshi Atoh, "*Control strategy of active power filter using multiple voltage source PWM converters,*" IEEE Transactions on I.A., vol. IA-22, No. 3, May/June 1986, pp. 460-465.

[8] Nastaran J., Cajhen R., Seliger M. and Jereb P., "*Active power filter for nonlinear AC loads,*" IEEE Transactions on P.E., vol. 9, No. 1, 1994, pp. 92-96.

[9] John H. R. Enslin, Jian Jhao, Rene Spee, *"Operation of unified power flow controller as harmonic isolation,"* IEEE Transactions on P.E., vol. 11, No. 6, Nov. 1996, pp. 776-784.

[10] M. Rastogi, N. Mohan and A. A. Edris, "*Hybrid active filtering of harmonic currents in power systems,*" IEEE Transactions on Power Delivery, vol. 10, No. 4, Oct. 1995, pp. 1994-2000.

[11] H. Akagi, Y. Kanazawa and A. Nabae, "*Instantaneous reactive power compensator comprising switching devices without energy storage components,*" IEEE Transactions on I.A., vol. IA-20, No. 3, May/June 1984, pp. 625-630.

[12] Fang-Zhang Peng, Hirofumi Akagi and Akira Nabae, "*A study of active power filters using quad-series voltage source PWM converters for harmonic compensation,*" IEEE Transactions on P.E., Vol 5, No. 1, Jan. 1990, pp. 9-15.

[13] S. Satieo , R. Devraj and D.A. Torrey, "*The design, implementation of three-phase active power filter based on sliding mode control,*" IEEE Transactions on I.A., vol. 31, No. 5, 1995, pp. 993-1000.

[14] Bhim Singh, Kamal Al-Haddad and Ambrish Chandra, "*A new control approach to three-phase Active filter for harmonics and reactive power compensation,*" IEEE Transactions on Power System, vol. 13, No. 1, Feb. 1998.

[15] Nasser H. Rashidi, "*Improved and less load dependent three phase current controlled inverter with hysteresis current controllers,*" IEEE Transactions on I.E., vol. 42, No. 3, June 1995, pp. 325-330.

[16] Hoang Le-Huy and Louis A. Dessaint, "*An adaptive current control scheme for PWM synchronous motor drives: analysis and simulation,*" IEEE Transactions on P.E., vol. 4, No. 4, Oct. 1989, pp. 480-495.

[17] Hong Le Huy, Karim Slimani, Philippe Viarouge, "*Analysis and implementation of a real-time predictive current controller for permanent-magnet synchronous servo drives,*" IEEE Transactions on I.E., vol. 41, No. 1, Feb. 1994, pp. 110-117.

[18] Astou Kawamura and Richard Hoft, "*Instantaneous feedback controlled PWM inverter with adaptive hysteresis,*" IEEE Transactions on I.A., vol. 20, No. 4, July/Aug. 1984, pp. 769-775.

[19] Bimal K. Bose, "*An adaptive hysteresis based current control technique of a voltage fed PWM inverter for machine drive system,*" IEEE Transactions on I.E., vol. 37, No. 5, Oct. 1990, pp. 402-408.

[20] Mehrdad Kazerani, Phoivos D. Ziogas and Geza Joos, "*A novel active current wave-shaping technique for solid-state input power factor conditioners,*" IEEE Transactions on I.E., Vol. 38, No. 1, Feb. 1991, pp. 72-78.

[21] Akira Nabae, Isao Takahashi and Hirofumi Akagi, "*A new neutral-point-clamped PWM inverter,*" IEEE Transactions on I.A., vol. IA-17, No. 5, Sept./Oct. 1981, pp. 518-523.

[22] Roberto Rojas, Tokuo Ohnishi and Takayuki Suzuki, "*Neutral-point-clamped inverter with improved voltage waveform and control range,*" IEEE Transactions on I.A., vol. 42, No. 6, Dec. 1995, pp. 587-594.

[23] Jih-Sheng Lai and Fang Zheng Peng, " *Multilevel converters - a new breed of power converters,*" IEEE Transactions on I.A., vol. 33, No. 3, May/June 1996, pp. 509-517.

[24] Fang Zheng Peng, Jih-Sheng Lai, John W. McKeever and James VanCoevering, "*A multi level voltage-source inverter with separate DC source for static var generation,*" IEEE Transactions on I.A., vol. 32, No. 5, Sept./Oct. 1996, pp. 1030-1037.

[25] Heinz Willi Van Der Broeck, Hans-Christoph Skudelny and Georg Viktor Stanke, "*Analysis and realization of a pulse width modulator based on voltage space vectors,*" IEEE Transactions on I.A., vol. 24, No. 1, Jan./Feb. 1988, pp. 142-150.

[26] V.T. Ranganathan, "*Space vector pulse width modulation - a status review,*" Sadhana, vol. 22, Part 3, Dec. 1997, pp. 675-688.

[27] Mario Marchesoni, "*High performance current control techniques for applications to multilevel high-power voltage source inverters,*" IEEE Transactions on P.E., vol. 7, No. 1, Jan. 1992, pp. 189-201.

[28] Yo-Han Lee, Bum-Seok Suh and Dong-Seok Hyun, "*A novel PWM scheme for a three level voltage source inverter with GTO thyristors,*" IEEE Transactions on I.A., vol. 32, No. 2, March/April. 1996, pp. 260-268.

[29] Hirofumi Akagi, "*Trends in active power line conditioners*," IEEE Transactions on P.E., vol. 9, No. 3, May 1994, pp. 263-268.

[30] Fang Zheng Peng and Jih-Sheng Lai, "*Generalized instantaneous reactive power theory for three-phase power system*," IEEE Transactions on I.& M., vol. 45, No. 1, Feb. 1996, pp. 293-297.

Appendix A

Simulation Of Various Load Circuits

The various load circuits simulated in chapter 3 are.

Three Phase Thyristor Load

The load circuit is shown in the fig. A.1. It can be modeled by the differential equation

$$L_l \frac{di_{dc}}{dt} + R_l i_{dc} = V_{rn} - V_{sn} \tag{A.1}$$

where V_{rn} and V_{sn} depends on the pair of thyristors conducting. V_{rn}, is the voltage of the phase which is connected to the point 'r', similarly V_{sn} is the voltage of the phase connected to the point 's'. Similarly the current also depends on the pair of thyristors conducting.

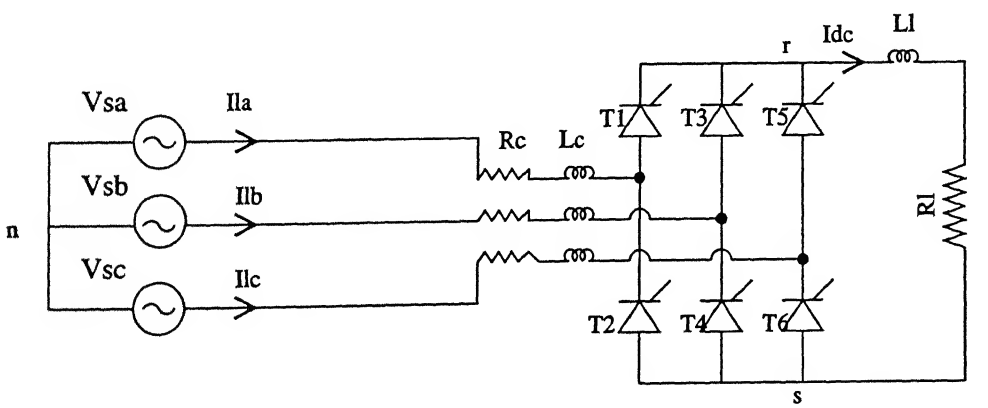

Figure A.1: Source supplying the thyristor load.

If T_1 and T_6 are conducting at a time, then phase 'a ' is connected to point 'r' and

phase 'c' is connected to point 's'. Thus V_{rn} and V_{sn} can be calculated as,

$$V_{rn} = V_{sa} - L_c\frac{di_{la}}{dt} - R_c i_{la} \tag{A.2}$$

$$V_{sn} = V_{sc} - L_c\frac{di_{lc}}{dt} - R_c i_{lc} \tag{A.3}$$

where V_{sa} and V_{sc} are the source voltages and $i_{la} = i_{dc}$, $i_{lb} = 0$ and $i_{lc} = -i_{dc}$.

During the commutation the equations for V_{rn} and V_{sn} are changed. Now after T_1, T_3 is fired. So the current from phase 'a' is transfered to phase 'b'. During the current transfer the equations for i_{la} and i_{lb} are given by,

$$V_{rn} = V_{sa} - L_c\frac{di_{la}}{dt} - R_c i_{la} \tag{A.4}$$

$$V_{rn} = V_{sb} - L_c\frac{di_{lb}}{dt} - R_c i_{lb} \tag{A.5}$$

adding equations A.4 and A.5 and using $i_{la} + i_{lb} = i_{dc}$.

$$V_{rn} = \frac{V_{sa} + V_{sb}}{2} - \frac{L_c di_{dc}}{2dt} - \frac{R_c i_{dc}}{2} \tag{A.6}$$

V_{sn} remains the same as equation A.3. Thus substituting V_{rn} and V_{sn} from equations A.2, A.3, A.6 (as the case may be) in equation A.1 and solving this differential equation load current i_{dc} is calculated. During the commutation interval, V_{rn} can be calculated from equation A.6. Then equations A.4 and A.5 can be used to solve for i_{la} and i_{lb}.

Resistive Load

The load circuit is shown in the fig. A.2. The respective load currents can be calculated by the following equations

$$I_{la} = \frac{V_{sa}}{R_{la}} \tag{A.7}$$

$$I_{lb} = \frac{V_{sb}}{R_{lb}} \tag{A.8}$$

$$I_{lc} = \frac{V_{sc}}{R_{lc}} \tag{A.9}$$

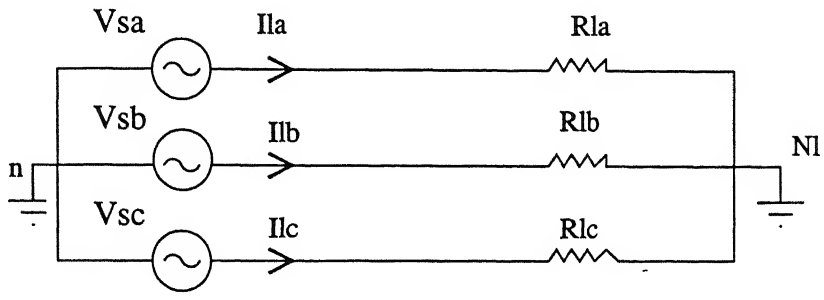

Figure A.2: Source supplying three phase unbalanced resistive load.

Single Phase Full Wave Rectifier Load

The load circuit is shown in the fig. A.3. The rectifier load is connected to phase 'a'. The circuit can be modeled by the following differential equation.

$$L_f \frac{di_{dc}}{dt} + R_f i_{dc} = V_{dc} \tag{A.10}$$

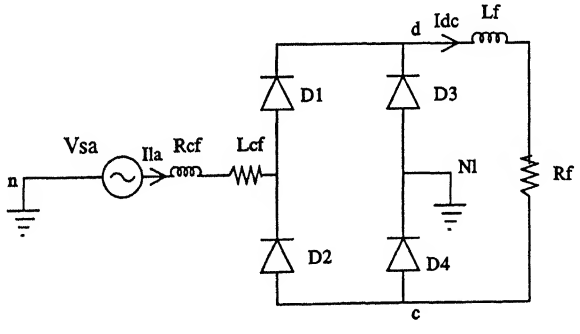

Figure A.3: Source supplying the full wave diode rectifier load.

If D_1 and D_4 are conducting then

$$V_{dc} = V_{sa} - L_c \frac{di_{la}}{dt} - R_c i_{la} \tag{A.11}$$

and $i_{la} = i_{dc}$.

If D_2 and D_3 are conducting then

$$V_{dc} = -V_{sa} + L_c \frac{di_{la}}{dt} + R_c i_{la} \tag{A.12}$$

and $i_{la} = -i_{dc}$.

Thus substituting V_{dc} from equation A.11 or A.12 (as the case may be) in the equation A.10 and solving this differential equation i_{dc} is calculated. Thus i_{la} can be

calculated.

Single Phase Half Wave Rectifier Load

The load circuit is shown in the fig. A.4. The rectifier load is connected to phase 'a'. The circuit can be modeled by the following differential equation.

$$L_h \frac{di_{la}}{dt} + R_h i_{la} = V_{dc} \tag{A.13}$$

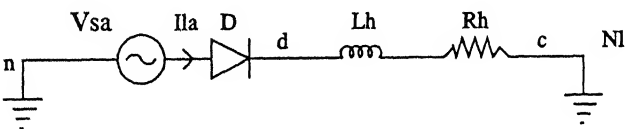

Figure A.4: Source supplying the half wave rectifier load.

If diode D is conducting then $V_{dc} = V_{sa}$.
If diode D is not conducting then $V_{dc} = 0$.
Thus solving equation A.13, i_{la} can be calculated.

.....	.....
.....	.....
.....	.....
.....	.....
.....	.....
.....	.....
.....	.....
.....	.....
.....	.....
.....	.....
.....	.....
.....	.....